Finite Difference Approach for the Measure Valued Vanishing Dispersion Limit of Burgers' Equation

Master's Thesis of Simon Laumer
Supervisor: Prof. Dr. Siddhartha Mishra

July 20, 2014

Abstract

We are concerned with the numerical computation of the measure valued vanishing dispersion limit (VDL) of Burgers' equation. Motivated by modern ideas concerning the numerical treatment of systems of conservation laws [5], we present an implicit finite difference scheme (FDS) with perturbation of the initial data and provide both theoretical and numerical indication that it indeed approximates the VDL.

Furthermore, we also present a Crank-Nicolson FDS for which we can't proof the above mentioned theoretical results but which as a KdV scheme works better than the implicit scheme. Indeed we shall see an improvement in the numerical results.

In order to have a reference for comparison, we lean on the work of Lax and Levermore [12] who theoretically investigated the mean and variance of the VDL.

Contents

1 Introduction

This thesis is embedded into the framework of *conservation laws* which form a class of PDE's appearing in many physical contexts. Basically, it is the PDE-formulation of

the fact that the local change of a certain quantity is equal to the flux of this quantity through the boundary of the local domain:

$$\frac{\mathrm{d}}{\mathrm{d}t}\int_\Omega u\,\mathrm{d}x = \int_{\partial\Omega} F(u)\cdot\,\mathrm{d}S.$$

Applying Gauss's formula $\int_{\partial\Omega} F\cdot\,\mathrm{d}S = \int_\Omega \mathrm{div}(F)\,\mathrm{d}x$, one then derives the corresponding PDE

$$u_t + \mathrm{div}(F(u)) = 0.$$

In the following, we shall give a short summary of well-known theory up to modern research topics concerning conservation laws and their numerical treatment. This will lead quite naturally to the *vanishing dispersion limit (VDL)* of Burgers' equation as theoretically investigated by Lax and Levermore (LaL) [12],[13],[14], but from the perspective of conservation laws and their *measure valued solutions*. The following introduction is mainly based on the work of DiPerna [4], Fjordholm and co-workers [5], and well-established theory that can be found for instance in [3].

1.1 Scalar Conservation Laws in One Space Dimension

In one space dimension, the *scalar conservation law* takes the form

$$\begin{aligned} u_t + f(u)_x &= 0, \quad x\in\mathbb{R}, t>0 \\ u(x,0) &= u_0(x), \quad x\in\mathbb{R}, \end{aligned} \tag{1}$$

where $f:\mathbb{R}\to\mathbb{R}$ is the *flux function*. One classical example of a non-linear flux is the Burgers' flux $f(u)=\frac{u^2}{2}$ which will be considered in this thesis.

It is well-known that even for smooth initial data, the classical solution of (1) generates infinite derivatives, so-called shocks, in finite time. It is therefore necessary to weaken the notion of solution in order to obtain existence of a global solution.

1.1.1 Weak Solutions, Entropy Conditions

The concept of solution is weakened such that it doesn't have to be differentiable anymore. This is formally done by shifting the derivatives onto a test function using integration by parts. More precisely, a function $u(x,t)$ is said to be a *weak solution* of (1) if for all compactly supported, smooth test functions $\varphi(\cdot,\cdot)\in C_c^\infty(\mathbb{R}\times\mathbb{R}_{\geq 0})$, the following integral equation holds:

$$\iint_{\mathbb{R}\times\mathbb{R}_{\geq 0}} u(x,t)\varphi_t(x,t) + f(u(x,t))\varphi_x(x,t)\,\mathrm{d}x\,\mathrm{d}t + \int_{\mathbb{R}} u_0(x)\varphi(x,0)\,\mathrm{d}x = 0. \tag{2}$$

Even though the concept of weak solutions gives existence, we lose uniqueness. This is why certain constraints have to be enforced, so-called *entropy conditions*. A pair (η,q) of functions $\mathbb{R}\to\mathbb{R}$ is an *entropy pair* if η is convex and if

$$q' = f'\eta'. \tag{3}$$

The function q is called an *entropy flux*. A weak solution $u(x,t)$ is then said to be an *entropy solution* if for all entropy pairs (η,q) and all non-negative, compactly supported, smooth test functions $0\leq\varphi(\cdot,\cdot)\in C_c^\infty(\mathbb{R}\times\mathbb{R}_{>0})$, the following integral inequality holds:

$$\iint_{\mathbb{R}\times\mathbb{R}_{\geq 0}} \eta(u(x,t))\varphi_t(x,t) + q(u(x,t))\varphi_x(x,t)\,\mathrm{d}x\,\mathrm{d}t \geq 0. \tag{4}$$

These entropy inequalities are forcing the weak solution to be the *vanishing viscosity limit (VVL)*, i.e. the strong L^2-limit $u = \lim_{\varepsilon \to 0} u^\varepsilon$ where u^ε is the smooth solution of

$$u_t^\varepsilon + f(u^\varepsilon)_x = \varepsilon u_{xx}^\varepsilon. \tag{5}$$

Indeed, the entropy inequality (4) is formally derived by multiplying the vanishing viscosity equation (5) with $\eta'(u^\varepsilon)$ and inserting (3). The inequality sign is then a consequence of the viscosity term $\varepsilon u_{xx}^\varepsilon$ together with the convexity of η. Thus, (4) makes sure that the entropy properties of the vanishing viscosity equation (5) are shared in the weak sense by the entropy solution. Kruzkhov [9] showed that this is indeed enough to prove uniqueness of the entropy solution. Moreover, it can be shown that the strong limit $u = \lim_{\varepsilon \to 0} u^\varepsilon$ exists which yields existence.

1.1.2 Numerical Solutions

There is a well-established theory of numerical methods converging to the entropy solution. Since we want to compute a solution that is characterized by integral (in)equalities, we work with so-called *finite volume schemes*. After discretizing space and time into cells $[x_{j-1/2}, x_{j+1/2}), [t_n, t_{n+1})$, the spatial cell averages $\frac{1}{\Delta x} \int_{x_{j-1/2}}^{x_{j+1/2}} u(x, t_n)\, \mathrm{d}x$ are approximated by the following explicit discrete scheme:

$$\frac{u_{j,n+1} - u_{j,n}}{\Delta t} + \frac{F_{j+1/2,n} - F_{j-1/2,n}}{\Delta x} = 0. \tag{6}$$

Here, $F_{j+1/2,n} = F_{j+1/2,n}(u_{j,n}, u_{j+1,n})$ is the *numerical flux*, and the mesh sizes Δx and Δt are linked via the CFL condition $\Delta t = \lambda \Delta x$.

In order to achieve convergence to the entropy solution, the numerical flux has to satisfy certain criteria of which the most important is *monotonicity*. This property allows us to establish discrete entropy inequalities which imply that as $\Delta x \to 0$, the computed solution will satisfy the entropy inequalities (4). One example of such a monotone flux is the *Godunov flux*:

$$F(u_j, u_{j+1}) = \begin{cases} \min_{u_j \le \theta \le u_{j+1}} f(\theta) & \text{if } u_j \le u_{j+1} \\ \max_{u_{j+1} \le \theta \le u_j} f(\theta) & \text{if } u_j \ge u_{j+1}. \end{cases}$$

For our numerical experiments, we use an initial function u_0 which satisfies the requirements of the LaL theory [12]. In particular, we choose the smooth, non-positive one-bump function

$$u_0(x) = \begin{cases} -e^{\frac{1}{2} - \frac{1}{(2x+2)^2} - \frac{1}{(2x-2)^2}} & \text{if } |x| < 1 \\ 0 & \text{else.} \end{cases}$$

Furthermore, we adjust the Burgers flux in order to be conformable to the KdV equation considered by LaL and therefore work with the flux $f(u) = -3u^2$.

The computed numerical solution with

$$\begin{aligned} N &= 500 \text{ spatial mesh points,} \\ \lambda &= 0.1 \text{ and} \\ t &= 0.1, 0.2, 0.3, 0.4 \end{aligned}$$

is shown in figure 1. One can clearly see how the initial bump function is skewed to the right and forms a shock which is then nicely resolved by the monotone scheme.

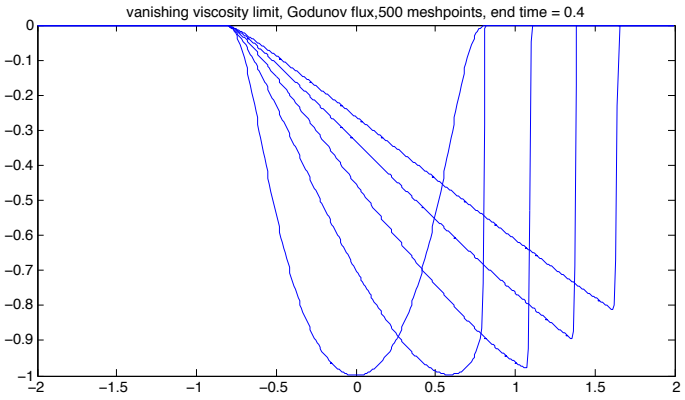

Figure 1: Entropy solution at the scalar level, computed with the Godunov finite volume scheme.

1.2 Systems of Conservation Laws

Most problems in physics are neither one-dimensional nor scalar. Therefore, we usually seek the solution $u : \mathbb{R}^d \times \mathbb{R}_{\geq 0} \to \mathbb{R}^N$ of a *multi-dimensional system of conservation laws*:

$$\begin{aligned} u_t + \nabla_x \cdot f(u) = 0, \quad x \in \mathbb{R}^d, t > 0 \\ u(x,0) = u_0(x), \quad x \in \mathbb{R}^d, \end{aligned} \tag{7}$$

where $f : \mathbb{R}^N \to \mathbb{R}^{d \times N}$ is the flux function.

In contrast to the scalar case, it is much harder to obtain (global) well-posedness results for such systems. There are some results available for one-dimensional systems ($d = 1$), see for instance [7],[1]. However, there are no global well-posedness results for generic systems in several space dimensions. Again, it is necessary to weaken the notion of solution hoping to get existence and uniqueness results.

1.2.1 Young Measures

Instead of looking at solutions $u(x,t)$ which can be exactly evaluated at each point (x,t), we turn to the concept of *measure valued solutions* introduced by DiPerna [4]. For that purpose, we have to introduce the notion of *Young measures*: For $D \subset \mathbb{R}^{k\ 1}$, we define $\mathbf{Y}(D, \mathbb{R}^N)$ to be the set of all measurable functions

$$\begin{aligned} \nu : D &\to \text{Prob}(\mathbb{R}^N), \\ y &\mapsto \nu_y. \end{aligned}$$

It can be shown that each Young measure ν can be written as a *random field* $v : D \times \Omega \to \mathbb{R}^N$ for some probability space $(\Omega, \mathcal{F}, P)$. The connection between the random field and the Young measure is given by

$$\nu_y(F) = P(\{\omega : v(y;\omega) \in F\}), \quad F \subset \mathbb{R}^N.$$

The Young measure ν is called the *law* of the random field v. Note that the class of measurable functions $u : D \to \mathbb{R}^N$ is included in the notion of Young measures since

[1] In our case, D will usually be $\mathbb{R}^d \times \mathbb{R}_{\geq 0}$.

$y \mapsto \delta_{u(y)}$ trivially defines a Young measure. Here, δ_ξ is the Dirac measure centered at $\xi \in \mathbb{R}^N$. Every Young measure that can be written as such a Dirac measure is called *atomic*.

Let g be any continuous function

$$g : \mathbb{R}^N \to \mathbb{R},$$
$$\xi = (\xi_0, \dots \xi_{N-1}) \mapsto g(\xi),$$

ν a Young measure and v the corresponding random field. We define the pairing of ν with g at y as

$$\langle \nu_y, g \rangle := \int_{\mathbb{R}^N} g(\xi) \, \mathrm{d}\nu_y(\xi)$$

which can be thought of as the expectation of the functional $g(v)$ at the point y. Having defined this pairing, we equip the set of Young measures with the topology of *narrow convergence*: ν^n is said to converge narrowly to ν (written $\nu^n \rightharpoonup \nu$) if

$$\int_D \varphi(y) \langle \nu_y^n, g \rangle \, \mathrm{d}y \to \int_D \varphi(y) \langle \nu_y, g \rangle \, \mathrm{d}y, \quad n \to \infty$$

for all $g \in C^0(\mathbb{R}^N)$ and $\varphi \in L^1(D)$.

Let v^ε be a sequence of measurable maps $D \to \mathbb{R}^N$ which converges weakly to v, i.e. $\int_D \varphi(y) v^\varepsilon(y) \, \mathrm{d}y \to \int_D \varphi(y) v(y) \, \mathrm{d}y$ for all $\varphi \in C_c^\infty(D)$. As was described by DiPerna [4], there is a subsequence such that for all continuous functions $g : \mathbb{R}^N \to \mathbb{R}$, the functionals $g(v^\varepsilon)$ also converge weakly. Moreover, there is a Young measure ν such that each of these weak limits is the pairing of ν with g, i.e. for all continuous functions g, we have

$$\int_D \varphi(y) g(v^\varepsilon(y)) \, \mathrm{d}y \to \int_D \varphi(y) \langle \nu_y, g \rangle \, \mathrm{d}y.$$

Thus, Young measures are a convenient way of describing the weak limit behavior of a sequence of functions and their functionals. The above statement is a special case of the fundamental theorem of Young measures which states that under some mild assumptions, each sequence of Young measures has a narrowly converging subsequence, see ([5], Theorem A.1).

1.2.2 Measure Valued Solutions

Coming back to systems of conservation laws, we define a Young measure $\nu \in \mathbf{Y}(\mathbb{R}^d \times \mathbb{R}_{\geq 0}, \mathbb{R}^N)$ to be a *measure valued (MV) solution* of (7) if

$$\begin{aligned} \iint_{\mathbb{R}^d \times \mathbb{R}_{\geq 0}} & \varphi_t(x,t) \langle \nu_{(x,t)}, \mathrm{id} \rangle + \nabla_x \varphi(x,t) \cdot \langle \nu_{(x,t)}, f \rangle \, \mathrm{d}x \, \mathrm{d}t \\ & + \int_{\mathbb{R}^d} \varphi(x,0) \langle \nu_{(x,0)}, \mathrm{id} \rangle \, \mathrm{d}x = 0 \end{aligned} \tag{8}$$

for all test functions $\varphi(\cdot,\cdot) \in C_c^\infty(\mathbb{R}^d \times \mathbb{R}_{\geq 0})$. Here, $\nu_{(\cdot,0)}$ is the atomic initial measure $\delta_{u_0(\cdot)}$, and therefore we have $\langle \nu_{(x,0)}, \mathrm{id} \rangle = u_0(x)$. However, there is nothing that prevents us from also allowing the initial measure $\nu_{(\cdot,0)}$ to be non-atomic. In the sequel, we shall denote this initial measure by $\sigma \in \mathbf{Y}(\mathbb{R}^d, \mathbb{R}^N)$.

Again, we have to impose certain entropy constraints hoping to enforce uniqueness of the MV solution. Let (η, q) be an entropy pair, i.e. functions $\eta : \mathbb{R}^N \to \mathbb{R}$ and

$q : \mathbb{R}^N \to \mathbb{R}^d$ such that η is convex, and $q' = \eta' \cdot f'$. We then define a MV solution ν to be an *entropy measure valued (EMV) solution* if

$$\iint_{\mathbb{R}^d \times \mathbb{R}_{\geq 0}} \varphi_t(x,t)\langle \nu_{(x,t)}, \eta\rangle + \nabla_x \varphi(x,t) \cdot \langle \nu_{(x,t)}, q\rangle \,\mathrm{d}x\,\mathrm{d}t + \int_{\mathbb{R}^d} \varphi(x,0)\langle \sigma_x, \eta\rangle \,\mathrm{d}x \geq 0 \tag{9}$$

for all non-negative test functions φ.

So far, there is no complete theory about existence and uniqueness of EMV solutions. However, as it was demonstrated in [5], there can be no uniqueness in the case of non-atomic initial data even at the scalar level. Nevertheless, we shall use the concept of non-atomic initial data for the sake of numerical computations as we shall explain below.

The question is how to find or construct MV solutions. As we discovered in the scalar case, it makes sense to add some regularizing term to the conservation law, i.e. a higher order derivative term, and then let the coefficient of this term go to zero. Thus, we get a sequence u^ε of smooth solutions. Assuming this sequence to be uniformly bounded in L^∞, we get a weakly converging subsequence. As mentioned in the previous subsection, we can then again extract a subsequence such that each functional $g(u^\varepsilon)$ converges weakly, and these weak limits can conveniently be described by a Young measure. It can then be shown that this Young measure is a MV solution. However, we expect to obtain a different MV solution for each type of regularization, and the entropy inequalities, if existing, are inherited from the regularized equation.

1.2.3 Perturbations in Numerical Computations

Suppose that a numerical scheme produces a solution $u^{\Delta x}$ such that each functional $g(u^{\Delta x})$ converges weakly. In order to compute an approximation of the corresponding Young measure, we pick a sequence $\Delta x_1 > \cdots > \Delta x_M$ and use the corresponding solutions $u^{\Delta x_1}, \dots u^{\Delta x_M}$ as samples. It turns out that in order to get enough samples for a reasonable approximation, one has to go to extremely small mesh refinements. Therefore, even though we know about the non-uniqueness of EMV solutions in the case of non-atomic initial data, we use small perturbations of the initial function in order to obtain a Young measure *for a fixed mesh size*. More precisely, the perturbation of the initial function is considered to be a random field, and doing sampling over the corresponding probability space, the numerical solution also becomes a random field. The corresponding Young measure is then taken to be the numerical approximation of the MV solution.

This perturbation approach is based on the stability of the MV solution with respect to small perturbations around atomic initial data. It is a remedy of the numerical nightmare of having to go to extremely small mesh refinements. We refer the reader to [5] where this approach was first developed and numerically tested.

1.3 Outline of Thesis

Nothing prevents us from considering MV solutions also in the scalar case. However, by a stability result that was proven in [5] and by the above mentioned theory of entropy solutions in the scalar case (section 1.1.1), we expect the EMV solution to be atomic. As a consequence of the entropy constraints, this is indeed the case. Moreover, the EMV solution turns out to be the vanishing viscosity limit (VVL). However, in contrast to diffusive regularization (e.g. vanishing viscosity), this thesis focuses on the MV solution obtained by the vanishing *dispersion* equation

$$u_t^\varepsilon + f(u^\varepsilon)_x = \varepsilon^2 u^\varepsilon_{xxx} \tag{10}$$

in the special case of Burgers' flux $f(u) = \frac{u^2}{2}$. The corresponding dispersive equation (10) is in fact the famous Korteweg-de Vries (KdV) equation. When substituting diffusion with dispersion, we lose the entropy constraints which force the EMV to be atomic. Therefore, we expect the measure valued vanishing dispersion limit (VDL) to be non-atomic. This is indeed the case and a consequence of the KdV solution being oscillatory. These KdV oscillations have a frequency of $O(\varepsilon^{-1})$ and occur after a certain *break time* which is independent of ε.

In a remarkable series of three papers [12], [13], [14], Lax and Levermore (LaL) theoretically computed the first two moments of the VDL of Burgers' equation. Motivated by their result and inspired by the numerical perturbation approach described in [5], we attempt to approximate the Young measure of the VDL with a finite difference scheme (FDS).

The outline of the thesis is as follows: We start with considering the VVL of Burgers' equation in section 2, and demonstrate the atomicity of the EMV solution both theoretically and numerically. In Chapter 3, we turn to the VDL and give a summary of the LaL theory together with a characterization of the VDL given by DiPerna [4]. This characterization is based on the KdV hierarchy of conservation laws and can be regarded as some kind of weaker entropy condition. In Chapter 4, we present an implicit FDS and prove that under some assumptions, the computed solution will satisfy DiPerna's characterization as $\Delta x \to 0$. This theoretical result is based on the FDS being implicit and diffusive. Attempting to get a reasonable approximation of the VDL, we then apply the perturbation approach and compare the computed solution with the LaL theory. To improve the numerical results, we furthermore present an almost diffusion-less Crank-Nicolson FDS in section 5. Unfortunately, we couldn't prove DiPerna's characterization for the Crank-Nicolson scheme.

Summarized, this thesis combines modern ideas arising in the numerical treatment of systems of conservation laws with the dispersive regularization of scalar conservation laws.

2 The EMV Solution of Burgers' Equation

In this section, we show that the entropy measure valued (EMV) solution at the scalar level coincides with the vanishing viscosity limit (VVL) and therefore is atomic. This is then also demonstrated numerically with the perturbation approach mentioned in subsection 1.2.3. We mainly base this section on ideas presented in [5].

2.1 The EMV Solution and Vanishing Viscosity

We consider the VVL of the scalar conservation law (1), i.e. the strong L^2-limit $u = \lim_{\varepsilon \to 0} u^\varepsilon$ where u^ε is the smooth solution of

$$u_t^\varepsilon + f(u^\varepsilon)_x = \varepsilon u_{xx}^\varepsilon. \tag{11}$$

Let (η, q) be an entropy pair so that in particular we have $q'(u) = f'(u)\eta'(u)$. Multiplying (11) with $\eta'(u^\varepsilon)$, we obtain the entropy property

$$\begin{aligned} \eta(u^\varepsilon)_t + q(u^\varepsilon)_x &= \varepsilon u_{xx}^\varepsilon \eta'(u^\varepsilon) \\ &= \varepsilon \eta(u^\varepsilon)_{xx} - \varepsilon \eta''(u^\varepsilon)(u_x^\varepsilon)^2 \\ &\leq \varepsilon \eta(u^\varepsilon)_{xx}, \end{aligned} \tag{12}$$

where the last step is due to the convexity of η. Note that the right hand side vanishes in the sense of distributions. It can be shown that the strong L^2-limit $u = \lim_{\varepsilon \to 0} u^\varepsilon$ exists which gives existence of an entropy solution of the scalar conservation law (1) because u inherits all entropy constraints from the above inequality (12). Furthermore,

as was shown by Kruzkhov [9], these entropy constraints make the entropy solution unique.

In the language of measure valued solutions, we can say that the measure valued VVL is atomic as a consequence of the strong L^2-convergence of u^ε to the entropy solution. However, we have to ask the question if the *EMV solution* subject to atomic initial data coincides with the VVL, i.e. if the EMV solution is atomic and coincides with the entropy solution. As was shown in ([5], Theorem 3.3), this is indeed the case. We reproduce this result together with the proof for the one-dimensional case $d = 1$:

Theorem 2.1.1 ([5], Theorem 3.3)**.** *Consider the scalar one-dimensional case $N = d = 1$. Let $u_0 \in L^\infty(\mathbb{R})$ and let $\sigma \in \mathbf{Y}(\mathbb{R}, \mathbb{R})$ be uniformly bounded, i.e. there exists a compact set $K \subset \mathbb{R}$ such that for all $x \in \mathbb{R}$: $supp(\sigma_x) \subset K$. Let $u \in L^\infty(\mathbb{R}\times\mathbb{R}_{\geq 0})$ be the entropy solution of the scalar conservation law* (1) *with initial data u_0. Furthermore, let ν be* any *EMV solution of* (1) *which attains the initial MV data σ in the sense*

$$\lim_{T\to 0} \frac{1}{T} \int_0^T \int_{\mathbb{R}} |\langle \nu_{(x,t)}, |\xi - u(x,t)|\rangle - \langle \sigma_x, |\xi - u_0(x)|\rangle| \,\mathrm{d}x \,\mathrm{d}t = 0.$$

Then, for all $t > 0$, we have the stability estimate

$$\int_{\mathbb{R}} \langle \nu_{(x,t)}, |u(x,t) - \xi|\rangle \,\mathrm{d}x \leq \int_{\mathbb{R}} \langle \sigma_x, |u_0(x) - \xi|\rangle \,\mathrm{d}x.$$

In particular, if $\sigma = \delta_{u_0(\cdot)}$, then $\nu = \delta_{u(\cdot,\cdot)}$.

Proof. We follow DiPerna [4] who proved the uniqueness of scalar EMV solutions subject to atomic initial data.

For $\xi \in \mathbb{R}$, let $(\eta(\xi, u), q(\xi, u))$ be the Kruzkhov entropy pair, defined as

$$\eta(\xi, u) := |\xi - u|, \quad q(\xi, u) := \operatorname{sgn}(\xi - u)(f(\xi) - f(u)).$$

By ([4], Theorem 4.1) we know that for any entropy solution u and any EMV solution ν of (1), we have

$$\int_{\mathbb{R}_{\geq 0}} \int_{\mathbb{R}} \varphi_t(x,t)\langle \nu_{(x,t)}, \eta(\xi, u(x,t))\rangle + \varphi_x(x,t)\langle \nu_{(x,t)}, q(\xi, u(x,t))\rangle \,\mathrm{d}x \,\mathrm{d}t \geq 0$$

for all test functions $0 \leq \varphi \in C_c^1(\mathbb{R} \times \mathbb{R}_{\geq 0})$. In particular the function

$$V(t) := \int_{\mathbb{R}} \langle \nu_{(x,t)}, |\xi - u(x,t)|\rangle \,\mathrm{d}x$$

is non-increasing. By hypothesis, the point $t = 0$ is a Lebesgue point for V, so $\lim_{t\to 0} V(t) = \int_{\mathbb{R}} \langle \sigma_x, |u_0(x) - \xi|\rangle \,\mathrm{d}x$. The result follows. □

This Theorem in particular proves that the EMV solution is atomic when subject to atomic initial data. Therefore, we see that the entropy constraints are forcing the EMV solution to be atomic and to coincide with the VVL.

2.2 Numerical Experiments

In this section which is a generalization of section 1.1.2, we present a numerical algorithm proposed in [5] to compute EMV solutions of conservation laws. We apply this algorithm to a monotone finite volume scheme at the scalar level and demonstrate the atomicity of the EMV solution numerically.

Finite Volume Scheme We discretize space into cells $\mathcal{C}_j = [x_{j-1/2}, x_{j+1/2})$ of size Δx and time into cells $[t_n, t_{n+1})$ of size Δt. The mesh widths Δx and Δt are linked via the CFL-number $\lambda = \frac{\Delta t}{\Delta x}$. The cell averages $\frac{1}{\Delta x}\int_{\mathcal{C}_j} u(x,t_n)\,\mathrm{d}x$ are approximated by the explicit scheme

$$\frac{u_{j,n+1}-u_{j,n}}{\Delta t} + \frac{F_{j+1/2,n}-F_{j-1/2,n}}{\Delta x} = 0$$

where $F_{j+1/2,n} = F_{j+1/2,n}(u_{j,n}, u_{j,n+1})$ is the numerical flux. As in subsection 1.1.2, we choose the Godunov flux

$$F(u_j, u_{j+1}) = \begin{cases} \min_{u_j \le \theta \le u_{j+1}} f(\theta) & \text{if } u_j \le u_{j+1} \\ \max_{u_{j+1} \le \theta \le u_j} f(\theta) & \text{if } u_j \ge u_{j+1} \end{cases}$$

which is both consistent and monotone. The resulting function $u^{\Delta x}(x,t)$ is defined to be piecewise constant, i.e.

$$u^{\Delta x}(x,t) = u_{j,n}, \quad (x,t) \in \mathcal{C}_j \times [t_n, t_{n+1}).$$

A consistent and monotone scheme such as the Godunov scheme satisfies some nice properties which imply convergence to the entropy solution: First, it satisfies a discrete maximum principle and thus, $u^{\Delta x}$ is uniformly bounded in L^∞. Second, it is TVD, i.e. the total variation of $u^{\Delta x}(\cdot,t)$ is non-increasing over time. Third, it satisfies discrete entropy inequalities using the Crandall-Majda numerical entropy fluxes [2].

Perturbation Algorithm To compute the MV solution associated to any numerical scheme, one has to consider the weak limits of $u^{\Delta x}$ and its functionals $g(u^{\Delta x})$ as $\Delta x \to 0$ and find the Young measure which characterizes these weak limits.[2] However, this is numerically very inefficient since the mesh sizes that are required in order to get a reasonable approximation are immensely small. We therefore follow [5] where the following algorithm ([5], Algorithm 4.6 and 4.8), based on perturbation of the initial function, is presented:

1. Let $(\Omega, \mathcal{F}, P)$ be a probability space. Fix $\varepsilon > 0$ and let $u_0^\varepsilon(\cdot,\cdot)$ be a random field $\mathbb{R}^d \times \Omega \to \mathbb{R}$ such that $||u_0^\varepsilon(\cdot;\omega) - u_0(\cdot)||_{L^1(\mathbb{R}^d)} \le \varepsilon$ for P-almost every ω.
2. Pick a random sample of M drawings of $u_0^\varepsilon(\cdot;\omega)$, denoting them by $u_0^{\varepsilon,k}(\cdot)$, $k = 1, \dots, M$.
3. Choose a numerical method (i.e. a finite volume scheme) and compute the numerical approximation $u^{\varepsilon,\Delta x,k}(\cdot,\cdot)$ for each sample $k = 1, \dots, M$.
4. Compute the approximated MV solution as

$$\nu^{\varepsilon,\Delta x,M}_{(x,t)} := \frac{1}{M}\sum_{k=1}^{M} \delta_{u^{\varepsilon,\Delta x,k}(x,t)}.$$

If the chosen numerical scheme satisfies the following properties:

1. *Uniform boundedness:*

$$||u^{\varepsilon,\Delta x,k}||_{L^\infty(\mathbb{R}^d \times \mathbb{R}_{\ge 0})} \le C, \quad \forall \omega, \varepsilon, \Delta x,$$

2. *Weak BV* (case $d = 1$): There exists $1 \le r < \infty$ such that

$$\lim_{\Delta x \to 0} \int_0^T \sum_j |u^{\varepsilon,\Delta x,k}(x_{j+1},t) - u^{\varepsilon,\Delta x,k}(x_j,t)|^r \Delta x\,\mathrm{d}t = 0, \quad \forall \omega,$$

[2] Since it can be shown that consistent and monotone schemes converge strongly at the scalar level, we immediately conclude that the resulting measure must be atomic. However, for the sake of illustrating the perturbation approach, we don't use this result here.

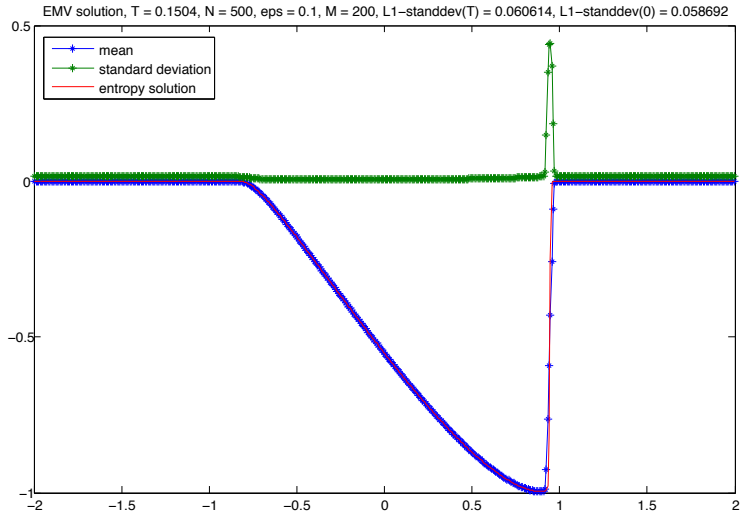

Figure 2: EMV solution (mean and standard deviation) at the scalar level, computed with the perturbation algorithm of [5] with the Godunov finite volume scheme.

3. *Discrete entropy inequality* (case $d = 1$): For an entropy pair (η, q), there is a numerical entropy flux $Q_{j+1/2,n}(u_{j,n}, u_{j+1,n})$ consistent with the entropy flux q such that

$$\frac{\eta(u_{j,n+1}) - \eta(u_{j,n})}{\Delta t} + \frac{Q_{j+1/2,n} - Q_{j-1/2,n}}{\Delta x} \leq 0, \quad \forall j, n, \omega,$$

then it can be shown that there is subsequence $(\Delta x, \varepsilon, M) \to (0, 0, \infty)$ such that $\nu^{\varepsilon,\Delta x,M}$ converges narrowly to an EMV solution of the corresponding conservation law. At the scalar level, the above three properties are satisfied by any consistent and monotone finite volume scheme.

The major advantage of the above algorithm is that for a reasonably small but fixed Δx, we can perform the above described perturbation and sampling process without having to go to extremely small mesh sizes, yet still obtain a good approximation. The computational cost of doing more sampling is increasing linearly whereas the computational cost of going to smaller mesh sizes grows at least quadratically (this follows from the CFL-condition).

We use the same smooth, non-positive one-bump initial function as in section 1.1.2 and perturb it by the random field $u_0(x;\omega) = u_0(x) + \omega\,\varepsilon$ with probability space $\Omega = [-1, 1]$ and uniform probability distribution. We show the numerical result for

$$\begin{aligned} N &= 500 \text{ mesh points}, \\ \text{CFL-number } \lambda &= 0.1, \\ \text{end time } T &= 0.15, \\ \text{perturbation level } \varepsilon &= 0.1 \text{ and} \\ \text{sample number } M &= 200 \end{aligned}$$

in figure 2. We observe that the L^1-norm of the standard deviation at $t = 0$ and $t = T$ is almost identical which is a strong indication that the computed approximation indeed converges to an atomic limit measure. However, we observe a narrow peak of

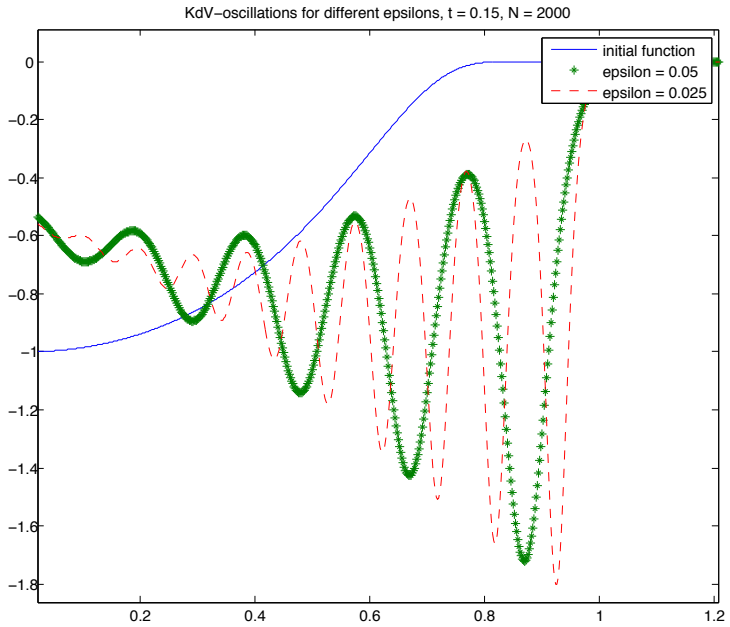

Figure 3: KdV solution for different ε, computed with the Crank-Nicolson FDS (62).

the standard deviation near the shock of the entropy solution. This can be explained by the fact that perturbations cause the solution to be shifted in space. Since we can at best hope for convergence in L^1, such a narrow peak is perfectly acceptable.

3 The Vanishing Dispersion Limit of Burgers' Equation

So far, we have seen that diffusive regularization (e.g. vanishing viscosity) at the scalar level forces the MV solution to be atomic as a consequence of the entropy constraints. Now, we turn to dispersive regularization in the special case of Burgers' equation. In order to conform to Lax and Levermore (LaL) [12], we adjust the flux function to be $f(u) = -3u^2$ and reverse the sign of the dispersive term so that our regularized equation finally is

$$u_t - 6uu_x + \varepsilon^2 u_{xxx} = 0. \tag{13}$$

This is in fact the famous Korteweg-de Vries (KdV) equation. From numerical computations, we know that the solution of KdV forms oscillations after a certain *break time*. The frequency of these oscillations is $O(\varepsilon^{-1})$ whereas the amplitude is independent of ε, see figure 3. Therefore, we may expect the VDL which is the narrow limit $\delta_{u(\cdot,\cdot)} \rightharpoonup \nu$ of equation (13) to be non-atomic.

LaL [12] computed the first two moments (i.e. mean and variance) of this limit measure ν theoretically. In section 3.1, we shall give a short summary of their work as far as it is relevant for our purpose. Since the LaL theory doesn't provide simple computable formulas, we shall discuss a numerical method developed by McLaughlin and Strain [15] to reproduce the LaL result approximatively in section 3.2. This will be

needed later in order to numerically test our finite difference schemes. Even though we lose infinitely many entropy constraints when substituting diffusion with dispersion, DiPerna [4] described a characterization of the VDL which is based on the infinite KdV hierarchy of conservation laws (reviewed in section 3.3) and which we shall present in section 3.4. This characterization can be regarded as some kind of weaker entropy condition and will be used it in section 4 to theoretically justify the implicit FDS.

3.1 Review of Lax and Levermore Theorie

In this section, we summarize some of the theoretical work done by LaL [12] who computed the first two moments of the VDL of Burgers' equation, i.e. the distributional limits $u(x,t;\,\varepsilon) \overset{*}{\to} \overline{u}$ and $u^2(x,t;\,\varepsilon) \overset{*}{\to} \overline{u^2}$ where $u(x,t;\,\varepsilon)$ is the KdV solution of equation (13).

The main tool used in the following theoretical considerations is the *inverse scattering method* which was first described in [6]: To each solution $u(x,t;\,\varepsilon)$ of KdV (13), we associate a one-parameter family of Schrödinger operators

$$\mathcal{L}(t) := -\,\varepsilon^2\partial_x^2 + u(x,t;\,\varepsilon).$$

If $u(x,t;\,\varepsilon)$ evolves according to the KdV equation, the eigenvalues of the operator $\mathcal{L}(t)$ are integrals of motion. Moreover, for each such $\mathcal{L}(t)$, we can define *scattering data* which consists of

1. the reflection coefficients $R(k)$,
2. the eigenvalues $-\eta_n^2, \quad n = 1,\dots,N(\,\varepsilon)$ and
3. the norming constants c_n associated to the eigenfunctions f_n of $\mathcal{L}(t)$.

Here, the number of eigenvalues $N(\,\varepsilon)$ is given by

$$N(\,\varepsilon) \cong \frac{1}{\varepsilon\pi}\Phi(0)$$

where

$$\Phi(\eta) := \operatorname{Re}\int_{-\infty}^{\infty}\sqrt{-u_0(y)-\eta^2}\,\mathrm{d}y.$$

The scattering data evolves in time in a surprisingly simple manner:

$$\begin{aligned} R(k,t) &= R(k)e^{4ik^3t/\,\varepsilon},\\ \eta_n(t) &= \eta_n,\\ c_n(t) &= c_n e^{4\eta_n^3 t/\,\varepsilon}. \end{aligned}$$

The crucial point is that one can reconstruct the solution $u(x,t;\,\varepsilon)$ from the scattering data. In particular, if all reflection coefficients $R(k)$ vanish, Kay and Moses gave the following formula for the solution $u(x,t;\,\varepsilon)$:

$$u(x,t;\,\varepsilon) = \partial_x^2 W(x,t;\,\varepsilon), \tag{14}$$

where

$$\begin{aligned} W(x,t;\,\varepsilon) &= -2\,\varepsilon^2\log\det(I+G(x,t;\,\varepsilon)),\\ G(x,t;\,\varepsilon) &= \varepsilon\left(\frac{e^{-(\eta_n x+\eta_m x)/\,\varepsilon}}{\eta_n+\eta_m}c_nc_m\right)_{n,m=1}^{N}. \end{aligned}$$

In order to make the reflection coefficients vanish, we have to choose the initial function $u_0(x)$ to be non-positive, C^1-smooth, decaying to 0 sufficiently fast as $x \to$

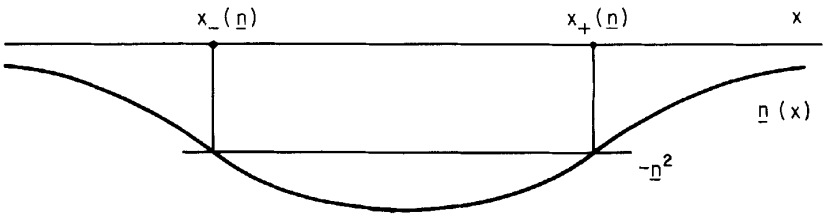

Figure 4: Definition of $x_\pm(\eta)$, ([12], Figure 1).

∞, and to have only one critical point x_0. For simplicity, we require $u_0(x_0) = -1$. Moreover, we then have to replace the exact scattering data of $u_0(x)$ with a WKB scattering data which has the property that the corresponding initial function $u_0(x;\,\varepsilon)$ converges to $u_0(x)$ strongly in L^2 as $\varepsilon \to 0$. In particular, the WKB scattering data is given as follows:

$$\begin{aligned} R(k) &= 0 \quad \forall k, \\ N(\varepsilon) &= \left\lceil \frac{1}{\varepsilon\pi}\Phi(0) \right\rceil, \\ \Phi(\eta_n) &= \left(n - \frac{1}{2}\right)\varepsilon\pi, \\ c_n &= e^{\theta_+(\eta_n)/\varepsilon}, \quad n = 1, \dots N(\varepsilon) \end{aligned}$$

where

$$\theta_+(\eta) := \eta x_+(\eta) + \int_{x_+(\eta)}^{\infty} \eta - (\eta^2 + u_0(y))^{1/2}\,\mathrm{d}y$$

and where $x_\pm(\eta)$ are defined by requiring

$$u_0(x_\pm(\eta)) = -\eta^2, \quad x_-(\eta) \le 0 \le x_+(\eta).$$

This is well defined because of the special structure of $u_0(x)$, see figure 4. Furthermore, we define the following two functions which we will need below:

$$\begin{aligned} \phi(\eta) &:= \int_{x_-(\eta)}^{x_+(\eta)} \frac{\eta}{(-u_0(y) - \eta^2)^{1/2}}\,\mathrm{d}y, \\ a(\eta, x, t) &:= \eta x - 4\eta^3 t - \theta_+(\eta). \end{aligned} \tag{15}$$

Coming back to the explicit formulas (14) ff., we write the determinant $\det(I + G)$ as

$$\det(I + G) = \sum_S \det(G_S)$$

where the sum ranges over all index subsets $S \subset \{1, \dots, N\}$ and where G_S is the principal minor of G with indices in S. It is then shown that this sum is dominated by its largest term. The corresponding approximation of $W(x, t;\,\varepsilon)$ is denoted by $Q^*(x, t;\,\varepsilon)$ and is the solution of a minimization problem. LaL then show that the locally uniform limit $Q^*(x, t) = \lim_{\varepsilon\to 0} Q^*(x, t;\,\varepsilon)$ exists and can also be characterized by a minimization problem. More precisely, we have the following

Theorem 3.1.1 (LaL [12], Theorem 2.2)**.**

$$\lim_{\varepsilon\to 0} Q^*(x, t;\,\varepsilon) = Q^*(x, t)$$

uniformly on compact subsets of x, t, where

$$Q^*(x,t) = \min\{Q(\psi; x, t) : \psi \in A\};$$

the admissible set A consisting of all Lebesgue measurable functions ψ on $[0,1]$,

$$0 \le \psi(\eta) \le \phi(\eta), \tag{16}$$

and $Q(\psi; x, t)$ denoting the quadratic form

$$\begin{aligned} Q(\psi; x, t) = \frac{4}{\pi} \int_0^1 a(\eta, x, t)\psi(\eta)\,\mathrm{d}\eta \\ - \frac{1}{\pi^2} \int_0^1 \int_0^1 \log\left(\frac{\eta-\mu}{\eta+\mu}\right)^2 \psi(\mu)\psi(\eta)\,\mathrm{d}\mu\,\mathrm{d}\eta. \end{aligned} \tag{17}$$

Finally, we have the following Theorem which characterizes the first two moments of the VDL:

Theorem 3.1.2 (LaL [12], Theorem 2.10 and 2.11)**.** *Let $u(x,t;\varepsilon)$ be the solution of the KdV equation 13 with initial WKB data $u_0(x;\varepsilon)$; then the distributional limits*

$$\begin{aligned} u(x,t;\varepsilon) &\overset{*}{\to} \overline{u}(x,t), \\ u^2(x,t;\varepsilon) &\overset{*}{\to} \overline{u^2}(x,t) \end{aligned}$$

exist, and

$$\begin{aligned} \overline{u}(x,t) &= \partial_{xx} Q^*(x,t), \\ \overline{u^2}(x,t) &= \frac{1}{3}\partial_{xt} Q^*(x,t). \end{aligned}$$

3.2 Numerical Method of McLaughlin and Strain

The numerical approach presented here is a simplified version of the method developed by McLaughlin and Strain [15]. The idea is to solve the minimization problem posed in Theorem 3.1.1 on a finite dimensional subspace $S_N \subset L^1(0,1)$ to get an approximation of the minimizing function $\psi(\eta)$. But unlike McLaughlin and Strain who choose S_N to be the space of continuous, piecewise linear functions, we choose it to be the space of piecewise constant functions.

3.2.1 The Method

We discretize the interval $[0,1]$ into N cells $[\eta_{i-1}, \eta_i), i = 1, \dots, N$ of size $\Delta\eta = \frac{1}{N}$. Let $S_N \subset L^1(0,1)$ denote the set of piecewise constant functions on this grid, and let $\psi^{\Delta\eta}(\eta)$ denote a function in S_N, i.e.

$$\psi^{\Delta\eta}(\eta) = \psi_i, \quad \eta \in [\eta_{i-1}, \eta_i).$$

Furthermore, denote by $\underline{\psi} := (\psi_i)_i$ the vector of the piecewise constant values corresponding to the function $\psi^{\Delta\eta}$. Assuming that we can evaluate the function $a(\eta, x, t)$ (see (15)) exactly,[3] we can compute the entries of a $N \times N$-matrix L and of a vector $\underline{a}$ such that

$$Q(\psi^{\Delta\eta}; x, t) = \underline{a}^T \underline{\psi} - \underline{\psi}^T L \underline{\psi} =: Q_N(\underline{\psi}) \tag{18}$$

[3]This is actually not true in our case, but $\theta_+(\eta)$ and thus also $a(\eta, x, t)$ can be computed by very accurate numerical integration.

(see (17) of Theorem 3.1.1) exactly. We then have to solve the following *finite dimensional minimization problem*:

$$\underline{\psi}^* := \operatorname{argmin}\{Q_N(\underline{\psi}) : 0 \le \psi_i \le \phi_i, i = 1, \dots, N\}$$

where $\phi_i := \phi(\eta_{i-1/2}), \eta_{i-1/2} := \frac{\eta_{i-1}+\eta_i}{2}$.

Our major concern is to find the regions where $\underline{\psi}^*$ meets the constraints $0 \le \psi_i^* \le \phi_i$. Let A denote the set of indices i such that $\psi_i^* = 0$ and B the set of indices such that $\psi_i^* = \phi_i$. Furthermore, define $C := A \cup B, I = \{1, \dots N\} \backslash C$ and introduce the following notation:

$$\begin{aligned} \underline{\psi}_X &:= (\psi_i)_{i \in X}, \quad X \subset \{1, \dots, N\}, \\ \underline{a}_X &:= (a_i)_{i \in X}, \quad X \subset \{1, \dots, N\}, \\ L_{XY} &:= L_{i \in X, j \in Y}, \quad X, Y \subset \{1, \dots, N\}. \end{aligned}$$

Suppose for the moment that we know the sets A and B in which case we can find $\underline{\psi}^*$ by the following stationary-point-equation:

$$\partial_{\underline{\psi}_I^*} Q_N(\underline{\psi}^*) = 0. \tag{19}$$

Note that this is a linear equation: Since we can rearrange the indices such that

$$L = \begin{pmatrix} L_{II} & L_{IC} \\ L_{CI} & L_{CC} \end{pmatrix}, \quad \underline{\psi} = \begin{pmatrix} \underline{\psi}_I \\ \underline{\psi}_C \end{pmatrix}, \quad \underline{a} = \begin{pmatrix} \underline{a}_I \\ \underline{a}_C \end{pmatrix},$$

we find by expanding (18) that

$$\begin{aligned} Q_N(\underline{\psi}) = \underline{a}_I^T \underline{\psi}_I + \underline{a}_C^T \underline{\psi}_C \\ - \underline{\psi}_I^T L_{II} \underline{\psi}_I - 2\underline{\psi}_C^T L_{CI} \underline{\psi}_I - \underline{\psi}_C^T L_{CC} \underline{\psi}_C, \end{aligned}$$

and therefore

$$\partial_{\underline{\psi}_I} Q_N(\underline{\psi}) = \underline{a}_I^T - 2\underline{\psi}_C^T L_{CI} - 2\underline{\psi}_I^T L_{II}.$$

The crucial issue therefore is how to find the sets A and B. First note that the following inequalities must be satisfied componentwise:

$$\partial_{\underline{\psi}_A^*} Q_N(\underline{\psi}^*) > 0, \quad \partial_{\underline{\psi}_B^*} Q_N(\underline{\psi}^*) < 0, \tag{20}$$

which is actually a consequence of the positive definiteness of the operator L. McLaughlin and Strain [15] now developed the following algorithm to construct A, B iteratively: We start with an initial guess for A, B and $\underline{\psi}$. Then, we solve equation (19) to compute $\underline{\psi}_I$ of the new iterate. There are two cases that can occur now: Either $\underline{\psi}$ is admissable, $0 \le \psi_i \le \phi_i, i \in I$, or not. In the first case, we check whether A, B satisfy the correct signs (20). If this is the case, we are done and the iteration stops. If not, we remove the index $i \in C = A \cup B$ for which $\partial_{\psi_i} Q_N(\underline{\psi})$ is furthest from correct[4] from the set C and add it to I. In the second case where $\underline{\psi}_I$ is not admissable, we interpolate between the old and new iterate as far as possible towards the new iterate until a constraint is met. The index for which this happens is then added to A resp. B, and the interpolation becomes the new iterate.

So far, we have computed an approximation for $Q^*(x,t)$ as described in Theorem 3.1.1 which we shall denote by $Q_N^*(x,t)$. In order to approximate $\overline{u}$ and $\overline{u^2}$, we have to numerically differentiate $Q_N^*(x,t)$, see Theorem 3.1.2. We do this by using

[4] i.e. among those $\partial_{\psi_i} Q_N(\underline{\psi}), i \in C$ for which the sign is not correct, we choose the one with the largest absolute value.

finite difference quotients in x and t. More precisely, we choose $(x_{-1}, x_0, x_1) := (x - \Delta x, x, x + \Delta x), (t_{-1}, t_0, t_1) := (t - \Delta t, t, t + \Delta t)$ and compute

$$\overline{u} \approx \frac{Q_N^*(x_1, t_0) - 2Q_N^*(x_0, t_0) + Q_N^*(x_{-1}, t_0)}{\Delta x^2},$$
$$\overline{u^2} \approx \frac{1}{3} \frac{Q_N^*(x_1, t_1) - Q_N^*(x_{-1}, t_1) - (Q_N^*(x_1, t_{-1}) - Q_N^*(x_{-1}, t_{-1})}{4\Delta x \Delta t}.$$

The numerical difficulty arising at this point is the fact that the numerical error $|Q^*(x,t) - Q_N^*(x,t)|$ essentially gets divided by Δx^2 resp. $\Delta x \Delta t$. This is why one has to be careful not to choose $\Delta x, \Delta t$ too small.

We close this subsection by emphasizing one important aspect of the McLaughlin algorithm: it is a *local* method, i.e. for each (x,t), a different minimization problem has to be solved. This is a major numerical drawback which we try to avoid when applying a FDS.

3.2.2 Numerical Experiments

We use the same initial function as in subsection 1.1.2 and show the resulting minimizing $\underline{\psi}^*$ for

$$N = 200,$$
$$(x,t) = (0.5, 0.15)$$

in figure 5. One can clearly see the regions A and B where $\psi_i = 0$ resp. $\psi_i = \phi_i$. Furthermore, we show the resulting approximation of the mean and standard deviation at $t = 0.15$ and with

$$N = 200,$$
$$\Delta x = 0.02,$$
$$\Delta t = 0.01$$

in figure 6. We see that the non-atomicity is propagating out of the shock to the left.

In section 7 of [14], LaL explicitly computed some numerical values of the mean and variance of the VDL at $t = 1$ with Riemann initial data

$$u_0^{step}(x) = \begin{cases} -1 & \text{if } x < 0, \\ 0 & \text{if } x \geq 0. \end{cases} \tag{21}$$

This is clearly not a function for which the LaL requirements are satisfied. In order to nevertheless use the explicit LaL values as a reference to test our simplified method of McLaughlin and Strain, we instead use a smooth function for which the LaL requirements are satisfied and which approximates the step function (21) in a reasonably large domain. More precisely, we choose some $l > 0$ and construct smooth one-bump cut-off-functions $u_0^\delta(x)$ such that

$$||u_0^{step} - u_0^\delta||_{L^1(-l,\infty)} \to 0, \quad \delta \to 0.$$

We set

$$N = 100,$$
$$\Delta x = 0.02,$$
$$\Delta t = 0.01$$

and show the resulting mean and standard deviation together with the LaL explicit values and the approximating initial functions corresponding to $l = 6$ and $l = 9$ in figure 7. On the right hand side of the plots, the LaL values and our computed solutions coincide very well. On the left hand side, we can observe the truncation error that arises because we cut off the Riemann initial data at $x = -l$. Obviously, this truncation error is worse for $l = 6$ then it is for $l = 9$.

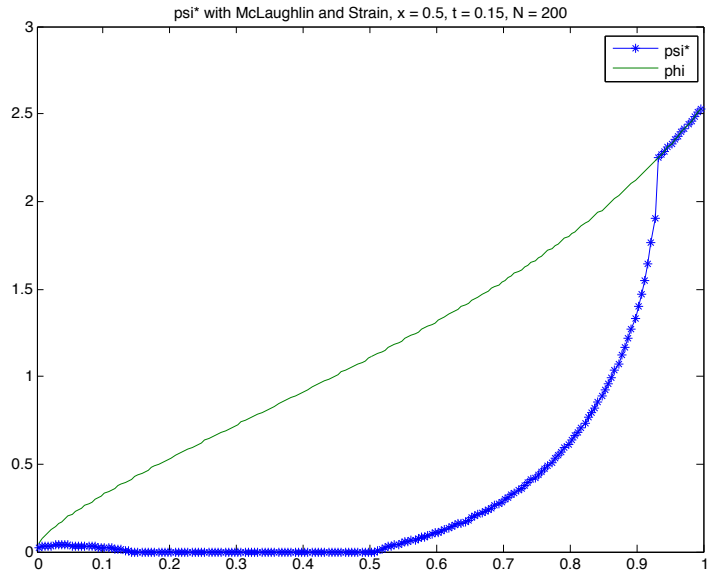

Figure 5: Minimizing function ψ^* as computed with the simplified method of McLaughlin and Strain.

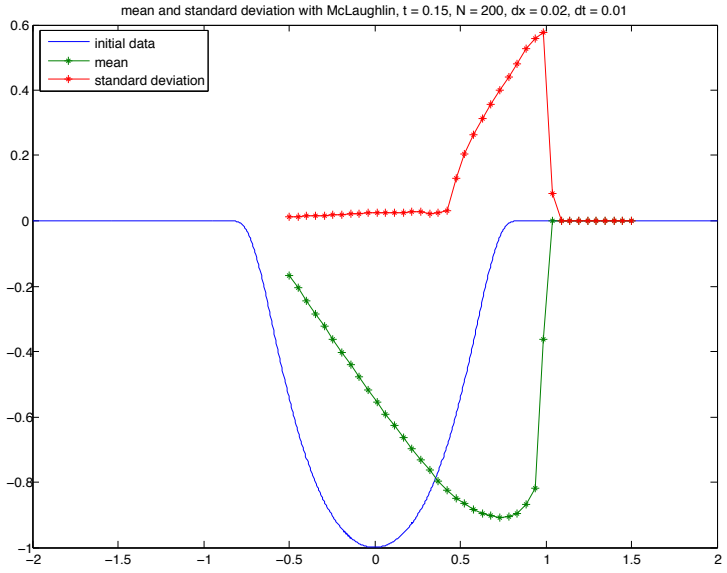

Figure 6: Mean $\overline{u}$ and standard deviation $\sqrt{\overline{u^2} - \overline{u}^2}$ of the VDL, computed with the simplified method of McLaughlin and Strain.

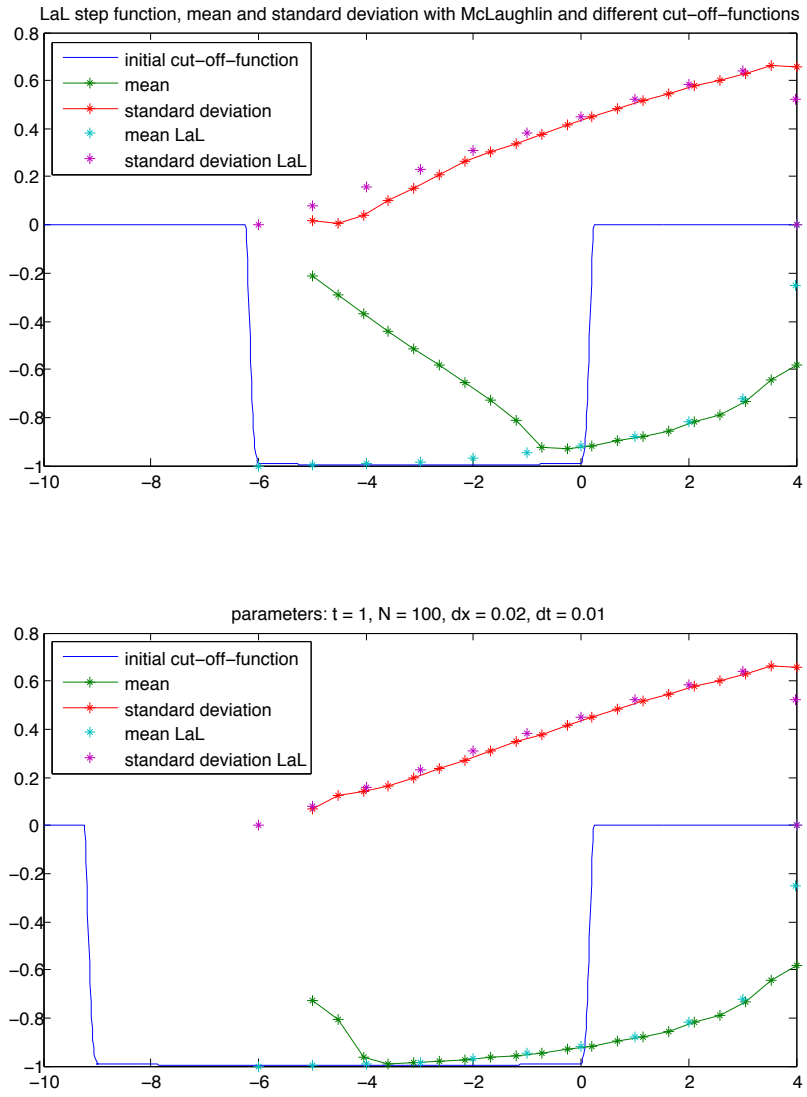

Figure 7: Mean and standard deviation of the VDL with Riemann initial function (21), computed with the simplified method of McLaughlin and Strain and different cut-off-functions and compared to the explicit values of LaL ([14], section 7).

3.2.3 Stability of the VDL w.r.t. Perturbation of Initial Data

There is no mathematical proof of whether the VDL is stable with respect to small perturbation around atomic initial data. In this subsection, we present numerical indication that this is indeed the case. We use the same initial function $u_0(x)$ as in subsection 1.1.2 and perturb it such that the LaL requirements are still satisfied. We use the following two different types of perturbations:

$$u_0^{\delta,(1)}(x) := u_0(x) + \delta u_0(2x+1) + \delta u_0(2x-1),$$
$$u_0^{\delta,(2)}(x) := u_0((1-\delta)x).$$

We then apply the simplified method of McLaughlin and Strain to the original and to the perturbed function using the same setting as in figure 6. In figures 8 and 9, we plot the L^1-errors of the mean and standard deviation against the L^1-norms of the perturbation. We observe that as the perturbation level tends to zero, also the mean and standard deviation of the perturbed problem are converging to the solution of the original problem. This indicates that the VDL is stable with respect to small perturbation around atomic initial data.

3.3 Aside: The KdV Hierarchy of Conservation Laws

It is well-known that the KdV equation (13) possesses infinitely many *integrals of motion*, i.e. there are infinitely many distinct polynomials $p_n(u, u_x, u_{xx}, \dots)$ of the KdV solution u and its x-derivatives such that $\int_{\mathbb{R}} p_n(u, u_x, u_{xx}, \dots)\,\mathrm{d}x$ is a conserved quantity. In fact, for every such polynomial p_n, there is a polynomial $q_n(u, u_x, u_{xx}, \dots)$ such that

$$\partial_t p_n + \partial_x q_n = 0, \quad n = 0, 1, 2, \dots. \tag{22}$$

This is sometimes also referred to as the *KdV hierarchy of conservation laws*. We call the polynomials p_n *conserved densities* and q_n the corresponding *fluxes*. We will need these KdV conservation laws in order to precisely discribe DiPerna's characterization of the VDL in the following section 3.4.

3.3.1 Summary of Miura et al

The following is a summary of the work of Miura et al done in [16]. It is a formal argument on how to construct infinitely many integrals of motion for the KdV equation.

Together with the KdV equation (13), we shall also consider the equation

$$v_t - 6v^2 v_x + \varepsilon^2 v_{xxx} = 0. \tag{23}$$

The connection between (23) and (13) is the following remarkable non-linear transformation: If v satisfies (23), then

$$u := v^2 \pm \varepsilon v_x \tag{24}$$

satisfies (13). Indeed, a direct calculation shows that

$$u_t - 6uu_x + \varepsilon^2 u_{xxx} = (2v \pm \varepsilon\partial_x)(v_t - 6v^2 v_x + \varepsilon v_{xxx}).$$

For a generalization of this connection between (13) and (23), we now introduce

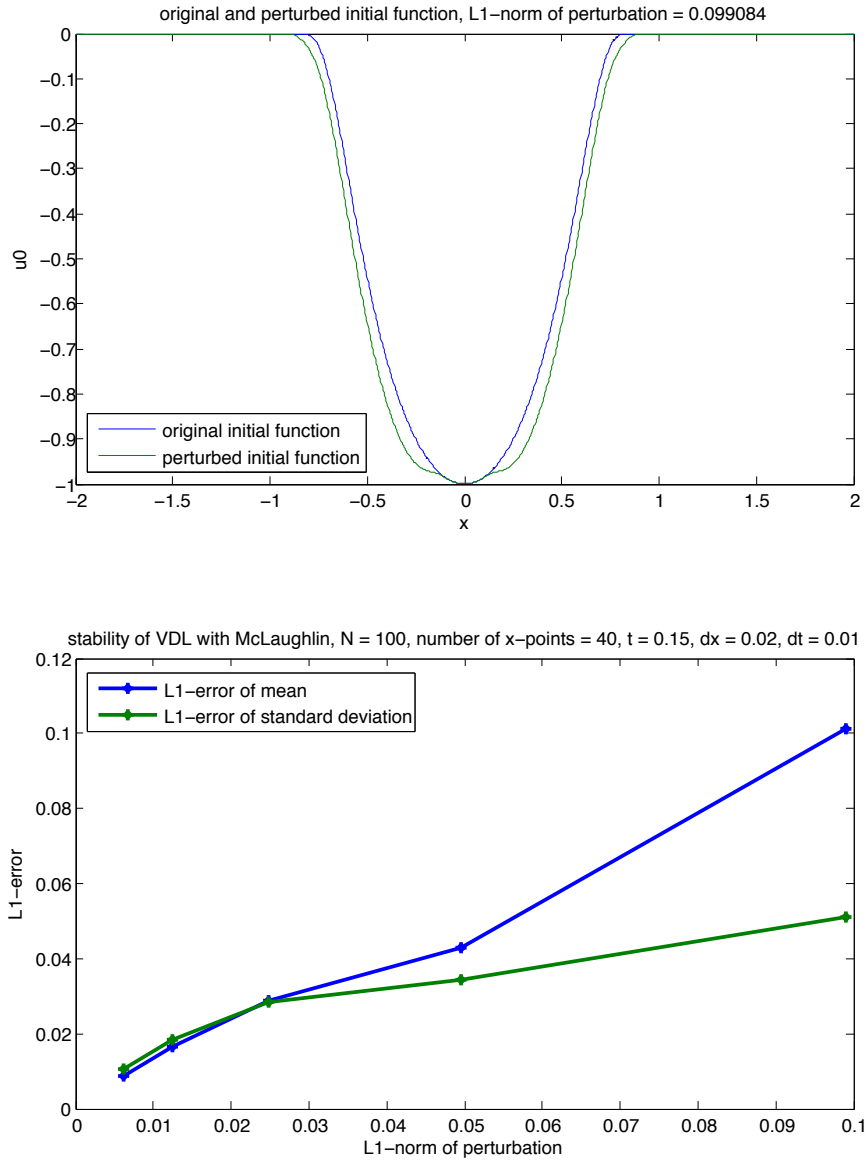

Figure 8: Stability check with simplified method of McLaughlin and Strain, first type of perturbation: Error plot for the mean and standard deviation.

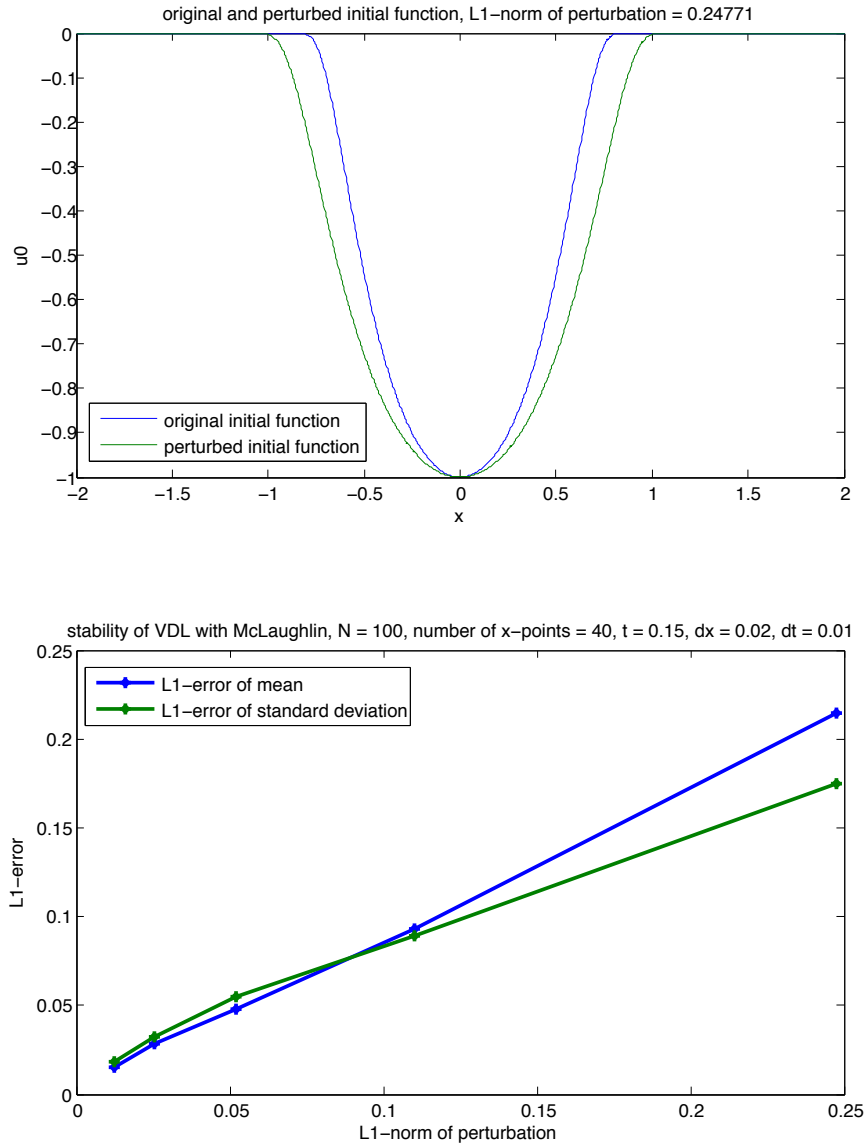

Figure 9: Stability check with simplified method of McLaughlin and Strain, second type of perturbation: Error plot for the mean and standard deviation.

the following transformation:

$$\begin{aligned} t' &= t \\ x' &= x + \frac{6}{\xi^2} t \\ u(x,t) &= u'(x',t') + \frac{1}{\xi^2} \\ v(x,t) &= \frac{\xi}{2} v'(x',t') + \frac{1}{\xi}. \end{aligned}$$

Then, equations (13) and (23) transform into

$$u'_{t'} - 6u'u'_{x'} + \varepsilon^2 u'_{x'x'x'} = 0 \tag{25}$$

and

$$\begin{aligned} & v'_{t'} - \frac{3\xi^2}{2} v'^2 v'_{x'} - 6v'v'_{x'} + \varepsilon^2 v'_{x'x'x'} = 0. \\ \Rightarrow\ & v'_{t'} + \left(-\frac{\xi^2}{2} v'^3 - 3v'^2 + \varepsilon^2 v'_{x'x'} \right)_{x'} = 0. \end{aligned} \tag{26}$$

It is important that the KdV equation (13) resp. (25) is invariant under this transformation. Furthermore, the transformation (24) becomes

$$u' = v' \pm \frac{\xi\,\varepsilon}{2} v'_{x'} + \frac{\xi^2}{4} v'^2. \tag{27}$$

Having done these preparations, we can now present the formal argument on how to construct infinitely many integrals of motion. By (26), $\int_{\mathbb{R}} v'\,\mathrm{d}x'$ is a conserved quantity. We now consider ξ to be a small perturbation parameter. Thus, v' is a perturbation of u', see (27). Consequently, we formally express v' as a sum

$$v' = \sum_{n=0}^{\infty} p_n \xi^n \tag{28}$$

with $p_0 = u'$. The crucial point is that equation (27) determines the coefficients $p_n, n = 1, 2, 3, \ldots$ as polynomials of u' and its x'-derivatives. By the independence of the terms $p_n \xi^n$, each p_n is a conserved quantity together with v'.

3.3.2 The Recursion Formula

From now on, we drop the primes for the sake of simplicity. This is no problem because the KdV equation (13) is invariant under the transformation that was carried out in the previous subsection.

Inserting the sum (28) into the transformation (27) and taking the + in (27), we get

$$u = \sum_{n=0}^{\infty} p_n \xi^n + \frac{\varepsilon\xi}{2} \sum_{n=0}^{\infty} \partial_x p_n \xi^n + \frac{\xi^2}{4} \left(\sum_{n=0}^{\infty} p_n \xi^n \right)^2.$$

Comparing coefficients yields the recursion formula

$$\begin{aligned} p_0 &= u \\ p_n &= -\frac{\varepsilon}{2} \partial_x p_{n-1} - \frac{1}{4} \sum_{i+j=n-2} p_i p_j, \quad n = 1, 2, 3, \ldots \end{aligned} \tag{29}$$

This gives for the first four polynomials:

$$\begin{aligned}
p_1 &= -\frac{\varepsilon}{2}u_x \\
p_2 &= \frac{\varepsilon^2}{4}u_{xx} - \frac{1}{4}u^2 \\
p_3 &= -\frac{\varepsilon^3}{8}u_{xxx} + \frac{\varepsilon}{2}uu_x \\
p_4 &= \frac{\varepsilon^4}{16}u_{xxxx} - \frac{5\,\varepsilon^2}{16}u_x^2 - \frac{3\,\varepsilon^2}{8}uu_{xx} + \frac{1}{8}u^3 \\
&\dots
\end{aligned}$$

We can see that p_1 and p_3 are exact derivatives which trivially are integrals of motion. In fact, one can always add exact x-derivatives to an integral of motion without substantially altering it. However, p_2 and p_4 seem to be genuinely distinct integrals of motion. This suggests that the distinct conserved densities we are looking for are only the polynomials $p_{2n}, n \in \mathbb{N}_0$.

To compute the polynomials q_n corresponding to p_n, we use the KdV equation (13) to write $\partial_t p_n$ without t-derivatives. Then we write the result as an exact x-derivative. For the sake of illustration, we carry out this calculation for q_2:

$$\begin{aligned}
-\partial_x q_2 = \partial_t p_2 &= \frac{\varepsilon^2}{4}u_{txx} - \frac{1}{2}uu_t \\
&= \frac{\varepsilon^2}{4}\left(6uu_x - \varepsilon^2 u_{xxx}\right)_{xx} - \frac{1}{2}u(6uu_x - \varepsilon^2 u_{xxx}) \\
&= \frac{\varepsilon^2}{4}\left(6uu_x - \varepsilon^2 u_{xxx}\right)_{xx} - (u^3)_x + \frac{\varepsilon^2}{2}uu_{xxx} \\
&= \frac{\varepsilon^2}{4}\left(6uu_x - \varepsilon^2 u_{xxx}\right)_{xx} - (u^3)_x + \frac{\varepsilon^2}{2}(uu_{xx})_x - \frac{\varepsilon^2}{4}(u_x^2)_x \\
\Rightarrow q_2 &= -\frac{\varepsilon^2}{4}(6uu_x - \varepsilon^2 u_{xxx})_x + u^3 - \frac{\varepsilon^2}{2}uu_{xx} + \frac{\varepsilon^2}{4}u_x^2.
\end{aligned}$$

3.3.3 The Rank

In the following, we are going to modify the KdV conservation laws (22) by splitting off exact x-derivatives from p_n and adding them to q_n. Actually, we never worry about q_n because we can always reconstruct it from p_n as explained in the previous subsection. We already mentioned that p_n remains an integral of motion after adding or subtracting an exact x-derivative to it. The goal of this operation is to decrease the order of derivatives appearing in p_n and q_n to a minimum.

We define the *rank* of a term $\partial_x^{i_1} u \cdots \partial_x^{i_m} u$ as

$$\operatorname{rank}[\partial_x^{i_1} u \cdots \partial_x^{i_m} u] := \sum_{l=1}^{m} 1 + \frac{i_l}{2}. \tag{30}$$

Note that x-differentiation increases the rank by $\frac{1}{2}$, and the rank of a product is the sum of the ranks of the factors.

The following Lemma is a first statement about the ranks of the polynomials p_n. In particular, it states that the rank of each polynomial p_n is indeed well-defined:

Lemma 3.3.1. *Each term of p_n as defined by the recursion* (29) *has rank $\frac{n}{2} + 1$.*

Proof. By induction: The case $n = 0$ is clear. For the induction step $n - 1 \to n$, we

use the recursion (29) to check that

$$\begin{aligned}\operatorname{rank}[\partial_x p_{n-1}] &= \operatorname{rank}[p_{n-1}] + \frac{1}{2} = \frac{n-1}{2} + 1 + \frac{1}{2} = \frac{n}{2} + 1\\ \operatorname{rank}[p_i p_j] &= \operatorname{rank}[p_i] + \operatorname{rank}[p_j] = \frac{i}{2} + 1 + \frac{j}{2} + 1 = \frac{n}{2} + 1.\end{aligned}$$

□

The next Lemma states that the polynomials p_n behave nicely with the regularization parameter ε. More precisely, it says that we can view p_n as polynomials of u, εu_x, $\varepsilon^2 u_{xx}, \dots$ with coefficients independent of ε:

Lemma 3.3.2. *Each term of p_n has the form $c\,\varepsilon^{i_1+\cdots+i_l}\partial_x^{i_1}u\cdots\partial_x^{i_l}u$ with c independent of ε.*

Proof. Follows by induction from the recursion (29). □

The next Lemma allows us to split off exact x-derivatives from the conserved densities p_n and thus reduce the order of derivatives appearing in them:

Lemma 3.3.3. *Each polynomial $p_n, n \geq 1$ can be written as*

$$p_n = P_n + \partial_x \tilde{p}_n$$

such that P_n is a polynomial of $u, u_x, \dots \partial_x^{l_n} u$, $l_n = \lceil \frac{n}{2} \rceil - 1$.

Proof. We construct P_n iteratively. First, set $P_n = p_n$ and $\tilde{p}_n = 0$. Now let $\partial_x^{i_1}u\cdots\partial_x^{i_l}u$ be a term of P_n and assume that $i_1 \geq \cdots \geq i_l$. If $m = 1$, then P_n already is an exact derivative and we are done. Assume therefore that $m \geq 2$ and suppose that $i_1 > \lfloor \frac{n}{2} \rfloor$. Since the rank of the considered term must be $\frac{n}{2} + 1$ (see Lemma 3.3.1), we conclude that

$$\begin{aligned}&\frac{i_1}{2} + \frac{i_2}{2} + 2 \leq \frac{n}{2} + 1\\ &\quad\Rightarrow i_1 + i_2 \leq n - 2\\ &\qquad\Rightarrow i_2 \leq n - 2 - \left\lfloor \frac{n}{2} \right\rfloor\\ &\qquad\Rightarrow i_2 \leq \left\lfloor \frac{n}{2} \right\rfloor - 1 < i_1 - 1.\end{aligned}$$

Therefore, we can split off an exact derivative

$$\partial_x^{i_1}u\cdots\partial_x^{i_l}u = -\partial_x^{i_1-1}u(\partial_x^{i_2}u\cdots\partial_x^{i_l}u)_x + (\partial_x^{i_1-1}u\cdots\partial_x^{i_l}u)_x$$

where the highest derivative appearing in the first term on the right hand side has order $\leq i_1 - 1$. Since we assumed $i_1 > \lfloor \frac{n}{2} \rfloor$, we can iterate this process to reduce the order of derivatives appearing in P_n to $\lfloor \frac{n}{2} \rfloor$. This also proves the Lemma for n being odd.

For n even, we can assume by the above that $i_1 = \frac{n}{2}$. We argue as before and find that

$$\begin{aligned}&i_1 + i_2 \leq n - 2\\ &\quad\Rightarrow i_2 \leq \frac{n}{2} - 2,\end{aligned}$$

which allows us to again reduce the order of derivative by one. □

We summarize our results in the following

Theorem 3.3.1. *For each $n \in \mathbb{N}_0$, there is a conserved densitiy P_n which is a polynomial of u, $\varepsilon u_x, \dots \varepsilon^{l_n}\partial_x^{l_n}u$,*

$$l_n = \begin{cases} 0 & , n = 0 \\ \lceil \frac{n}{2} \rceil - 1 & , n \geq 1 \end{cases}$$

with coefficients independent of ε, and a corresponding polynomial flux Q_n such that $\partial_t P_n + \partial_x Q_n = 0$.

3.4 The DiPerna Characterization

In this section, we will further investigate the KdV hierarchy of conservation laws in order to reproduce DiPerna's characterization of the VDL as given in ([4], section 7).

3.4.1 The KdV Conservation Laws Revisited

As already mentioned, the distinct conserved densities for the KdV equation are only the polynomials P_n (see Theorem 3.3.1) for n even. We therefore set $U_k := P_{2k-2}$ and $V_k := Q_{2k-2}, k \geq 1$. Thus, the distinct KdV conservation laws are

$$\partial_t U_k + \partial_x V_k = 0, \quad k = 1, 2, 3, \dots \tag{31}$$

We take a closer look at the fluxes V_k which we construct by the conservation law (31) itself: We differentiate U_k with respect to t, insert the KdV equation (13) to get rid of all t-derivatives, and finally write the result as an exact x-derivative. From Lemma 3.3.1, we know that the rank of U_k is k. By the KdV equation (13), differentiation with respect to t increases the rank by $\frac{3}{2}$. We conclude that the rank of V_k is $k+1$. Moreover, by Lemma 3.3.3, we know that for $k \geq 2$, U_k is a polynomial of u, $\varepsilon u_x, \dots, \varepsilon^{k-2}\partial_x^{k-2}u$. Again by the KdV equation (13), we conclude that for $k \geq 2$, the highest derivative appearing in V_k is of order k. Finally, note that Lemma 3.3.2 holds also for V_k, i.e. for $k \geq 2$, V_k is a polynomial of u, $\varepsilon u_x, \dots, \varepsilon^k \partial_x^k u$ with coefficients independent of ε. These considerations motivate the following definition:

Definition 3.4.1. *For each $k \in \mathbb{N}_{\geq 1}$, we define the k-*jet *J_k^ε to be the k-tuple $J_k^\varepsilon := (u, \varepsilon u_x, \dots \varepsilon^{k-1}\partial_x^{k-1}u)$. Note that J_k^ε can be viewed as a function $\mathbb{R} \times \mathbb{R}_{\geq 0} \to \mathbb{R}^k$.*

By this definition, U_k is a polynomial of J_{k-1}^ε, and V_k is a polynomial of J_{k+1}^ε (for $k \geq 2$). From now on, we shall always make the following

Assumption 3.4.1. *The k-jet J_k^ε is bounded in $L^\infty(\mathbb{R} \times \mathbb{R}_{\geq 0}, \mathbb{R}^k)$ uniformly in ε.*

We intend to modify the conservation law (31) (which so far is a statement involving the $k+1$-jet) such that as $\varepsilon \to 0$, it implies a statement concerning the k-jet. Let $\partial_x^{i_1}u \cdots \partial_x^{i_l}u$ be a term of V_k and assume $i_1 \geq \cdots \geq i_l$ and $i_1 = k$. Since the rank of V_k is $k+1$, we argue as in the proof of Lemma 3.3.3 to conclude that $i_2 \leq k-2$. Therefore, we write

$$\partial_x^{i_1}u \cdots \partial_x^{i_l}u = -\partial_x^{i_1-1}u(\partial_x^{i_2}u \cdots \partial_x^{i_l}u)_x + (\partial_x^{i_1-1}u \cdots \partial_x^{i_l}u)_x.$$

Remember that the coefficient of the considered term has the form $c\,\varepsilon^{i_1+\cdots+i_l}$. Since $i_2 \leq k-2$, the first term on the right hand side therefore is a polynomial of the k-jet. Moreover, by Assumption 3.4.1, the second term on the right hand side vanishes in the sense of distributions as $\varepsilon \to 0$. We get the following

Lemma 3.4.1. *The KdV conservation laws* (31) *can be written as*

$$\partial_t U_k + \partial_x F_k + \partial_x^2 W_k = 0,$$

where U_k and F_k are polynomials of J_{k-1}^ε resp. J_k^ε and where $\partial_x^2 W_k$ vanishes in the sense of distributions as $\varepsilon \to 0$.

For $k = 1$, the conservation law of Lemma 3.4.1 is the KdV equation itself. Therefore, we conclude that $U_1 = u$ and $F_1 = -3u^2$, or written as polynomials: $U_1(\xi) = \xi$ and $F_1(\xi) = -3\xi^2$. For the sake of illustration, we also present the case $k = 2$ explicitly: Up to multiplication with a constant, the conserved density for the 2-jet is $U_2 = \frac{u^2}{2}$. The corresponding conservation law can be obtained directly by multiplying the KdV equation (13) with u:

$$\begin{aligned} uu_t - 6u^2u_x + \varepsilon^2 uu_{xxx} &= 0 \\ \Rightarrow \left(\frac{u^2}{2}\right)_t - (2u^3)_x + (\varepsilon^2 uu_{xx})_x - \varepsilon^2 u_x u_{xx} &= 0 \\ \Rightarrow \left(\frac{u^2}{2}\right)_t - (2u^3)_x + (\varepsilon^2 uu_x)_{xx} - (\varepsilon^2 u_x^2)_x - \left(\frac{\varepsilon^2 u_x^2}{2}\right)_x &= 0. \end{aligned}$$

We conclude that $F_2 = -2u^3 - \frac{3\varepsilon^2 u_x^2}{2}$ and $W_2 = \varepsilon^2 uu_x$, or written as polynomials:

$$\begin{aligned} U_2(\xi_0, \xi_1) &= \frac{\xi_0^2}{2} \\ F_2(\xi_0, \xi_1) &= -2\xi_0^3 - \frac{3}{2}\xi_1^2. \end{aligned}$$

3.4.2 KdV-Hierarchy-Based Characterization of the VDL

We now turn to DiPerna's characterization of the VDL which is based on the KdV hierarchy of conservation laws as given in Lemma 3.4.1. By the assumed boundedness of the k-jet, see Assumption 3.4.1, we get a weakly converging subsequence $J_k^\varepsilon \overset{*}{\rightharpoonup} (\overline{u}_0, \dots, \overline{u}_{k-1})$. As was described at the end of subsection 1.2.1, there is a subsequence such that J_k^ε converges narrowly to a k-dimensional Young measure $\nu^k = (\nu_0^k, \dots \nu_{k-1}^k) \in \mathbf{Y}(\mathbb{R} \times \mathbb{R}_{\geq 0}, \mathbb{R}^k)$:

$$\iint_{\mathbb{R}\times\mathbb{R}_{\geq 0}} \varphi(x,t) g(J_k^\varepsilon)\, \mathrm{d}x\, \mathrm{d}t \to \iint_{\mathbb{R}\times\mathbb{R}_{\geq 0}} \varphi(x,t) \langle \nu^k, g\rangle\, \mathrm{d}x\, \mathrm{d}t, \quad \varepsilon \to 0$$

for all test functions φ and all continuous functions g. We call such a Young measure ν^k a *Young measure associated with an L^∞-stable k-jet*. Note that the first component ν_0^k is the VDL.

DiPerna's characterization states a connection between the components of the Young measure ν^k using the notion of MV solutions to systems of conservation laws (see subsection 1.2.2):

Theorem 3.4.1 (DiPerna [4], Theorem 7.2)**.** *For each $k \geq 1$, the Young measure ν^k associated with an L^∞-stable k-jet of a KdV solution sequence is a MV solution to a system of k conservation laws of the form*

$$\partial_t U^k(u_1, \dots u_k) + \partial_x F^k(u_1, \dots u_k) = 0, \quad U^k, F^k : \mathbb{R}^k \to \mathbb{R}^k.$$

Here, the components of U^k resp. F^k are $U_1, \dots U_k$ resp. $F_1, \dots F_k$ as given in Lemma 3.4.1.

Remark 3.4.1. *More specifically, this means that the Young measure ν^k associated with an L^∞-stable k-jet satisfies the following property: For all test functions φ and $l = 1, \dots k$:*

$$\iint_{\mathbb{R}\times\mathbb{R}_{\geq 0}} \varphi_t(x,t) \langle \nu^k_{(x,t)}, U_l\rangle\, \mathrm{d}x\, \mathrm{d}t + \iint_{\mathbb{R}\times\mathbb{R}_{\geq 0}} \varphi_x(x,t) \langle \nu^k_{(x,t)}, F_l\rangle\, \mathrm{d}x\, \mathrm{d}t = 0 \tag{32}$$

where we view the polynomials U_l, F_l as functions

$$\begin{aligned} &U_l, F_l : \mathbb{R}^k \to \mathbb{R} \\ &(u_1, \dots u_k) \mapsto U_l(u_1, \dots, u_l), F_l(u_1, \dots, u_l). \end{aligned}$$

Proof. Follows immediately from Lemma 3.4.1 and the narrow convergence $\delta_{J_k^\varepsilon} \rightharpoonup \nu^k$. □

Note that this characterization looks similar to the entropy constraints given in (9). However, it is much weaker since it also includes x-derivatives of the KdV solution and the polynomials U_k are not necessarily convex.

We call a k-dimensional measure $\nu^k = (\nu_0^k, \dots \nu_{k-1}^k)$ which satisfies the DiPerna characterization a *k-jet MV solution* and the corresponding equation (32) the *k-jet MV equation*. In the following section, we shall prove that any k-dimensional Young measure associated with our implicit FDS satisfies the k-jet MV equation provided we choose the rate at which ε tends to zero as $\Delta x \to 0$ properly. This will provide indication that the computed measure indeed approximates the VDL.

4 Implicit Finite Difference Scheme

We come to the main part of this thesis where we present an implicit finite difference scheme (FDS) attempting to approximate the vanishing dispersion limit (VDL). This approach is motivated by [5] where finite volume schemes together with perturbation of the initial data are used to approximate EMV solutions of systems of conservation laws. However, such an EMV is the result of vanishing viscosity rather than vanishing dispersion. Also, dispersive regularization doesn't offer infinitely many entropy inequalities. Moreover, we have seen that in the special case of a one-dimensional scalar conservation law, the EMV solution is atomic whereas we presume that the VDL is non-atomic. There is therefore no theoretical background to fall back on which could indicate that a FDS will provide the correct VDL. Thus, we aim to present both theoretical and numerical indication that our FDS does indeed approximate the VDL.

After introducing the scheme in section 4.1, we shall prove in section 4.2 that under the assumption of discrete L^∞-boundedness, the associated limit measure is a MV solution. Moreover, we will prove in section 4.4 that the limit measure associated with a uniformly bounded discrete k-jet satisfies DiPerna's characterization as described in Theorem 3.4.1, i.e. it satisfies the k-jet MV equation (32). For the sake of illustration, we shall first prove the case $k = 2$ in section 4.3 before moving on to the general case. However, for each k, this theoretical result depends on the rate at which the dispersion coefficient ε tends to zero as $\Delta x \to 0$. To satisfy the whole infinite KdV hierarchy of conservation laws, this rate would have to be slower than any polynomial rate $\varepsilon = \Delta x^r$.

It is no accident that we call our scheme a finite *difference* scheme instead of finite *volume* scheme. Indeed, it was originally designed as an approximation for the KdV equation. With the methods presented in [10] and [11], it can be proven to converge to the classical differentiable KdV solution (for fixed ε). Consequently, our scheme was designed to approximate a classical solution in contrast to a weak or even MV solution. We shall see that we indeed rely on how accurately we can reproduce the oscillations of the KdV solution. This is why we shall furthermore present a generalization of the implicit finite difference equation in section 4.6 which allows for a better approximation of the classical KdV solution while still satisfying the DiPerna characterization. We shall use this generalized scheme to finally perform numerical experiments in section 4.7 and compare the results with the simplified method of McLaughlin and Strain which was presented in section 3.2.

4.1 The Scheme

The implicit finite difference scheme (FDS) which we present in this section was first developed in [8] as an approximation for the KdV equation. For fixed ε, it was proven to converge to the classical KdV solution in [10].

From now on, we consider the space-periodic case, i.e. $x \in \mathbb{R}/\mathbb{Z}$.[5] After defining the finite difference equation, we will describe how to obtain an approximative MV solution from it. Finally, we shall discuss the diffusiveness of the scheme.

4.1.1 Preparations Concerning the Discrete Environment

We discretize space by a Δx-equispaced grid $(x_j)_{j\in\mathbb{Z}/N\mathbb{Z}}$ of N gridpoints where $x_j = j\Delta x$ and $\Delta x = \frac{1}{N}$. Also, we discretize time into mesh points $(t_n)_{n\in\mathbb{N}_0}$ where $t_n = n\Delta t$. The mesh sizes Δx and Δt are linked linearly via the CFL-number $\lambda = \frac{\Delta t}{\Delta x}$.

For a discrete function

$$\begin{aligned} \mathbb{Z}/N\mathbb{Z} \times \mathbb{N}_0 &\to \mathbb{R} \\ (j,n) &\mapsto v_{j,n}, \end{aligned}$$

we define the following operators:

$$\begin{aligned} Ev_{j,n} &:= \frac{v_{j-1,n} + v_{j,n} + v_{j+1,n}}{3} \\ D_+v_{j,n} &:= \frac{v_{j+1,n} - v_{j,n}}{\Delta x} \\ D_-v_{j,n} &:= \frac{v_{j,n} - v_{j-1,n}}{\Delta x} \\ D_0v_{j,n} &:= \frac{v_{j+1,n} - v_{j-1,n}}{2\Delta x} \\ D_-^tv_{j,n} &:= \frac{v_{j,n} - v_{j,n-1}}{\Delta t} \\ &\dots \end{aligned} \tag{33}$$

Note that the first four (spatial) operators can be viewed as $N \times N$-matrices. Furthermore, we define the *discrete spatial inner product*

$$(v_j, w_j)_{\Delta x} := \sum_{j=1}^{N} v_j w_j \Delta x$$

which induces the norm $||\cdot||_{\Delta x}$. From now on, we shall abbreviate $\sum_{j=1}^{N}$ with $\sum_j$ for the sake of simplicity.

We shall need the following *Sobolev-type inequalities*:

Lemma 4.1.1. *$\exists C > 0$ s.t. $\forall \Delta x, \forall (v_j)_j, \forall \varepsilon' > 0$:*

$$||D_+v_j||_{\Delta x}^2 \le \frac{C}{\varepsilon'}||v_j||_{\Delta x}^2 + \varepsilon'^2||D_+^3v_j||_{\Delta x}^2 \tag{34}$$

$$||D_+^2v_j||_{\Delta x}^2 \le \frac{C}{\varepsilon'^2}||v_j||_{\Delta x}^2 + \varepsilon'||D_+^3v_j||_{\Delta x}^2. \tag{35}$$

Proof. First, by simple integration by parts and Young's inequality with ε, we find that

$$\begin{aligned} \int \varphi_x^2 \,\mathrm{d}x &\le \frac{C}{\varepsilon'} \int \varphi^2 \,\mathrm{d}x + \varepsilon'^2 \int \varphi_{xxx}^2 \,\mathrm{d}x \\ \int \varphi_{xx}^2 \,\mathrm{d}x &\le \frac{C}{\varepsilon'^2} \int \varphi^2 \,\mathrm{d}x + \varepsilon' \int \varphi_{xxx}^2 \,\mathrm{d}x \end{aligned}$$

for any smooth periodic function φ. Then, by a result that was proven by Sjöberg in ([17], Lemma 2.2), these inequalities can be transferred to the discrete case. □

[5] For the initial function $u_0(x)$ we considered so far (see subsection 1.1.2), this is no substantial restriction since $u_0(x) = 0$ for $|x|$ big enough. We therefore assume that also $u(x,t) = 0$ for $|x|$ big enough and t small enough.

Moreover, it can easily be checked that the following *discrete Leibniz rules* hold:

$$\begin{aligned} D_+(v_j w_j) &= D_+ v_j w_j + v_{j+1} D_+ w_j, \\ D_-(v_j w_j) &= D_- v_j w_j + v_{j-1} D_- w_j, \\ D_0(v_j w_j) &= D_0 v_j w_{j-1} + v_{j+1} D_0 w_j, \\ D_-^t(v_n w_n) &= D_-^t v_n w_n + v_{n-1} D_-^t w_n. \end{aligned}$$

Also, *discrete integration by parts* can be done as follows:

$$\begin{aligned} (D_+ v_j, w_j)_{\Delta x} &= -(v_j, D_- w_j)_{\Delta x} \\ (D_0 v_j, w_j)_{\Delta x} &= -(v_j, D_0 w_j)_{\Delta x}. \end{aligned}$$

4.1.2 The Finite Difference Equation

We define the discrete function $u_{j,n}$ which is supposed to approximate the KdV solution $u(x_j, t_n)$ of (13) to be the solution of the discrete implicit finite difference equation

$$\begin{aligned} D_-^t u_{j,n} - 6E u_{j,n} D_0 u_{j,n} + \varepsilon^2 D_+^2 D_- u_{j,n} = 0, \quad j \in \mathbb{Z}/N\mathbb{Z}, n \in \mathbb{N}_{\geq 1}, \\ u_{j,0} = u_0(x_j), \quad j \in \mathbb{Z}/N\mathbb{Z}. \end{aligned} \tag{36}$$

The backward operator D_-^t makes this scheme implicit. For each time step, it is therefore necessary to solve a non-linear equation. This is done by the following *fixed-point iteration*:

$$\begin{aligned} u_{j,n,(m+1)} &= u_{j,n-1} + 6\Delta t E u_{j,n,(m)} D_0 u_{j,n,(m)} - \varepsilon^2 \Delta t D_+^2 D_- u_{j,n,(m+1)}, \quad m \geq 0, \\ u_{j,n,(0)} &= u_{j,n-1}. \end{aligned} \tag{37}$$

In this iteration, it is still necessary to solve a linear system for each iteration step. Even though this is computationally very costly, it is necessary in order to prove convergence of the iteration *for fixed* ε, see [11]. It is far from being obvious whether the iteration converges if ε is decreasing at a rate $\varepsilon = \Delta x^r$. Nevertheless, we don't investigate this issue further at this point since the convergence of the iteration can always be checked experimentally.

We furthermore have to specify the behavior of ε as $\Delta x \to 0$. We simply set

$$\varepsilon = c\Delta x^r, \quad r > 0 \tag{38}$$

where c is a constant. The influence of the rate r on the solution will be discussed extensively in the following subsections.

We close this subsection by giving some motivation for each term in the finite difference equation (36). The discrete time derivative is chosen to be a backward operator because implicity is well-known to provide stability. In our case, it will be needed to derive weak BV properties. The non-linear term is discretized such that it satisfies the continuous property $(vv_x, v)_{L^2(\mathbb{R}/\mathbb{Z})} = 0$ discretely. Indeed, we find that

$$(E v_j D_0 v_j, v_j)_{\Delta x} = 0.$$

Furthermore, the discrete dispersion term is chosen such that a property similar to $(u, u_{xxx})_{L^2(\mathbb{R}/\mathbb{Z})} = 0$ holds discretely. Indeed, using discrete integration by parts and the Cauchy-Schwartz inequality, we find that

$$\begin{aligned} (D_+^2 D_- v_j, v_j)_{\Delta x} &= (D_- v_j, D_-^2 v_j)_{\Delta x} \\ &= \frac{(D_- v_j, D_- v_j)_{\Delta x} - (D_- v_j, D_- v_{j-1})_{\Delta x}}{\Delta x} \geq 0. \end{aligned}$$

This inequality will allow us to always neglect the third order term when deriving weak BV estimates. However, the symmetric operator D_0^3 would in fact satisfy an

even better property, namely $(D_0^3 v_j, v_j)_{\Delta x} = 0$. As a result, it produces a better approximation of the KdV solution which is the reason why it was preferred above the asymmetric operator $D_+^2 D_-$ in [11]. Nevertheless, we shall stick to $D_+^2 D_-$ for the moment because it allows us to apply the discrete Sobolev-type inequalities of Lemma 4.1.1.

4.1.3 Construction of the Approximative Young Measure

After having defined the discrete finite difference equation (36) to obtain the discrete function $(j,n) \mapsto u_{j,n}$, we turn to producing an approximative Young measure. We shall present two approaches: the straightforward *weak limit approach* and the *perturbation approach* of [5]. In order to do that, we define the piecewise constant function

$$u^{\Delta x}(x,t) = u_{j,n}, \quad (x,t) \in [x_j, x_{j+1}) \times [t_n, t_{n+1}).$$

Weak Limit Approach: The most straightforward approach to compute the Young measure associated with a numerical scheme is to compute the weak limits of $u^{\Delta x}$ and its functionals $g(u^{\Delta x})$ as $\Delta x \to 0$ and determine the Young measure which characterizes these weak limits, see subsection 1.2.1. In practice, this is done by choosing a sequence $\Delta x_m \to 0$ and defining the approximative Young measure as

$$\nu_{(x,t)}^{(\Delta x_m)_m, M} := \frac{1}{M} \sum_{m=1}^{M} \delta_{u^{\Delta x_m}(x,t)}.$$

However, one has to go to very small mesh sizes Δx_m in order to obtain enough samples. This is computationally very costly which is why we next introduce the

Perturbation Approach: (Compare to section 2.2.) Following [5], we perturb the initial data with a random field $u_0(x;\omega)$ over a probability space $(\Omega, \mathcal{F}, P)$. The FDS will then produce the random field $u^{\Delta x}(x,t;\omega)$ whose law $\nu^{\Delta x}$ is taken to be the approximative Young measure. Since it is not possible to compute $u^{\Delta x}(x,t;\omega)$ for each $\omega \in \Omega$, we apply a Monte-Carlo method: We choose M independent, identically distributed drawings of $u_0(x;\omega)$ and denote them by $u_0^m(x), m = 1, \dots M$. The FDS will then produce M functions $u^{\Delta x, m}(x,t)$ and the approximative Young measure is defined to be

$$\nu_{(x,t)}^{\Delta x, M} := \frac{1}{M} \sum_{m=1}^{M} \delta_{u^{\Delta x, m}(x,t)}.$$

It remains to specify how the random field $u_0(x;\omega)$ is constructed. We postpone this issue to section 4.7 where we shall explicitly do numerical experiments.

The perturbation approach is numerically more efficient then the weak limit approach since the numerical complexity grows linearly with the number of samples M. The rate at which the numerical complexity grows with decreasing Δx is much worse.

Remembering the DiPerna characterization (Theorem 3.4.1), we actually not only want to compute the one-dimensional VDL but also the k-dimensional k-jet MV solution $\nu^k = (\nu_0^k, \dots \nu_{k-1}^k)$. We define the discrete k-jet as

$$J_k^{j,n} := (u_{j,n}, \varepsilon D_+ u_{j,n}, \dots \varepsilon^{k-1} D_+^{k-1} u_{j,n})$$

which yields the function $J_k^{\Delta x} := (u^{\Delta x}, \dots \varepsilon^{k-1} D_+^{k-1} u^{\Delta x})$. Then, we repeat the above procedures for each component. This yields the approximative k-jet MV solutions

$$\nu_{(x,t)}^{(\Delta x_m)_m, M, k} = (\nu_{0,(x,t)}^{(\Delta x_m)_m, M, k}, \dots \nu_{k-1,(x,t)}^{(\Delta x_m)_m, M, k})$$

resp.

$$\nu^{\Delta x,M,k}_{(x,t)} = (\nu^{\Delta x,M,k}_{0,(x,t)}, \dots \nu^{\Delta x,M,k}_{k-1,(x,t)}).$$

Even though these are the explicit methods wherewith we will compute the approximative Young measures, we shall for the sake of theoretical proofs consider the narrow limits

$$\delta_{u^{\Delta x}(\cdot,\cdot)} \rightharpoonup \nu$$

resp. for the k-jet

$$\delta_{J^{\Delta x}_k(\cdot,\cdot)} \rightharpoonup \nu^k = (\nu^k_0, \dots \nu^k_{k-1}).$$

Up to a subsequence, the existence of these limits is a consequence of assuming $u^{\Delta x}$ resp. $J^{\Delta x}_k$ to be bounded in L^∞ uniformly in Δx.

4.1.4 Numerical Diffusion

The fact that the FDS is implicit adds a considerable amount of diffusion to it. Indeed, we shall exploit this fact when deriving weak BV estimates below. In addition, the asymmetric discretization of the third order term is another source of diffusion. In this section, we take a closer look at this third order finite difference term and approximate it using Taylor sequences. This will indicate that our finite difference equation approximates the solution of Burgers' equation with dispersive *and* diffusive regularization rather than just dispersive regularization.

In a canonical way, the discrete operators D_+, D_- and D_0 can also be applied to functions $v : \mathbb{R} \to \mathbb{R}$, e.g. $D_+v(x) = \frac{v(x+\Delta x)-v(x)}{\Delta x}$. We then find that

$$D^2_+ D_- v(x) = \frac{v(x+2\Delta x) - 3v(x+\Delta x) + 3v(x) - v(x-\Delta x)}{\Delta x^3}.$$

For each term of the enumerator, we use a Taylor sequence to approximate it around x:

$$\begin{aligned}
v(x+2\Delta x) &= v(x) + 2\Delta x v'(x) + \frac{4\Delta x^2}{2} v''(x) \\
&\quad + \frac{8\Delta x^3}{6} v'''(x) + \frac{16\Delta x^4}{24} v''''(x) + O(\Delta x^5), \\
v(x+\Delta x) &= v(x) + \Delta x v'(x) + \frac{\Delta x^2}{2} v''(x) \\
&\quad + \frac{\Delta x^3}{6} v'''(x) + \frac{\Delta x^4}{24} v''''(x) + O(\Delta x^5), \\
v(x-\Delta x) &= v(x) - \Delta x v'(x) + \frac{\Delta x^2}{2} v''(x) \\
&\quad - \frac{\Delta x^3}{6} v'''(x) + \frac{\Delta x^4}{24} v''''(x) + O(\Delta x^5).
\end{aligned}$$

This yields

$$D^2_+ D_- v(x) = v'''(x) + \frac{\Delta x}{2} v''''(x) + O(\Delta x^2)$$

which is a mixture of dispersion $v'''(x)$ and diffusion $\frac{\Delta x}{2} v''''(x)$. This indicates that instead of approximating the KdV solution, we are rather approximating the modified equation

$$\partial_t u - 6uu_x + \varepsilon^2 u_{xxx} + \frac{\varepsilon^2 \Delta x}{2} u_{xxxx} = 0.$$

Already at this stage we see that the smaller we choose the rate r in (38), the smaller the diffusion becomes compared to dispersion. More precisely, the smaller r is, the faster the diffusion coefficient $\frac{\Delta x^{1+2r}}{2}$ goes to zero compared to the dispersion coefficient Δx^{2r}. This already indicates that the smaller we choose r, the closer we get to the VDL.

The existence of numerical diffusion in the third order term is a consequence of its asymmetry. To avoid this asymmetry, we would have to bring the symmetric operator D_0 into play. However, this would make the application of the Sobolev-type inequalities of Lemma 4.1.1 impossible. Furthermore, it is a well-known principle that diffusion adds stability to the numerical equation.

4.2 MV Solution, or: 1-jet MV solution

We assume that the numerical solution $u^{\Delta x}(x,t)$ is bounded in $L^\infty(\mathbb{R}/\mathbb{Z}\times(0,T))$ uniformly in Δx. Here, $T = n_{end}\Delta t$ is a fixed end time. From this assumed uniform boundedness, we get a subsequence $\Delta x_m \to 0$ such that $u^{\Delta x_m}$ converges narrowly to a Young measure ν:

$$\delta_{u^{\Delta x_m}(\cdot,\cdot)} \rightharpoonup \nu, \quad m\to\infty.$$

We call ν the *Young measure associated with the implicit FDS.* We shall prove that ν is a MV solution of Burgers' equation $u_t - (3u^2)_x = 0$ if $\Delta x = o(\varepsilon)$ or, more concretely, $\varepsilon = \Delta x^r, r < 1$. Note that being a MV solution is equivalent to satisfying the 1-jet MV equation.

4.2.1 Weak BV for the 1-jet MV equation

As it was the case in subsection 2.2, we will need some *weak BV property.* In particular, we shall need

$$\sum_{n=0}^{n_{end}} ||u_{j+1,n} - u_{j,n}||^2_{\Delta x}\Delta t \to 0, \quad \Delta x \to 0$$

(we shall abbreviate $\sum_{n=0}^{n_{end}}$ with $\sum_n$). This is achieved using the properties of each term of the finite difference equation (36) as explained at the end of subsection 4.1.2.

We multiply the finite difference equation (36) with $u_{j,n}$ and sum over j. Using the properties $(Ev_jD_0v_j, v_j)_{\Delta x} = 0$ and $(D_+^2D_-v_j, v_j)_{\Delta x} \geq 0$ we conclude that

$$\begin{aligned}(u_{j,n}, u_{j,n} - u_{j,n-1})_{\Delta x} &\leq 0 \qquad (39)\\ \Rightarrow ||u_{j,n}||^2_{\Delta x} &\leq (u_{j,n}, u_{j,n-1})_{\Delta x}\\ &\leq ||u_{j,n}||_{\Delta x}||u_{j,n-1}||_{\Delta x}\\ &\leq \frac{1}{2}||u_{j,n}||^2_{\Delta x} + \frac{1}{2}||u_{j,n-1}||^2_{\Delta x}\\ \Rightarrow ||u_{j,n}||^2_{\Delta x} &\leq ||u_{j,n-1}||^2_{\Delta x}. \qquad (40)\end{aligned}$$

Assuming L^∞-boundedness, the last estimate (40) isn't really needed. Nevertheless, it shows one of the nice properties of the scheme. Turning again to (39), we apply the basic equality $a(a-b) = \frac{1}{2}a^2 - \frac{1}{2}b^2 + \frac{1}{2}(a-b)^2$ (it is here that we make use of the implicity) to obtain

$$||u_{j,n}||^2_{\Delta x} - ||u_{j,n-1}||^2_{\Delta x} + ||u_{j,n} - u_{j,n-1}||^2_{\Delta x} \leq 0. \qquad (41)$$

Summing over n and exploiting the arising telescoping sum for the first two terms yields

$$\sum_n ||u_{j,n} - u_{j,n-1}||^2_{\Delta x} \leq ||u_{j,0}||^2_{\Delta x} - ||u_{j,n_{end}}||^2_{\Delta x} \leq ||u_0||^2_{L^\infty(\mathbb{R})}$$
$$\Rightarrow \sum_n ||D^t_- u_{j,n}||^2_{\Delta x} \Delta t \leq \frac{||u_0||^2_{L^\infty(\mathbb{R})}}{\Delta t}. \tag{42}$$

Here, the finite difference equation (36) comes into play again. From it, we directly estimate its third order derivative term as

$$\sum_n ||\,\varepsilon^2 D^2_+ D_- u_{j,n}||^2_{\Delta x} \Delta t \leq 2 \sum_n ||6E u_{j,n} D_0 u_{j,n}||^2_{\Delta x} \Delta t + 2 \sum_n ||D^t_- u_{j,n}||^2_{\Delta x} \Delta t. \tag{43}$$

The second term on the right hand side is bounded by (42). For the first term, we use the assumed L^∞-boundedness of $u^{\Delta x}$ and Lemma 4.1.1, (34) together with (40) to estimate

$$2 \sum_n ||6E u_{j,n} D_0 u_{j,n}||^2_{\Delta x} \Delta t \leq 72 ||u^{\Delta x}||^2_{L^\infty} \left(\frac{CT}{\varepsilon'} ||u_0||^2_{L^\infty} + \varepsilon'^2 \sum_n ||D^3_+ u_{j,n}||^2_{\Delta x} \Delta t \right).$$

Inserting this into (43) and setting $\varepsilon' = \frac{1}{12||u^{\Delta x}||_{L^\infty}} \varepsilon^2$, we conclude that

$$\sum_n ||\,\varepsilon^2 D^3_+ u_{j,n}||^2_{\Delta x} \Delta t \leq \frac{4||u_0||^2_{L^\infty(\mathbb{R})}}{\Delta t} + \frac{1728 ||u^{\Delta x}||^3_{L^\infty} ||u_0||^2_{L^\infty} CT}{\varepsilon^2}.$$

Applying once more Lemma 4.1.1, (34) together with (40) yields

$$\sum_n ||D_+ u_{j,n}||^2_{\Delta x} \Delta t \leq \frac{CT}{\varepsilon'} ||u_0||^2_{L^\infty} + \varepsilon'^2 \left(\frac{4||u_0||^2_{L^\infty(\mathbb{R})}}{\Delta t\, \varepsilon^4} + \frac{1728 ||u^{\Delta x}||^3_{L^\infty} ||u_0||^2_{L^\infty} CT}{\varepsilon^6} \right)$$

from which we conclude that there is a constant C' such that

$$\sum_n ||D_+ u_{j,n}||^2_{\Delta x} \Delta t \leq C' \left(\frac{1}{\varepsilon'} + \frac{\varepsilon'^2}{\Delta x\, \varepsilon^4} + \frac{\varepsilon'^2}{\varepsilon^6} \right)$$
$$\Rightarrow \sum_n ||u_{j+1,n} - u_{j,n}||^2_{\Delta x} \Delta t \leq C' \left(\frac{\Delta x^2}{\varepsilon'} + \frac{\varepsilon'^2 \Delta x}{\varepsilon^4} + \frac{\varepsilon'^2 \Delta x^2}{\varepsilon^6} \right). \tag{44}$$

Setting $\varepsilon' = \Delta x^s$ and remembering that $\varepsilon = \Delta x^r$, the right hand side can be written as

$$C' \left(\Delta x^{2-s} + \Delta x^{2s+1-4r} + \Delta x^{2s+2-6r} \right).$$

Since s is arbitrary, we can make this vanish as $\Delta x \to 0$ if $r < 1$. So we have proven the following

Lemma 4.2.1 (Weak BV for 1-jet)**.** *Let $u_{j,n}$ be the discrete function computed by the scheme* (36)*. Assuming it to be uniformly bounded in L^∞ and fixing the rate $\varepsilon = \Delta x^r$ at some $r < 1$, we have the following weak BV property:*

$$\sum_{j=1}^{N} \sum_{n=0}^{n_{end}} (u_{j+1,n} - u_{j,n})^2 \Delta x \Delta t \to 0, \quad \Delta x \to 0.$$

4.2.2 Proof of 1-jet MV equation

We are now ready to prove the 1-jet MV equation for the limit measure ν associated with the implicit FDS (in other words, we prove that the limit measure ν is a MV solution of Burgers' equation $u_t - (3u^2)_x = 0$):

Theorem 4.2.1 (1-jet MV equation)**.** *Let ν be the one-dimensional Young measure associated with the implicit FDS, i.e. $\delta_{u^{\Delta x}(\cdot,\cdot)} \rightharpoonup \nu, \Delta x \to 0$. Assuming $u^{\Delta x}$ to be uniformly bounded in $L^\infty(\mathbb{R}/\mathbb{Z} \times (0,T))$ and fixing the rate $\varepsilon = \Delta x^r$ at some $r < 1$, ν will be a MV solution of Burgers' equation $u_t - (3u^2)_x = 0$. In other words, ν satisfies the 1-jet MV equation*

$$\iint_{\mathbb{R}/\mathbb{Z}\times(0,T)} \varphi_t(x,t)\langle \nu_{(x,t)}, \xi\rangle \,\mathrm{d}x\,\mathrm{d}t - \iint_{\mathbb{R}/\mathbb{Z}\times(0,T)} \varphi_x(x,t)\langle \nu_{(x,t)}, 3\xi^2\rangle \,\mathrm{d}x\,\mathrm{d}t = 0$$

for all test functions $\varphi \in C_c^\infty(\mathbb{R}/\mathbb{Z} \times (0,T))$, and therefore is a 1-jet MV solution.

Proof. Let $\varphi \in C_c^\infty(\mathbb{R}/\mathbb{Z} \times (0,T))$ be a test function and define its local averages $\varphi_{j,n} := \frac{1}{\Delta x \Delta t}\int_{x_j}^{x_{j+1}}\int_{t_n}^{t_{n+1}} \varphi(x,t)\,\mathrm{d}x\,\mathrm{d}t$. We then multiply the scheme (36) with $\varphi_{j,n}$ and sum over j, n:

$$\sum_{j,n} D_-^t u_{j,n}\varphi_{j,n}\Delta x\Delta t - \sum_{j,n} 6Eu_{j,n}D_0u_{j,n}\varphi_{j,n}\Delta x\Delta t + \varepsilon^2 \sum_{j,n} D_+^2 D_- u_{j,n}\varphi_{j,n}\Delta x\Delta t = 0. \tag{45}$$

It can easily be verified that $6Ev_jD_0v_j = D_+(v_{j-1}^2 + v_j^2 + v_jv_{j-1})$. Therefore, we can do discrete integration by parts for each term of (45) to obtain

$$\sum_{j,n} u_{j,n}D_+^t\varphi_{j,n}\Delta x\Delta t - \sum_{j,n}(u_{j-1,n}^2 + u_{j,n}^2 + u_{j,n}u_{j-1,n})D_-\varphi_{j,n}\Delta x\Delta t + \varepsilon^2\sum_{j,n} u_{j,n}D_+D_-^2\varphi_{j,n}\Delta x\Delta t = 0. \tag{46}$$

It is for the second term that we need the weak BV property of Lemma 4.2.1: We write

$$\begin{aligned}&\sum_{j,n}(u_{j-1,n}^2 + u_{j,n}^2 + u_{j,n}u_{j-1,n})D_-\varphi_{j,n}\Delta x\Delta t \\ &\quad= \sum_{j,n} 3u_{j,n}^2 D_-\varphi_{j,n}\Delta x\Delta t + \sum_{j,n}(u_{j-1,n}^2 + u_{j,n}u_{j-1,n} - 2u_{j,n}^2)D_-\varphi_{j,n}\Delta x\Delta t\end{aligned}$$

where the last term vanishes as $\Delta x \to 0$ by the assumed L^∞-boundedness and the weak BV property of Lemma 4.2.1. We can now write (46) as

$$\sum_{j,n} u_{j,n}D_+^t\varphi_{j,n}\Delta x\Delta t - \sum_{j,n} 3u_{j,n}^2 D_-\varphi_{j,n}\Delta x\Delta t + \varepsilon^2\sum_{j,n} u_{j,n}D_+D_-^2\varphi_{j,n}\Delta x\Delta t = o(1)$$

Remembering the definition of $\varphi_{j,n}$ and $u^{\Delta x}$, this can be written as an integral equation:

$$\begin{aligned}&\iint_{\mathbb{R}/\mathbb{Z}\times(0,T)} u^{\Delta x}(x,t)D_+^t\varphi(x,t)\,\mathrm{d}x\,\mathrm{d}t \\ &\quad- \iint_{\mathbb{R}/\mathbb{Z}\times(0,T)} 3(u^{\Delta x}(x,t))^2 D_-\varphi(x,t)\,\mathrm{d}x\,\mathrm{d}t \\ &\quad+ \varepsilon^2\iint_{\mathbb{R}/\mathbb{Z}\times(0,T)} u^{\Delta x}(x,t)D_+D_-^2\varphi(x,t)\,\mathrm{d}x\,\mathrm{d}t = o(1).\end{aligned}$$

The last term on the left hand side vanishes as $\varepsilon \to 0$. The 1-jet MV equation follows now immediately from the narrow convergence $\delta_{u^{\Delta x}(\cdot,\cdot)} \rightharpoonup \nu, \Delta x \to 0$. □

In the following sections, we shall similarly prove the 2-jet MV equation and the general k-jet MV equation for higher-dimensional Young measures associated with the implicit FDS. The proofs are going to be more technical but still of the same spirit.

4.3 2-jet MV Solution

We assume that the discrete 2-jet $J_2^{\Delta x}(x,t) = (u^{\Delta x}(x,t),\, \varepsilon D_+ u^{\Delta x}(x,t))$ is bounded in $L^\infty(\mathbb{R}/\mathbb{Z}\times(0,T))$ uniformly in Δx. We can then extract a subsequence $\Delta x_m \to 0$ such that $J_2^{\Delta x_m}$ converges narrowly to a two-dimensional Young measure $\nu^2 = (\nu_0^2, \nu_1^2)$:

$$\delta_{J_2^{\Delta x_m}(\cdot,\cdot)} \rightharpoonup \nu^2, \quad m \to \infty.$$

We call ν^2 the *two-dimensional Young measure associated with the implicit FDS*. We shall prove that ν^2 is a 2-jet MV solution if $\varepsilon = \Delta x^r, r < \frac{1}{4}$.

4.3.1 Auxiliary Lemmas for the 2-jet MV equation

We shall need two more auxiliary Lemmas of which the first was already stated in [11]:

Lemma 4.3.1 ([11], Lemma 3.2)**.**

$$\forall (v_j)_j, (w_j)_j : (D_0(v_j w_j), w_j)_{\Delta x} = \frac{\Delta x}{2}(D_+ v_j D_0 w_j, w_j)_{\Delta x} + \frac{1}{2}(w_{j-1} D_0 v_j, w_j)_{\Delta x}$$

Remark 4.3.1. *In fact, Lemma 4.3.1 is the very core of this thesis. A.Sjöberg also used it in [[17], p.575], and the main steps in the derivation of the essential Lemmas 4.3.2 and 4.4.2 below are based on it.*

Proof. Manipulate the right hand side using the definition of D_+, the discrete Leibniz rule $D_0(v_j w_j) = v_{j+1} D_0 w_j + w_{j-1} D_0 v_j$ and discrete integration by parts $(D_0 w_j, v_j w_j)_{\Delta x} = -(w_j, D_0(v_j w_j))_{\Delta x}$. □

Lemma 4.3.2.

$$\begin{aligned}\forall (v_j)_j : (D_+(6E v_j D_0 v_j), D_+ v_j)_{\Delta x} &= 2(D_+ v_j D_0 v_j, D_+ v_j)_{\Delta x} \\ &\quad + \Delta x (D_+ v_j D_0 D_+ v_j, D_+ v_j)_{\Delta x} \\ &\quad + (D_- v_j D_0 v_j, D_+ v_j)_{\Delta x}.\end{aligned}$$

Remark 4.3.2. *We would like to stress the importance of Lemma 4.3.2: It allows us to use the assumed boundedness of the discrete 2-jet for the term $(D_+(6E v_j D_0 v_j), D_+ v_j)_{\Delta x}$ which will appear when deriving weak BV properties below. Note in particular the Δx in front of the second term on the right hand side.*

Proof. First note that $6E v_j D_0 v_j = 2 v_j D_0 v_j + 2 D_0(v_j^2)$. This and the discrete Leibniz rule for D_+ yield

$$\begin{aligned}(D_+(6E v_j D_0 v_j), D_+ v_j)_{\Delta x} &= 2(D_+(v_j D_0 v_j), D_+ v_j)_{\Delta x} \\ &\quad + 2(D_+ D_0(v_j^2), D_+ v_j)_{\Delta x} \\ &= 2(D_+ v_j D_0 v_j, D_+ v_j)_{\Delta x} \\ &\quad + 2(v_{j+1} D_+ D_0 v_j, D_+ v_j)_{\Delta x} \\ &\quad + 2(D_0(D_+ v_j v_j), D_+ v_j)_{\Delta x} \\ &\quad + 2(D_0(D_+ v_j v_{j+1}), D_+ v_j)_{\Delta x}.\end{aligned}$$

Doing discrete integration by parts for D_0 in the last term, it cancels with the second term. The Lemma then follows by applying Lemma 4.3.1 to the third term. □

4.3.2 Weak BV for the 2-jet MV equation

As before, we shall need certain weak BV properties. In particular, for the 2-jet, we will need

$$\varepsilon^4 \sum_n ||D_+^3 u_{j,n}||_{\Delta x}^2 \Delta t \sum_n ||u_{j,n} - u_{j,n-1}||_{\Delta x}^2 \Delta t \to 0, \quad \Delta x \to 0,$$
$$\varepsilon^2 \sum_n ||D_+ u_{j+1,n} - D_+ u_{j,n}||_{\Delta x}^2 \Delta t \to 0, \quad \Delta x \to 0,$$
$$\varepsilon^2 \sum_n ||D_+^2 u_{j+1,n} - D_+^2 u_{j,n}||_{\Delta x}^2 \Delta t \to 0, \quad \Delta x \to 0.$$

Note that in the following, the constant C might change since we abstain from introducing a new name every time a new bounding constant comes up. We apply D_+ to the finite difference equation (36), multiply it with $D_+ u_{j,n}$ and sum over j. Using again the property $(D_+^2 D_- v_j, v_j)_{\Delta x} \geq 0$ and applying Lemma 4.3.2, we conclude that

$$\begin{aligned}\frac{1}{\Delta t}(D_+ u_{j,n}, D_+ u_{j,n} - D_+ u_{j,n-1})_{\Delta x} &= 2(D_+ u_{j,n} D_0 u_{j,n}, D_+ u_{j,n})_{\Delta x} \\ &\quad + \Delta x (D_+ u_{j,n} D_0 D_+ u_{j,n}, D_+ u_{j,n})_{\Delta x} \\ &\quad + (D_- u_{j,n} D_0 u_{j,n}, D_+ u_{j,n})_{\Delta x}.\end{aligned}$$

By the assumed L^∞-boundedness of the discrete 2-jet, we can find a constant C such that the right hand side is bounded by $\frac{C}{\varepsilon^3}$. Applying the identity $a(a-b) = \frac{1}{2}a^2 - \frac{1}{2}b^2 + \frac{1}{2}(a-b)^2$ for the left hand side, we get

$$||D_+ u_{j,n}||_{\Delta x}^2 - ||D_+ u_{j,n-1}||_{\Delta x}^2 + ||D_+ u_{j,n} - D_+ u_{j,n-1}||_{\Delta x}^2 \leq \frac{C\Delta t}{\varepsilon^3}.$$

Summing over n and exploiting the arising telescoping sum for the first two terms yields

$$\begin{aligned}\sum_n ||D_+ u_{j,n} - D_+ u_{j,n-1}||_{\Delta x}^2 \Delta t &\leq \frac{C\Delta t}{\varepsilon^3} + \Delta t ||D_+ u_{j,0}||_{\Delta x}^2 - \Delta t ||D_+ u_{j,n_{end}}||_{\Delta x}^2 \\ &\leq \frac{C\Delta t}{\varepsilon^3} + \Delta t ||u_0'||_{L^\infty}^2 \\ \Rightarrow \sum_n ||D_-^t D_+ u_{j,n}||_{\Delta x}^2 \Delta t &\leq \frac{C}{\Delta t\, \varepsilon^3}. \end{aligned} \tag{47}$$

Here, we again bring the finite difference equation (36) (whereto we applied D_+) into play to estimate its fourth order derivative term as

$$\begin{aligned}\sum_n ||\,\varepsilon^2 D_+^3 D_- u_{j,n}||_{\Delta x}^2 \Delta t &\leq 2 \sum_n ||D_+(6E u_{j,n} D_0 u_{j,n})||_{\Delta x}^2 \Delta t \\ &\quad + 2 \sum_n ||D_-^t D_+ u_{j,n}||_{\Delta x}^2 \Delta t. \end{aligned} \tag{48}$$

The second term on the right hand side is bounded by (47). For the first term, we apply the discrete Leibniz rule for D_+ and obtain two terms of which the first contains two first order derivatives and the second contains a second order derivative. Since we assume the discrete 2-jet to be bounded, we only have to worry about the second order derivative. Applying the Sobolev-type inequality (34) of Lemma 4.1.1 to $v_j = D_+ u_{j,n}$, we bound it by $\frac{C}{\varepsilon'} \sum_n ||D_+ u_{j,n}||_{\Delta x}^2 \Delta t + \varepsilon'^2 \sum_n ||D_+^4 u_{j,n}||_{\Delta x}^2 \Delta t$. Inserting everything into (48) and choosing $\varepsilon' \sim \varepsilon^2$ properly[6], this implies

$$\sum_n ||\,\varepsilon^2 D_+^4 u_{j,n}||_{\Delta x}^2 \Delta t \leq \frac{C}{\Delta t\, \varepsilon^3} + \frac{C}{\varepsilon^4}$$

[6] i.e. setting $\varepsilon' = c\,\varepsilon^2$ and choosing c properly

where we can neglect the last term because $\Delta t = o(\varepsilon)$.

At this point, we apply the Sobolev-type inequality (35) of Lemma 4.1.1 to $v_j = D_+ u_{j,n}$ and obtain by the above inequality:

$$\begin{aligned}\sum_n ||D_+^3 u_{j,n}||_{\Delta x}^2 \Delta t &\leq \frac{C}{\varepsilon'^2} \sum_n ||D_+ u_{j,n}||_{\Delta x}^2 \Delta t + \frac{C\,\varepsilon'}{\Delta t\,\varepsilon^7} \\ &\leq \frac{C}{\varepsilon'^2\,\varepsilon^2} + \frac{C\,\varepsilon'}{\Delta t\,\varepsilon^7}. \end{aligned} \tag{49}$$

We are now ready to state the following Lemma:

Lemma 4.3.1 (Weak BV for 2-jet)**.** *Let $J_2^{j,n} = (u_{j,n}, \varepsilon D_+ u_{j,n})$ be the discrete 2-jet computed by the scheme* (36)*. Assuming it to be uniformly bounded in L^∞ and fixing the rate $\varepsilon = \Delta x^r$ at some $r < \frac{1}{4}$, we have the following weak BV properties:*

$$\begin{aligned}\varepsilon^4 \sum_n ||D_+^3 u_{j,n}||_{\Delta x}^2 \Delta t \sum_n ||u_{j,n} - u_{j,n-1}||_{\Delta x}^2 \Delta t \to 0, \quad \Delta x \to 0, \\ \varepsilon^2 \sum_n ||D_+ u_{j+1,n} - D_+ u_{j,n}||_{\Delta x}^2 \Delta t \to 0, \quad \Delta x \to 0, \\ \varepsilon^2 \sum_n ||D_+^2 u_{j+1,n} - D_+^2 u_{j,n}||_{\Delta x}^2 \Delta t \to 0, \quad \Delta x \to 0.\end{aligned}$$

Proof. By the Sobolev-type inequality (35) (setting $\varepsilon' = 1$) of Lemma 4.1.1, the quantity $\sum_n ||D_+^2 u_{j,n}||_{\Delta x}^2 \Delta t$ satisfies the same bound as in (49). We therefore have the two bounds

$$\begin{aligned}\varepsilon^2 \sum_n ||D_+ u_{j+1,n} - D_+ u_{j,n}||_{\Delta x}^2 \Delta t \leq \frac{C\Delta x^2}{\varepsilon'^2} + \frac{C\,\varepsilon'\Delta x}{\varepsilon^5}, \\ \varepsilon^2 \sum_n ||D_+^2 u_{j+1,n} - D_+^2 u_{j,n}||_{\Delta x}^2 \Delta t \leq \frac{C\Delta x^2}{\varepsilon'^2} + \frac{C\,\varepsilon'\Delta x}{\varepsilon^5}.\end{aligned}$$

Also, by (49) and (42), we have

$$\varepsilon^4 \sum_n ||D_+^3 u_{j,n}||_{\Delta x}^2 \Delta t \sum_n ||u_{j,n} - u_{j,n-1}||_{\Delta x}^2 \Delta t \leq \frac{C\Delta x\,\varepsilon^2}{\varepsilon'^2} + \frac{C\,\varepsilon'}{\varepsilon^3}.$$

The Lemma follows if these three bounds vanish as $\Delta x \to 0$. Since $r < \frac{1}{4} < \frac{1}{2}$ and therefore $\Delta x = o(\varepsilon^2)$, the first two bounds are dominated by the third one. Setting $\varepsilon' = \Delta x^s$ and $\varepsilon = \Delta x^r$, we write this last bound as

$$C(\Delta x^{1+2r-2s} + \Delta x^{s-3r}).$$

Since s is arbitrary, we can make this vanish as $\Delta x \to 0$ if $r < \frac{1}{4}$. □

4.3.3 Proof of 2-jet MV equation

We are now ready to prove the 2-jet MV equation for the 2-dimensional limit measure $\nu^2 = (\nu_0^2, \nu_1^2)$ associated with the implicit FDS:

Theorem 4.3.1 (2-jet MV equation)**.** *Let $\nu^2 = (\nu_0^2, \nu_1^2)$ be the two-dimensional Young measure associated with the implicit FDS, i.e. $\delta_{J_2^{\Delta x}(\cdot,\cdot)} \rightharpoonup \nu^2, \Delta x \to 0$. Assuming $J_2^{\Delta x}$ to be uniformly bounded in $L^\infty(\mathbb{R}/\mathbb{Z} \times (0,T))$ and fixing the rate $\varepsilon = \Delta x^r$ at some*

$r < \frac{1}{4}$, ν^2 will be a 2-jet MV solution. In other words, ν^2 satisfies the 2-jet MV equation[7]

$$\iint_{\mathbb{R}/\mathbb{Z}\times(0,T)} \varphi_t(x,t)\langle \nu^2_{(x,t)}, \xi_0^2/2\rangle \,\mathrm{d}x\,\mathrm{d}t - \iint_{\mathbb{R}/\mathbb{Z}\times(0,T)} \varphi_x(x,t)\langle \nu^2_{(x,t)}, 2\xi_0^3 + 3\xi_1^2/2\rangle \,\mathrm{d}x\,\mathrm{d}t = 0$$

for all test functions $\varphi \in C_c^\infty(\mathbb{R}/\mathbb{Z}\times(0,T))$, and therefore is a 2-jet MV solution.

For the following proofs, we introduce the following terminology: We say that a discrete function $v_{j,n}$ vanishes *in the sense of distributions (i.t.s.o.d.)* if for all test functions $\varphi \in C_c^\infty(\mathbb{R}/\mathbb{Z}\times(0,T))$:

$$\sum_{j,n} v_{j,n}\varphi_{j,n}\Delta x\Delta t \to 0, \quad \Delta x \to 0$$

where $\varphi_{j,n} = \frac{1}{\Delta x\Delta t}\int_{x_j}^{x_{j+1}}\int_{t_n}^{t_{n+1}} \varphi(x,t)\,\mathrm{d}x\,\mathrm{d}t$ are the local averages.

Proof. The strategy of the proof is to do the same manipulations as at the end of subsection 3.4.1 discretely. The difficulties arise whenever having to apply the Leibniz rule in the discrete setting. The arising errors must be shown to vanish i.t.s.o.d. which is why we need the weak BV properties. Since we don't want to worry about this issue when dealing with the time derivative term, we make sure that we can apply the discrete Leibniz rule for the discrete time derivative *exactly*.

We multiply the finite difference equation (36) with $\frac{u_{j,n-1}+u_{j,n}}{2}$ and directly apply the discrete Leibniz rule to the first term:

$$\frac{1}{2}D_-^t(u_{j,n}^2) - 6Eu_{j,n}D_0u_{j,n}\frac{u_{j,n-1}+u_{j,n}}{2} + \varepsilon^2 D_+^2D_-u_{j,n}\frac{u_{j,n-1}+u_{j,n}}{2} = 0.$$

Next, we want to get rid of the $u_{j,n-1}$'s in the second and third term. It is mainly for this step that we need the weak BV properties. We write

$$\frac{1}{2}D_-^t(u_{j,n}^2) - 6Eu_{j,n}D_0u_{j,n}u_{j,n} + R_{j,n}^{(1)} + \varepsilon^2 D_+^2D_-u_{j,n}u_{j,n} + R_{j,n}^{(2)} = 0 \tag{50}$$

where

$$R_{j,n}^{(1)} = 6Eu_{j,n}D_0u_{j,n}\frac{u_{j,n}-u_{j,n-1}}{2},$$
$$R_{j,n}^{(2)} = \varepsilon^2 D_+^2D_-u_{j,n}\frac{u_{j,n-1}-u_{j,n}}{2}.$$

The error $R_{j,n}^{(2)}$ vanish i.t.s.o.d. by the first weak BV property of Lemma 4.3.1. The same is true for $R_{j,n}^{(1)}$ because of the boundedness of the 2-jet and inequality (42).

We turn to the second term of equation (50). First, we write it as an exact discrete derivative by noting that $6Ev_jD_0v_jv_j = D_+(v_j^2v_{j-1}+v_jv_{j-1}^2)$. To get rid of all j-index shifts, we write

$$6Eu_{j,n}D_0u_{j,n}u_{j,n} = D_+(2u_{j,n}^3) + D_+R_{j,n}^{(3)},$$
$$R_{j,n}^{(3)} = u_{j,n}^2u_{j-1,n} + u_{j,n}u_{j-1,n}^2 - 2u_{j,n}^3$$

where $D_+R_{j,n}^{(3)}$ vanishes i.t.s.o.d. by similar arguments as above.

[7] See the end of subsection 3.4.1 for the derivation of U_2, F_2.

Finally, we approach the third order derivative term of equation 50. We do the following manipulations applying the discrete Leibniz rule several times:

$$\begin{aligned} D_+^2 D_- v_j v_j &= D_-(D_+^2 v_j v_{j+1}) - D_+^2 v_j D_+ v_j \\ D_+^2 v_j v_{j+1} &= D_+(D_+ v_j v_j) - (D_+ v_j)^2 \\ D_+^2 v_j D_+ v_j &= \underbrace{D_+ D_- v_{j+1} D_0 v_{j+1}}_{=\frac{1}{2} D_+((D_+ v_j)^2)} + D_+ D_- v_{j+1} \underbrace{(D_- v_{j+1} - D_0 v_{j+1})}_{=\frac{1}{2}(D_- v_{j+1} - D_+ v_{j+1})}. \end{aligned}$$

Therefore, we conclude that

$$\begin{aligned} \varepsilon^2 D_+^2 D_- v_j v_j = &-D_-((\varepsilon D_+ v_j)^2) - \frac{1}{2} D_+((\varepsilon D_+ v_j)^2) \\ &+ \varepsilon^2 D_- D_+(D_+ v_j v_j) - \frac{1}{2}\varepsilon^2 D_+ D_- v_{j+1}(D_- v_{j+1} - D_+ v_{j+1}) \end{aligned}$$

where the last two terms vanish i.t.s.o.d.: For the third term, this follows quickly by the boundedness of the 2-jet. For the fourth term, we apply discrete integration by parts once to get rid of the second derivative term and apply the last two weak BV properties of Lemma 4.3.1.

Taking everything together, we have derived the following discrete 2-jet equation:

$$\frac{1}{2} D_-^t(u_{j,n}^2) - D_+(2u_{j,n}^3) - D_-((\varepsilon D_+ u_{j,n})^2) - \frac{1}{2} D_+((\varepsilon D_+ u_{j,n})^2) = R_{j,n} \qquad (51)$$

where $R_{j,n}$ vanishes i.t.s.o.d. Multiplying (51) with $\varphi_{j,n}$, summing over j, n and doing discrete integration by parts, we get the following integral equation:

$$\begin{aligned} &\iint_{\mathbb{R}/\mathbb{Z}\times(0,T)} \frac{(u^{\Delta x}(x,t))^2}{2} D_+^t \varphi(x,t)\,\mathrm{d}x\,\mathrm{d}t \\ &\quad - \iint_{\mathbb{R}/\mathbb{Z}\times(0,T)} 2(u^{\Delta x}(x,t))^3 D_-\varphi(x,t)\,\mathrm{d}x\,\mathrm{d}t \\ &\quad - \iint_{\mathbb{R}/\mathbb{Z}\times(0,T)} \frac{3(\varepsilon D_+ u^{\Delta x}(x,t))^2}{2} \frac{D_-\varphi(x,t) + 2D_+\varphi(x,t)}{3}\,\mathrm{d}x\,\mathrm{d}t = o(1). \end{aligned}$$

The 2-jet MV equation follows now immediately from the narrow convergence $\delta_{J_2^{\Delta x}(\cdot,\cdot)} \rightharpoonup \nu^2, \Delta x \to 0$. □

4.4 Generalization: k-jet MV Solutions

In this section, we generalize the results of the previous sections about the 1- resp. 2-jet to general k-jets: We assume that the discrete k-jet

$$J_k^{\Delta x}(x,t) = (u^{\Delta x}(x,t), \dots \varepsilon^{k-1} D_+^{k-1} u^{\Delta x}(x,t))$$

is bounded in $L^\infty(\mathbb{R}/\mathbb{Z}\times(0,T))$ uniformly in Δx. We can then extract a subsequence $\Delta x_m \to 0$ such that $J_k^{\Delta x}$ converges narrowly to a k-dimensional Young measure $\nu^k = (\nu_0^k, \dots \nu_{k-1}^k)$:

$$\delta_{J_k^{\Delta x_m}(\cdot,\cdot)} \rightharpoonup \nu^k, \quad m \to \infty.$$

We call ν^k the *k-dimensional Young measure associated with the implicit FDS.* We shall prove that ν^k is a k-jet MV solution if $\varepsilon = \Delta x^r$ and r small enough.

4.4.1 Auxiliary Lemmas for the k-jet MV equation

To prove the weak BV properties that are necessary for the general case, we also need general Lemmas: The first is a generalization of the discrete Leibniz rule and the second is a generalization of Lemma 4.3.2.

Lemma 4.4.1 (Discrete Leibniz)**.** *Let $m \geq 0$. Then:*

$$D_+^m(v_j w_j) = \sum_{l=0}^{m} \begin{pmatrix} m \\ l \end{pmatrix} D_+^{m-l} v_{j+l} D_+^l w_j.$$

Proof. By induction: For $m = 0$, the Lemma is trivial. For the induction step $m \to m+1$, we compute

$$\begin{aligned}
D_+^{m+1}(v_j w_j) &= D_+ \sum_{l=0}^{m} \begin{pmatrix} m \\ l \end{pmatrix} D_+^{m-l} v_{j+l} D_+^l w_j \\
&= \sum_{l=0}^{m} \begin{pmatrix} m \\ l \end{pmatrix} D_+^{m+1-l} v_{j+l} D_+^l w_j + \sum_{l=0}^{m} \begin{pmatrix} m \\ l \end{pmatrix} D_+^{m-l} v_{j+l+1} D_+^{l+1} w_j \\
&= \sum_{l=0}^{m} \begin{pmatrix} m \\ l \end{pmatrix} D_+^{m+1-l} v_{j+l} D_+^l w_j + \sum_{l=1}^{m+1} \begin{pmatrix} m \\ l-1 \end{pmatrix} D_+^{m+1-l} v_{j+l} D_+^l w_j \\
&= \sum_{l=0}^{m+1} \begin{pmatrix} m+1 \\ l \end{pmatrix} D_+^{m+1-l} v_{j+l} D_+^l w_j.
\end{aligned}$$

□

Lemma 4.4.2. *Let $k \geq 1$. Assume uniform L^∞-boundedness of the discrete k-jet $J_k^{j,n}$. Then, $\exists C > 0$ s.t. $\forall \Delta x, \forall n$:*

$$\left| \left(D_+^{k-1}(E u_{j,n} D_0 u_{j,n}), D_+^{k-1} u_{j,n} \right)_{\Delta x} \right| \leq \frac{C}{\varepsilon^{2k-1}}.$$

Proof. For the case $k = 1$, we have already seen that $\sum_j E v_j D_0 v_j v_j = 0$.

Now let $k \geq 2$. Since $3 E v_j D_0 v_j = D_0(v_j^2) + v_j D_0 v_j$ and by the above Leibniz-Lemma 4.4.1, we have

$$\begin{aligned}
&3(D_+^{k-1}(E u_{j,n} D_0 u_{j,n}), D_+^{k-1} u_{j,n})_{\Delta x} \\
&\quad = (D_+^{k-1} D_0(u_{j,n}^2), D_+^{k-1} u_{j,n})_{\Delta x} + (D_+^{k-1}(u_{j,n} D_0 u_{j,n}), D_+^{k-1} u_{j,n})_{\Delta x} \\
&\quad = \sum_{l=0}^{k-2} \begin{pmatrix} k-1 \\ l \end{pmatrix} \left(D_0(D_+^{k-1-l} u_{j+l,n} D_+^l u_{j,n}), D_+^{k-1} u_{j,n} \right)_{\Delta x} \\
&\qquad\quad + \left(D_0(u_{j+k-1,n} D_+^{k-1} u_{j,n}), D_+^{k-1} u_{j,n} \right)_{\Delta x} \\
&\qquad + \sum_{l=0}^{k-2} \begin{pmatrix} k-1 \\ l \end{pmatrix} \left(D_+^{k-1-l} u_{j+l,n} D_0 D_+^l u_{j,n}, D_+^{k-1} u_{j,n} \right)_{\Delta x} \\
&\qquad\quad + \left(u_{j+k-1,n} D_0 D_+^{k-1} u_{j,n}, D_+^{k-1} u_{j,n} \right)_{\Delta x}.
\end{aligned}$$

Doing discrete integration by parts for D_0, we see that the second and fourth term

cancel. Therefore, writing the first summand of the first sum separately, we get

$$\begin{aligned}
&3(D_+^{k-1}(Eu_{j,n}D_0u_{j,n}), D_+^{k-1}u_{j,n})_{\Delta x} \\
&\quad = (D_0(D_+^{k-1}u_{j,n}u_{j,n}), D_+^{k-1}u_{j,n})_{\Delta x} \\
&\qquad + \sum_{l=1}^{k-2} \begin{pmatrix} k-1 \\ l \end{pmatrix} \left(D_0(D_+^{k-1-l}u_{j+l,n}D_+^l u_{j,n}), D_+^{k-1}u_{j,n}\right)_{\Delta x} \\
&\qquad + \sum_{l=0}^{k-2} \begin{pmatrix} k-1 \\ l \end{pmatrix} \left(D_+^{k-1-l}u_{j+l,n}D_0D_+^l u_{j,n}, D_+^{k-1}u_{j,n}\right)_{\Delta x}.
\end{aligned}$$

Note that all derivatives appearing in the two sums are of order $\leq k-1$. Therefore, by the assumed L^∞-boundedness of the discrete k-jet, they can be bounded by $\frac{C}{\varepsilon^{2k-1}}$. To treat the first term on the right hand side, we use (and here is the point) Lemma 4.3.1 which yields in this case

$$\begin{aligned}
(D_0(D_+^{k-1}u_{j,n}u_{j,n}), D_+^{k-1}u_{j,n})_{\Delta x} = &\frac{\Delta x}{2}(D_+u_{j,n}D_0D_+^{k-1}u_{j,n}, D_+^{k-1}u_{j,n})_{\Delta x} \\
&+ \frac{1}{2}(D_+^{k-1}u_{j-1,n}D_0u_{j,n}, D_+^{k-1}u_{j,n})_{\Delta x}
\end{aligned}$$

which can also be bounded by $\frac{C}{\varepsilon^{2k-1}}$ due to the Δx in front of the first term. □

4.4.2 Weak BV for the k-jet MV equation

We generalize the weak BV results of Lemma 4.3.1 in the following

Lemma 4.4.1 (Weak BV for k-jet)**.** *Let*

$$J_k^{j,n} = (u_{j,n}, \dots \varepsilon^{k-1}D_+^{k-1}u_{j,n})$$

be the discrete k-jet computed by the scheme (36)*. Assuming it to be uniformly bounded in L^∞, we have the following weak BV properties:*

$$\forall l_1, l_2 \leq k+1: \quad \left|\varepsilon^m \sum_{j,n} |D_+^{l_1}u_{j+j_0,n}(D_+^{l_2}u_{j+1,n} - D_+^{l_2}u_{j,n})|\Delta x\Delta t\right| \to 0,$$

$$\forall l_1 \leq k+1, l_2 \leq k-1: \quad \left|\varepsilon^m \sum_{j,n} |D_+^{l_1}u_{j+j_0,n}(D_+^{l_2}u_{j,n} - D_+^{l_2}u_{j,n-1})|\Delta x\Delta t\right| \to 0,$$

as $\Delta x \to 0$, provided we fix the rate $\varepsilon = \Delta x^r$ at some $r < \frac{1}{6(l_1+l_2)+1-6m}$.

Proof. We shall do essentially the same steps as in subsection 4.3.2 but with higher derivatives. We apply D_+^{k-1} to the finite difference equation (36), multiply with $D_+^{k-1}u_{j,n}$ and sum over j. Using again the property $(D_+^2D_-v_j, v_j)_{\Delta x} \geq 0$ for the third order term, the bound of Lemma 4.4.2 for the nonlinear term, and the equality $a(a-b) = \frac{1}{2}a^2 - \frac{1}{2}b^2 + \frac{1}{2}(a-b)^2$ for the time derivative term, we conclude that

$$||D_+^{k-1}u_{j,n}||_{\Delta x}^2 - ||D_+^{k-1}u_{j,n-1}||_{\Delta x}^2 + ||D_+^{k-1}u_{j,n} - D_+^{k-1}u_{j,n-1}||_{\Delta x}^2 \leq \frac{C\Delta t}{\varepsilon^{2k-1}}.$$

Summing over n and exploiting the arising telescoping sum for the first two terms yields

$$\begin{aligned}
\sum_n ||D_+^{k-1}u_{j,n} - D_+^{k-1}u_{j,n-1}||_{\Delta x}^2\Delta t &\leq \frac{C\Delta t}{\varepsilon^{2k-1}} + \Delta t||D_+^{k-1}u_{j,0}||_{\Delta x}^2 \\
&\quad - \Delta t||D_+^{k-1}u_{j,n_{end}}||_{\Delta t}^2 \\
&\leq \frac{C\Delta t}{\varepsilon^{2k-1}} + \Delta t||u_0^{(k-1)}||_{L^\infty}^2 \\
\Rightarrow \sum_n ||D_+^{k-1}D_-^t u_{j,n}||_{\Delta t}^2\Delta t &\leq \frac{C}{\Delta t\,\varepsilon^{2k-1}}. \qquad (52)
\end{aligned}$$

Here, we again bring the finite difference equation (36) (whereto we applied D_+^{k-1}) into play to estimate its highest order derivative term as

$$\sum_n ||\,\varepsilon^2 D_+^{k+2} u_{j,n}||_{\Delta x}^2 \Delta t \le 2\sum_n ||D_+^{k-1}(6Eu_{j,n} D_0 u_{j,n})||_{\Delta x}^2 + 2\sum_n ||D_+^{k-1} D_-^t u_{j,n}||_{\Delta x}^2. \tag{53}$$

The second term on the right hand side is bounded by (52). For the first term, we use the discrete Leibniz rule of Lemma 4.4.1:

$$\begin{aligned}\sum_n ||D_+^{k-1}(Eu_{j,n} D_0 u_{j,n})||_{\Delta x}^2 \Delta t &\le C\sum_{l=0}^{k-1}\sum_n ||D_+^{k-1-l} Eu_{j+l,n} D_+^l D_0 u_{j,n}||_{\Delta x}^2 \Delta t \\ &= C\sum_{l=0}^{k-2}\sum_n ||D_+^{k-1-l} Eu_{j+l,n} D_+^l D_0 u_{j,n}||_{\Delta x}^2 \Delta t \\ &\quad + C\sum_n ||Eu_{j+k-1,n} D_+^{k-1} D_0 u_{j,n}||_{\Delta x}^2 \Delta t.\end{aligned}$$

Note that in the first sum, only derivatives of order $\le k-1$ appear. By the assumed boundedness of the k-jet, it can therefore be bounded by $\frac{C}{\varepsilon^{2k}}$. For the second term, we apply the Sobolev-type inequality (34) of Lemma 4.1.1 to $v_j = D_+^{k-1} u_{j,n}$:

$$\begin{aligned}\sum_n ||Eu_{j+k-1,n} D_+^{k-1} D_0 u_{j,n}||_{\Delta x}^2 \Delta t &\le C\sum_n ||D_+^k u_{j,n}||_{\Delta x}^2 \Delta t \\ &\le \frac{C}{\varepsilon'}\sum_n \underbrace{||D_+^{k-1} u_{j,n}||_{\Delta x}^2}_{\le \frac{C}{\varepsilon^{2k-2}}} \Delta t \\ &\quad + \varepsilon'^2 \sum_n ||D_+^{k+2} u_{j,n}||_{\Delta x}^2 \Delta t.\end{aligned}$$

Inserting this into (53) and choosing $\varepsilon' \sim \varepsilon^2$ properly[8], we conclude that

$$\sum_n ||D_+^{k+2} u_{j,n}||_{\Delta x}^2 \Delta t \le \frac{C}{\Delta t\, \varepsilon^{2k+3}} + \frac{C}{\varepsilon^{2k+4}} \tag{54}$$

where we can neglect the last term because $\Delta t = o(\varepsilon)$.

Since k is actually arbitrary, we conclude that

$$\begin{aligned}\forall 3 \le l \le k+2: \quad &\sum_n ||D_+^l u_{j,n}||_{\Delta x}^2 \Delta t \le \frac{C}{\Delta t\, \varepsilon^{2l-1}} \\ \Rightarrow \forall 2 \le l \le k+1: \quad &\sum_n ||D_+^l u_{j+1,n} - D_+^l u_{j,n}||_{\Delta x}^2 \Delta t \le \frac{C\Delta x}{\varepsilon^{2l+1}}.\end{aligned} \tag{55}$$

Furthermore, by the Sobolev-type inequality (35) of Lemma 4.1.1, we get

$$\begin{aligned}\sum_n ||D_+^{k+1} u_{j,n}||_{\Delta x}^2 \Delta t &\le \frac{C}{\varepsilon'^2}\sum_n ||D_+^{k-1} u_{j,n}||_{\Delta x}^2 \Delta t \\ &\quad + \varepsilon' \sum_n ||D_+^{k+2} u_{j,n}||_{\Delta x}^2 \Delta t \\ &\le \frac{C}{\varepsilon'^2\, \varepsilon^{2k-2}} + \frac{C\,\varepsilon'}{\Delta t\, \varepsilon^{2k+3}}\end{aligned}$$

[8] i.e. setting $\varepsilon' = c\,\varepsilon^2$ and choosing c properly

which, because k is arbitrary, again implies that

$$\forall 2 \le l \le k+1: \quad \sum_n ||D_+^l u_{j,n}||_{\Delta x}^2 \Delta t \le \frac{C}{\varepsilon'^2\, \varepsilon^{2l-4}} + \frac{C\,\varepsilon'}{\Delta t\, \varepsilon^{2l+1}}. \tag{56}$$

Since ε' is arbitrary, the Lemma now follows by the Cauchy-Schwartz inequality and inequalities (52),(55) and (56) (note that (52) can also be generalized because k is arbitrary). □

4.4.3 Proof of k-jet MV equation

We are now ready to prove the k-jet MV equation for the k-dimensional limit measure $\nu^k = (\nu_0^k, \dots \nu_{k-1}^k)$ associated with the implicit FDS:

Theorem 4.4.1 (k-jet MV equation)**.** *Let $\nu^k = (\nu_0^k, \dots \nu_{k-1}^k)$ be the k-dimensional Young measure associated with the implicit FDS, i.e. $\delta_{J_k^{\Delta x}(\cdot,\cdot)} \rightharpoonup \nu^k, \Delta x \to 0$. Assuming $J_k^{\Delta x}$ to be uniformly bounded in $L^\infty(\mathbb{R}/\mathbb{Z} \times (0,T))$ and fixing the rate $\varepsilon = \Delta x^r$ at some small enough r, ν^k will be a k-jet MV solution. In other words, ν^k satisfies the k-jet MV equations*[9]

$$\begin{aligned}\forall 1 \le l \le k: \quad & \iint_{\mathbb{R}/\mathbb{Z}\times(0,T)} \varphi_t(x,t) \langle \nu^k_{(x,t)}, U_l \rangle \,\mathrm{d}x\,\mathrm{d}t \\ & + \iint_{\mathbb{R}/\mathbb{Z}\times(0,T)} \varphi_x(x,t) \langle \nu^k_{(x,t)}, F_l \rangle \,\mathrm{d}x\,\mathrm{d}t = 0\end{aligned}$$

for all test functions $\varphi \in C_c^\infty(\mathbb{R}/\mathbb{Z} \times (0,T))$, and therefore is a k-jet MV solution.

Proof. The strategy of this proof is actually different then the proofs of Theorems 4.2.1 and 4.3.1. For instance in the case of the 2-jet, we started with the finite difference equation (36) and then derived the discrete 2-jet equation (51). In each step of the derivation, we made sure that the arising errors vanish i.t.s.o.d. We have seen that this approach brings up some technicalities involving discrete Leibniz manipulations. To do the general case, it is actually easier to start with the discrete k-jet equation and then prove that the error vanishes i.t.s.o.d.

Let

$$\partial_t U_l + \partial_x F_l + \partial_x^2 W_l = 0 \tag{57}$$

be the KdV conservation law as in Lemma 3.4.1. Remember that U_l is a polynomial of the $l-1$-jet, F_l is a polynomial of the l-jet, and W_l vanishes in the sense of distributions. We define the discrete quantities

$$\begin{aligned} U_{j,n} &:= U_l(u_{j,n}, \dots \varepsilon^{l-2} D_+^{l-2} u_{j,n}), \\ F_{j,n} &:= F_l(u_{j,n}, \dots \varepsilon^{l-1} D_+^{l-1} u_{j,n}), \\ W_{j,n} &:= W_l(u_{j,n}, \dots \varepsilon^{l-1} D_+^{l-1} u_{j,n}), \end{aligned}$$

and write down the *discrete l-jet equation* as

$$D_-^t U_{j,n} + D_+ F_{j,n} + D_+^2 W_{j,n} =: R_{j,n}. \tag{58}$$

Our goal is to prove that $R_{j,n}$ vanishes i.t.s.o.d.

[9] see Remark 3.4.1

Let $\varepsilon^{i_1+\cdots i_m} D_+^{i_1} u_{j,n} \cdots D_+^{i_m} u_{j,n}$ be a term of $U_{j,n}$. Using the discrete Leibniz rule[10] and inserting the scheme (36), we compute:

$$\begin{aligned} D_-^t(D_+^{i_1} u_{j,n} \cdots D_+^{i_m} u_{j,n}) &= \sum_{\beta=1}^{m} D_+^{i_1} u_{j,n-1} \cdots D_-^t D_+^{i_\beta} u_{j,n} \cdots D_+^{i_m} u_{j,n} \\ &= \sum_{\beta=1}^{m} D_+^{i_1} u_{j,n-1} \cdots D_+^{i_\beta} (6Eu_{j,n} D_0 u_{j,n}) \cdots D_+^{i_m} u_{j,n} \\ &\quad - \varepsilon^2 \sum_{\beta=1}^{m} D_+^{i_1} u_{j,n-1} \cdots D_+^{i_\beta} D_+^2 D_- u_{j,n} \cdots D_+^{i_m} u_{j,n}. \end{aligned}$$

Note that $i_1, \dots i_m \leq l-2 \leq k-2$. Therefore, by the second weak BV property derived in Lemma (4.4.1), we can get rid of the n-index shifts:

$$\begin{aligned} D_-^t(D_+^{i_1} u_{j,n} \cdots D_+^{i_m} u_{j,n}) &= \sum_{\beta=1}^{m} D_+^{i_1} u_{j,n} \cdots D_+^{i_\beta} (6Eu_{j,n} D_0 u_{j,n}) \cdots D_+^{i_m} u_{j,n} \\ &\quad - \varepsilon^2 \sum_{\beta=1}^{m} D_+^{i_1} u_{j,n} \cdots D_+^{i_\beta} D_+^2 D_- u_{j,n} \cdots D_+^{i_m} u_{j,n} \\ &\quad + R_{j,n}^{(1)} \end{aligned}$$

where $R_{j,n}^{(1)}$ vanishes i.t.s.o.d. provided that $\varepsilon = \Delta x^r$ and r small enough. Applying the discrete Leibniz rule once more for the first term on the right hand side, we conclude that $D_-^t U_{j,n}$ is a polynomial of $u_{j,n}, \dots D_+^{l+1} u_{j,n}$ and j-shifts thereof, i.e. there is a polynomial Q^U such that

$$D_-^t U_{j,n} = \underbrace{Q^U((u_{j+j',n})_{j'}, \dots (D_+^{l+1} u_{j+j',n})_{j'})}_{=:Q_{j,n}^U} + R_{j,n}^{(1)}.$$

Even simpler considerations imply that also for $D_+ F_{j,n} + D_+^2 W_{j,n}$, there is a polynomial Q^{FW} such that

$$D_+ F_{j,n} + D_+^2 W_{j,n} = \underbrace{Q^{FW}((u_{j+j',n})_{j'}, \dots (D_+^{l+1} u_{j+j',n})_{j'})}_{=:Q_{j,n}^{FW}}.$$

We now make the following crucial observation: If we replaced each discrete derivative with a continuous one and each $u_{j+j',n}$ with $u(x_j, t_n)$, the two quantities Q^U and Q^{FW} would add up to zero by (57). Therefore, we can estimate the discrete quantity $Q_{j,n}^U + Q_{j,n}^{FW}$ by comparing pairwise terms

$$D_+^{i_1} u_{j+j'_1,n} \cdots D_+^{i_m} u_{j+j'_m,n} - D_+^{i_1} u_{j+j''_1,n} \cdots D_+^{i_m} u_{j+j''_m,n} \tag{59}$$

where only the j-shifts are different. Note that the rank of $\partial_x F_l + \partial_x^2 W_l$ is $l + \frac{3}{2}$ (see subsection 3.4.1). Assume that $i_1 \geq \cdots \geq i_m$. If i_3 exists, it must therefore satisfy $i_3 \leq \frac{2l-3}{3} \leq k-1$, and therefore each factor $D_+^{i_\beta} u_{j+j'_\beta,n}$ resp. $D_+^{i_\beta} u_{j+j''_\beta,n}$ with $\beta \geq 3$ is bounded by the assumed boundedness of the discrete k-jet. Since furthermore $i_1, \dots i_m \leq l+1 \leq k+1$, we can estimate the above difference (59) by the first weak

[10] Using the discrete Leibniz rule iteratively, one can quickly see that

$$D_-^t(v_n^{(1)} \cdots v_n^{(m)}) = \sum_{\beta=1}^{m} v_{n-1}^{(1)} \cdots v_{n-1}^{(\beta-1)} D_-^t v_n^{(\beta)} v_n^{(\beta+1)} \cdots v_n^{(m)}.$$

BV property of Lemma 4.4.1. This proves that the error $R_{j,n}$ in the discrete k-jet equation (58) vanishes i.t.s.o.d.

The rest of the proof is now standard: We multiply the discrete k-jet equation (58) with $\varphi_{j,n}$, sum over j, n and do discrete integration by parts to obtain the integral equation

$$\iint_{\mathbb{R}/\mathbb{Z}\times(0,T)} U_l^{\Delta x}(x,t) D_+^t \varphi(x,t)\,\mathrm{d}x\,\mathrm{d}t + \iint_{\mathbb{R}/\mathbb{Z}\times(0,T)} F_l^{\Delta x}(x,t) D_- \varphi(x,t)\,\mathrm{d}x\,\mathrm{d}t = o(1)$$

where $U_l^{\Delta x}(x,t) = U_l(J_{l-1}^{\Delta x}(x,t))$ and $F_l^{\Delta x}(x,t) = F_l(J_l^{\Delta x}(x,t))$. The k-jet MV equations follow now immediately from the narrow convergence $\delta_{J_k^{\Delta x}(\cdot,\cdot)} \rightharpoonup \nu^k, \Delta x \to 0$. □

4.5 Interpretation of the Theoretical Result

We have seen that the k-dimensional Young measure associated with the implicit FDS is a k-jet MV solution provided that the rate $\varepsilon = \Delta x^r$ is slow enough. In fact, we have seen that being a k-jet MV solution requires $r \to 0$ as $k \to \infty$. It seems therefore that it is not possible to satisfy the whole infinite DiPerna characterization with a fixed polynomial rate. Also, we have seen in subsection 4.1.4 that we are approximating the modified equation

$$u_t - 6uu_x + \underbrace{\varepsilon^2}_{=:\mu_{disp}} u_{xxx} + \underbrace{\frac{\varepsilon^2 \Delta x}{2}}_{=:\mu_{diff}} u_{xxxx} = 0$$

rather than the KdV equation $u_t - 6uu_x + \varepsilon^2 u_{xxx} = 0$. This indicates that we are computing a MV solution of Burgers' equation which is the result of both dispersive *and diffusive* regularization! The smaller the rate r is, the smaller the diffusion coefficient μ_{diff} becomes compared to the dispersion coefficient μ_{disp}. More precisely, we consider the diffusion coefficient μ_{diff} to be a power of μ_{disp}:

$$\mu_{diff} = c\mu_{disp}^s.$$

We presume that as the rate s tends to infinity, the limit of the above dispersive-diffusive equation is the VDL. In our case, we can quickly verify that $s = \frac{1+2r}{2r}$ and thus $s \to \infty$ as $r \to 0$. This indicates that for each rate r, the Young measure associated with the implicit FDS might be different, but that we get closer and closer to the VDL as $r \to 0$.

There is also another interpretation of why we need a slow rate $\varepsilon = \Delta x^r$. The VDL is measure valued as a consequence of KdV oscillations which occur after a certain break time which is independent of ε and whose frequency is $O(\varepsilon^{-1})$. Therefore, computing the VDL depends on approximating these oscillations as accurately as possible. For a fixed ε, our scheme converges to the KdV solution as $\Delta x \to 0$. Thus, we interpret the above theoretical results as follows: *A slower rate $\varepsilon = \Delta x^r$ means a better resolution of the KdV equation and therefore makes for a better approximation of the VDL.* This interpretation is not only consistent with our theoretical results, but also with mere common sense.

Numerical experiments show that schemes with a symmetrical third order discretization such as D_0^3 or $D_+D_-D_0$ approximate the KdV solution better than our discretization $D_+^2 D_-$ which is mainly due to the absence of numerical diffusion. Nevertheless, we haven't chosen such a symmetrical discretization for computing the VDL simply because the essential Sobolev-type Lemma 4.1.1 can't be applied to them. We shall address this issue in the next section.

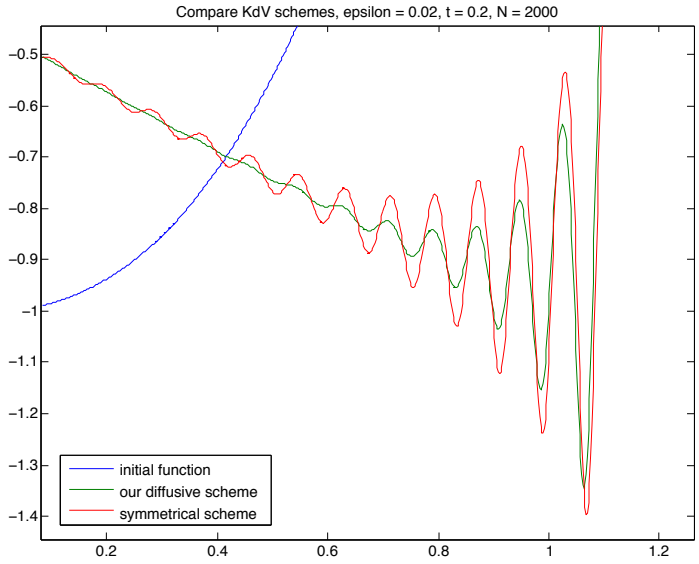

Figure 10: KdV oscillations: Comparison of the diffusive asymmetric third order discretization $D_+^2 D_-$ and the diffusion-less symmetric $D_+ D_- D_0$ discretization.

4.6 Generalized Scheme

Numerical experiments show that the KdV solution is better approximated if the third order term is discretized in a *symmetrical* manner. This is clearly not the case for the scheme (36). As an example, we look at the third order discretization $D_+ D_- D_0$. If we perform a Taylor approximation as in section 4.1.4, we find that

$$D_+ D_- D_0 v(x) = v_{xxx}(x) + \frac{\Delta x^2}{4} v_{xxxxx}(x) + O(\Delta x^3).$$

We see that there is no numerical diffusion in such a symmetric discrete dispersive term. Since it is a well-known fact that diffusion causes sharp peaks to spread out, we would prefer a diffusion-less discretization above a diffusive discretization because the VDL is the result KdV oscillations which get finer and finer as $\varepsilon \to 0$. In figure 10, we compare the numerical KdV solutions of the implicit scheme for the dispersions $D_+^2 D_-$ and $D_+ D_- D_0$. We see that the symmetric scheme resolves the oscillations much better than the dispersive-diffusive scheme.

We therefore believe that a symmetric third order discretization would also better approximate the VDL. However, it makes the application of the Sobolev-type Lemma 4.1.1 impossible. As a consequence, all weak BV properties which were derived in the previous sections don't hold. In fact, diffusion is needed in order to prove all of the above results.

We therefore need a scheme which is still diffusive while being closer to the symmetric discretization $D_+ D_- D_0$. We propose the following *generalized scheme*:

$$D_-^t u_{j,n} - E u_{j,n} D_0 u_{j,n} + \varepsilon^2 D_\delta^{(3)} u_{j,n} = 0 \tag{60}$$

where

$$D_\delta^{(3)} := \left(\frac{1}{2} + \delta\right) D_+^2 D_- + \left(\frac{1}{2} - \delta\right) D_+ D_-^2, \quad 1 \geq \delta > 0.$$

Note that for $\delta = 0$, this discretization is exactly $D_+D_-D_0$, and for $\delta = 1$, we get our implicit FDS with the third order discretization $D_+^2D_-$.

For small δ, this discretization is almost diffusion-less since Taylor approximation shows that

$$D_\delta^{(3)}v(x) = v_{xxx}(x) + \delta\Delta x v_{xxxx}(x) + O(\Delta x^2).$$

At the same time, we can still apply the Sobolev-type Lemma 4.1.1 because the triangle inequality implies that

$$\begin{aligned} 2\delta||D_+^3 v_j||_{\Delta x} &= \left(\frac{1}{2}+\delta\right)||D_+^2D_-v_j||_{\Delta x} - \left(\frac{1}{2}-\delta\right)||D_+D_-^2v_j||_{\Delta x} \\ &\leq ||D_\delta^{(3)}v_j||_{\Delta x}. \end{aligned}$$

It is even possible to let $\delta \to 0$ as $\Delta x \to 0$ with a rate $\delta = \Delta x^s$. However, the results of the previous sections then only hold for even smaller rates $\varepsilon = \Delta x^r$.

4.7 Numerical Experiments

In this section, we carry out numerical experiments with the generalized implicit FDS (60) using the two approaches described in subsection 4.1.3. Using the McLaughlin results as a reference, we shall see that the implicit FDS seems to approximate the correct VDL as $\Delta x, r \to 0$ and that the perturbation approach is much more efficient than the weak limit approach. Furthermore, replacing the Monte-Carlo method with a fixed uniform grid of the probability space will improve the results even more.

We shall then apply this last deterministic perturbation method to a Riemann initial data for which LaL [14] computed explicit numerical values. Despite the overall satisfactory results, we shall address some concerns about the accuracy of our method. Finally, we close this section with some considerations about the numerical complexity.

4.7.1 Weak Limit Approach

In the weak limit approach, we choose a sequence $\Delta x_1, \dots \Delta x_M$ and use the numerical solutions $u^{\Delta x_1}(x,t), \dots u^{\Delta x_M}(x,t)$ as samples to compute the approximative Young measure

$$\nu_{(x,t)}^{(\Delta x_m)_m,M} := \frac{1}{M}\sum_{m=1}^{M}\delta_{u^{\Delta x_m}(x,t)}.$$

We can easily compute the mean and variance of this measure as

$$\begin{aligned} \mathbb{E}(\nu_{(x,t)}^{(\Delta x_m)_m,M}) &= \frac{1}{M}\sum_{m=1}^{M}u^{\Delta x_m}(x,t), \\ \mathrm{Var}(\nu_{(x,t)}^{(\Delta x_m)_m,M}) &= \frac{1}{M}\sum_{m=1}^{M}(u^{\Delta x_m}(x,t))^2 - \mathbb{E}(\nu_{(x,t)}^{(\Delta x_m)_m,M})^2. \end{aligned}$$

To determine the sequence $\Delta x_1, \dots \Delta x_M$, we choose a minimal value N_{min} and a maximal value N_{max}. After fixing a sample number M, we divide the interval $[N_{min}, N_{max}]$ logarithmically into M points $N_{min} = N_1, N_2, \dots N_M = N_{max}$ such that $N_{m-1}/N_m = const.$ for all $m = 2, \dots M$. We then set $\Delta x_m := \frac{1}{\lceil N_m \rceil}$. Furthermore, we fix some ε_0 and choose the constant c in $\varepsilon = c\Delta x^r$ such that $\varepsilon_0 = c\Delta x_1^r$.

We use the generalized scheme (60) with $\delta = 0.01$ and present the results for

$$\begin{aligned} N_{min} &= 400, \\ N_{max} &= 8000, \\ r &= \frac{1}{2}, \frac{1}{4}, \\ M &= 10, 100, \\ t &= 0.15, \\ \varepsilon_0 &= 0.06 \text{ and} \\ \lambda &= 0.5 \end{aligned}$$

in figure 11. We see that the mean and standard deviation seem to converge for increasing sample number M. However, the standard deviation is nowhere near the McLaughlin result. In the region *away from the shock*, the variance increases for decreasing r. However, in the shock-region, we don't see an improvement as r decreases. On the contrary, the mean becomes more oscillatory. This can be explained by the fact that a smaller rate r results in a smaller range of the dispersion coefficient ε if N_{min} and N_{max} are fixed. As a consequence, the statistics get worse. However, keeping the range of ε unaltered would result in a larger range $[N_{min}, N_{max}]$ for decreasing r and thus an enormous increase of the computational complexity.

All in all, we have to say that the numerical results of the weak limit approach are very unsatisfactory.

4.7.2 Perturbation Approach

In the perturbation approach, we artificially create a measure valued initial data by perturbing the initial function. This perturbation is best described by a random field $u_0(x;\omega)$. Doing Monte-Carlo sampling over the corresponding random field $\omega \in \Omega$ and solving the numerical scheme for each initial sample $u_0^m(x), m = 1, \dots M$, we get the approximative Young measure by setting

$$\nu_{(x,t)}^{\Delta x, M} := \frac{1}{M} \sum_{m=1}^{M} \delta_{u^{\Delta x, m}(x,t)}$$

where $u^{\Delta x, m}(x,t)$ is the numerical solution of the m-th sample.

We are left with specifying how to perturb the initial function. We present two approaches: the *Monte-Carlo-left-right-shift-approach (MC-LR-approach)*

$$u_0(x;\omega) = u_0(x + \omega\, \varepsilon')$$

and the *Monte-Carlo-up-down-shift-approach (MC-UD-approach)*

$$u_0(x;\omega) = u_0(x) + \omega\, \varepsilon'.$$

Here, ε' is the perturbation level and $\omega \in \Omega = [-1, 1]$ with uniform distribution is the probability space.

We set

$$\begin{aligned} M &= 200, \\ N &= 2000, \\ \varepsilon &= 0.03, 0.06 \\ t &= 0.15, \\ \varepsilon' &= 0.1 \text{ and} \\ \lambda &= 0.5 \end{aligned}$$

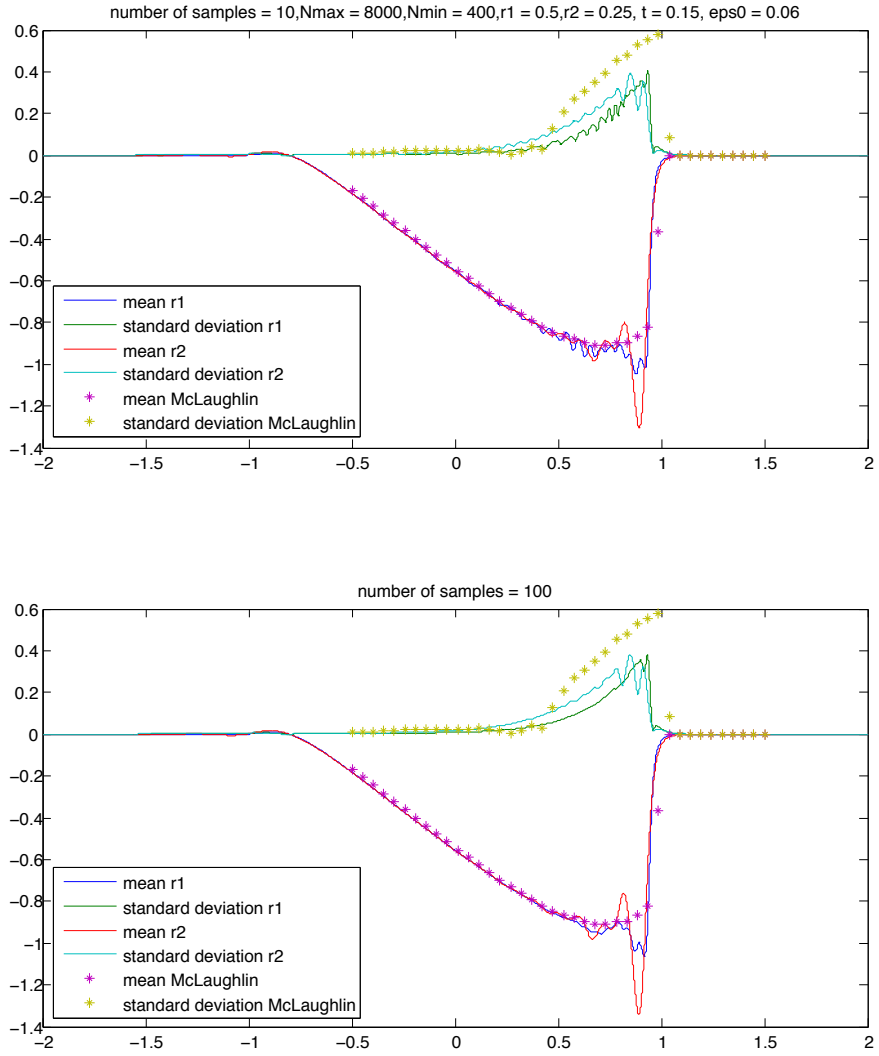

Figure 11: Approximative Young measure (mean and standard deviation) with implicit FDS and weak limit approach for different rates r and different sample numbers M, compared to simplified method of McLaughlin and Strain.

and use the generalized scheme (60) with $\delta = 0.01$. The results are shown in figure 12. They are both similar and much better than the weak limit approach *with considerably less computing time*. We see that for fixed $M, \Delta x$, the results get better for *larger* dispersion coefficient ε. This is explained by the following two reasons: First, the KdV solution is better approximated for larger ε if Δx is fixed. Second, a larger ε imitates the behavior of a smaller rate r because a smaller rate r means that ε tends to zero slower as $\Delta x \to 0$. Despite the improvement compared to the weak limit approach, both mean and standard deviation show considerable coarse fluctuations.

4.7.3 Uniform Left-Right-Shifts

Considering the MC-LR-approach and keeping in mind that the whole problem is translation invariant, we presume that we can minimize the Monte-Carlo error by the following *uniform-left-right-shift-approach (UNI-LR-approach)*: Instead of drawing M random samples $\omega \in \Omega = [-1, 1]$, we fix a uniform grid $\omega_i = \frac{2i}{M} - 1, i = 1, \dots M$ on the probability space. Furthermore, we observe that the sampling process is indeed not necessary for left-right-shifts: By the translation invariance, it is enough to compute only one sample and use the numerical solution within the region $[x - \varepsilon', x + \varepsilon']$ for the statistics. Having to compute only one solution also allows us to go to a finer mesh resolution.

We set

$$\begin{aligned} N &= 8000, \\ \varepsilon &= 0.03 \\ t &= 0.15, \\ \varepsilon' &= 0.1 \text{ and} \\ \lambda &= 0.5 \end{aligned}$$

and use the generalized scheme (60) with $\delta = 0.01$. The results are shown in figure 13 where we can observe a considerable improvement compared to the Monte-Carlo method from figure 12.

4.7.4 Other Example: Riemann Problem

In section 7 of [14], LaL explicitly computed some numerical values of the mean and variance of the VDL with the Riemann initial data (21). This gives an excellent reference for testing our FDS. Since this is not a periodic problem, we feed the scheme from left and right with -1 resp. 0. We set

$$\begin{aligned} N &= 8000, \\ \varepsilon &= 0.2, \\ t &= 1, \\ \varepsilon' &= 1 \text{ and} \\ \lambda &= 0.1 \end{aligned}$$

and apply the UNI-LR-approach with the generalized scheme (60) with $\delta = 0.01$. The result is shown in figure 14. Basically, we can make the same observations as in the previous subsections. Again, we see that the non-atomicity is propagating out of the shock to the left.

4.7.5 Criticism, Resolving the KdV Solution

Even though the numerical results of the UNI-LR-approach seem quite promising, we shall explain in this subsection that using only the mean and standard deviation as a reference might be partly misleading.

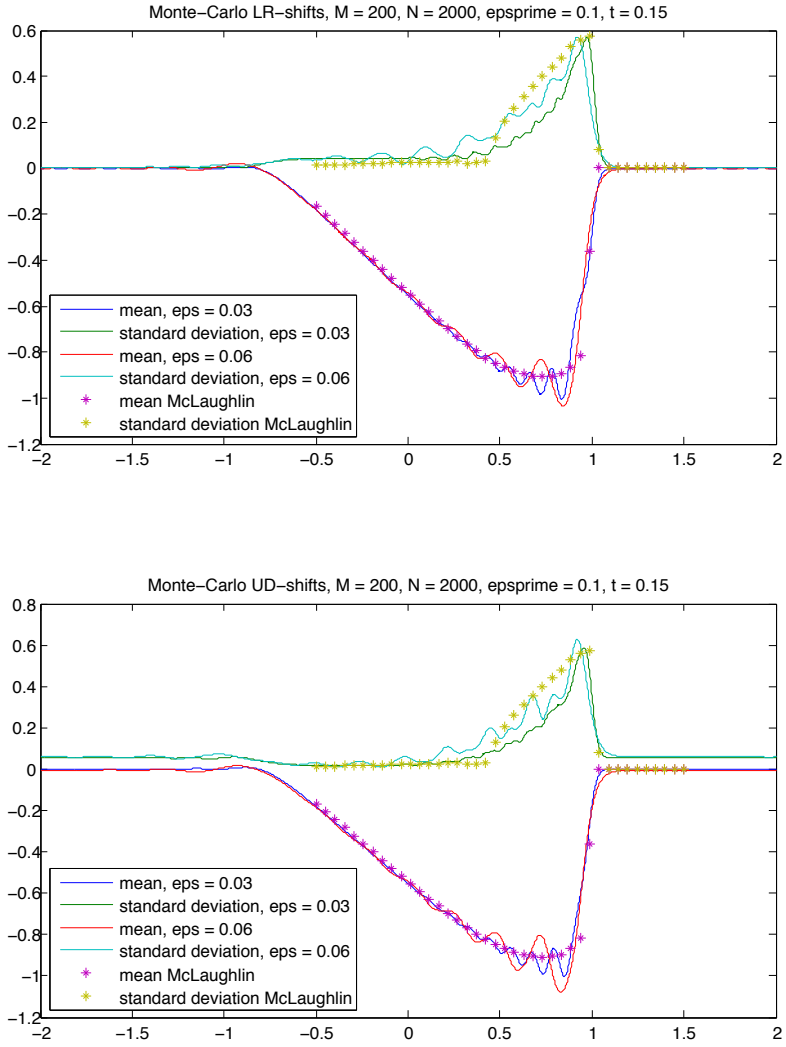

Figure 12: Approximative Young measure (mean and standard deviation) with implicit FDS and MC-LR-approach resp. MC-UD-approach and different ε, compared to simplified method of McLaughlin and Strain.

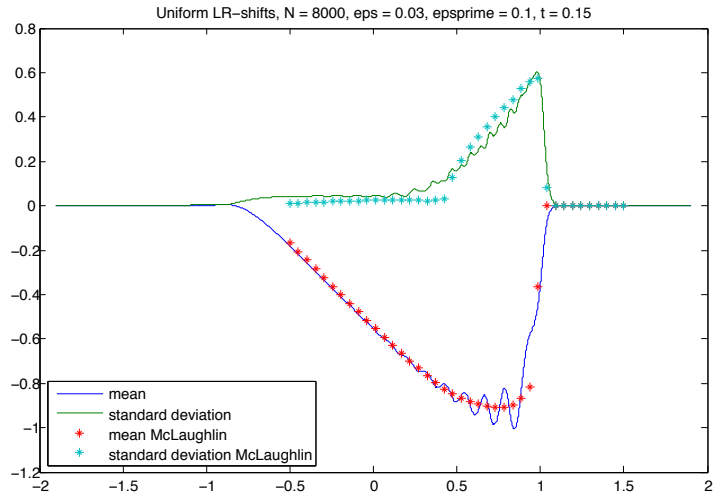

Figure 13: Approximative Young measure (mean and standard deviation) with implicit FDS and UNI-LR-approach, compared to simplified method of McLaughlin and Strain.

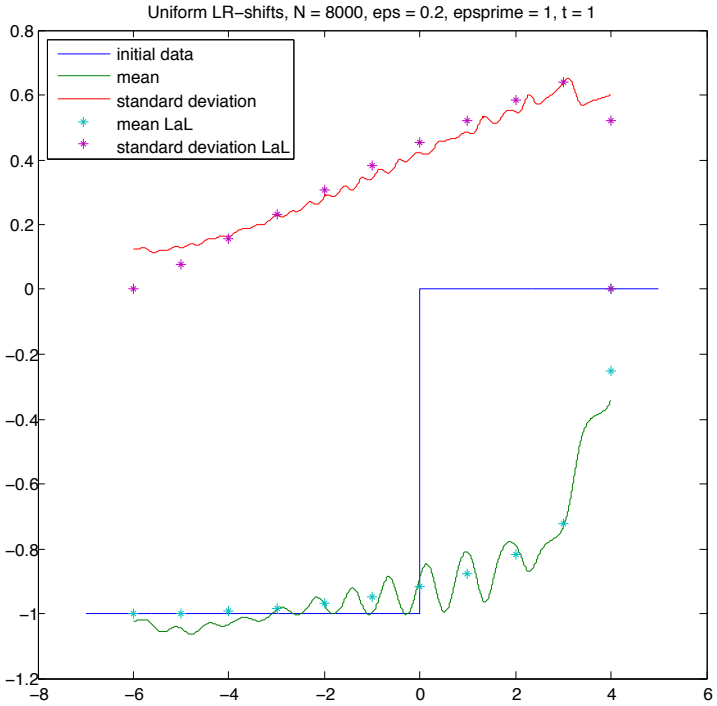

Figure 14: UNI-LR-approach for Riemann initial data, compared to explicit values of LaL ([14], section 7).

In order to do a sound statistical analysis in the perturbation approach, we would like to choose the dispersion coefficient ε very small compared to the perturbation level ε'. It is a fact however that for fixed Δx, the FDS works worse and worse for decreasing ε. Because of the numerical diffusiveness and implicity of the FDS, we have to choose ε quite large in order to be enough oscillatory. In other words, to get a good approximation of the KdV oscillations, we have to choose either ε large or Δx small. As a consequence of these conflicting requirements, the perturbation level ends up being of the same order of magnitude as the dispersion coefficient. Considering in particular the UNI-LR-approach, the shift-region $[x-\varepsilon', x+\varepsilon']$ has about the size of at most two KdV oscillation periods. Even though this gives satisfactory approximations of the mean and standard deviation, we have to doubt whether the approximation of the *whole* Young measure is faithful.

The correctness of the computed Young measure depends mainly on how accurate the FDS can resolve the KdV oscillations. Going back to the LaL theory of section 3.1 and remembering the formulas (14) ff. which we can actually implement numerically, we get a good reverence solution for these KdV oscillations. We set

$$\begin{aligned} \varepsilon &= 0.05, 0.01, \\ N &= 8000, \\ t &= 0.15 \text{ and} \\ \lambda &= 0.5 \end{aligned}$$

and show the KdV oscillations generated with the generalized scheme (60) together with the LaL reference in figure 15. We see that even though there is a shift in x, the *shape* and the *amplitude* of the KdV oscillations is reasonably resolved for $\varepsilon = 0.05$. But already for $\varepsilon = 0.01$, the result gets much worse.

4.7.6 Numerical Complexity

We experimentally investigate the numerical complexity of the implicit FDS as $\Delta x \to 0$. We do this by measuring the computing times for different mesh resolutions N. Performing a best linear fit of the logarithmic plot shown in figure 16, we see that

$$\text{computing time} \approx O(N^2),$$

i.e. the computational complexity grows at a quadratic rate with the mesh resolution N. Since Δx and Δt are linked linearly via the CFL-number $\lambda = \frac{\Delta t}{\Delta x}$, this computational complexity is to be expected provided that we can solve one time step in $O(N)$ time. This is rather surprising for an implicit scheme and also not entirely true since the best linear fit yields a rate which is slightly above 2, see figure 16. Nevertheless, the almost quadratic rate in the case of our implicit scheme can be explained by

- assuming that the number of iterations in (37) is uniformly bounded,
- noting that the inverse matrix needed in order to solve one iteration step only has to be computed once for the entire process,

and by taking into account that MATLAB has optimized algorithms for computing matrix-vector-multiplications and inverting matrices.

In the context of the weak limit approach, adding one single sample while keeping the ratio $\mu := \Delta x_{m-1}/\Delta x_m$ fixed means multiplying the computing time by μ^2, and thus

$$\text{computing time} \approx O(\mu^{2M}).$$

This exponential rate is much worse than the linear rate at which the computing time of the perturbation approach grows with increasing sample number M.

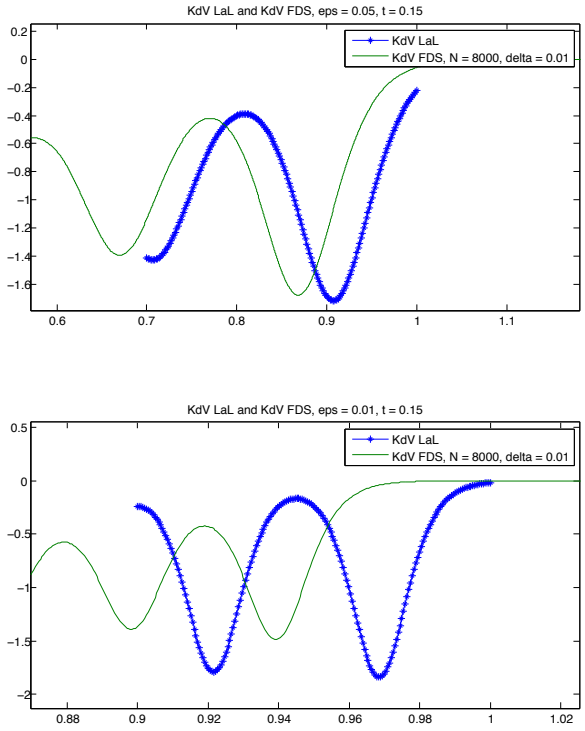

Figure 15: KdV oscillations for $\varepsilon = 0.05$ resp. $\varepsilon = 0.01$ computed with the implicit FDS and compared to LaL reference.

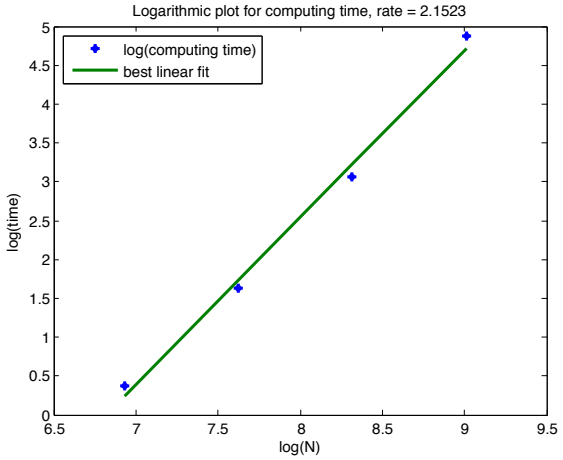

Figure 16: Numerical complexity of the implicit FDS together with the best linear fit of the logarithmic plot.

In addition to these considerations concerning the computational complexity, there is another advantage of the perturbation approach compared to the weak limit approach: The sampling process can be computationally optimized by using *parallel computing*. This is much harder if not impossible for the weak limit approach since every new sample has a different mesh size Δx.

Lastly, we would like to point out that the UNI-LR-approach avoids the sampling process completely which again means an enormous increase of efficiency.

4.8 Conjecture: Limit Measure is Vanishing Dispersion Limit

4.8.1 The r-Limit Measure

We have seen that the k-dimensional Young measure associated with the implicit FDS is a k-jet MV solution provided that the rate $\varepsilon = \Delta x^r$ is slow enough. We have also seen that the scheme (36) approximates Burgers' equation with a mixture of dispersive and diffusive regularization where the diffusive term tends to zero faster than the dispersive term as $r \to 0$. We have conjectured that for each r, the Young measure associated with the implicit FDS is different, and that we get closer and closer to the VDL as $r \to 0$. We shall make this more precise in this section.

For each k, let r_k be the rate $\varepsilon = \Delta x^{r_k}$ such that the k-dimensional Young measure $\nu^k = (\nu_0^k, \dots \nu_{k-1}^k)$ associated with the implicit FDS is a k-jet MV solution. By the fundamental theorem of Young measures (see [5], Theorem A.1) and by a simple diagonalization argument, we conclude that there is a subsequence k_l such that for each j, the one-dimensional components $\nu_j^{k_l}$ converge narrowly:

$$\forall j: \quad \nu_j^{k_l} \rightharpoonup \nu_j, \quad l \to \infty.$$

Formally, we get an infinite-dimensional measure $(\nu_0, \nu_1, \dots)$ which we call the *r-limit measure associated with the implicit FDS*. By narrow convergence, we get the following

Theorem 4.1 (r-Limit Measure)**.** *Let $(\nu_0, \nu_1, \dots)$ be the r-limit measure associated with the implicit FDS. Then, for each k, the first k components $(\nu_0, \dots \nu_{k-1})$ of the r-limit measure are a k-jet MV solution. In other words, the r-limit measure satisfies the whole infinite DiPerna characterization.*

This Theorem indicates that the first component ν_0 of the r-limit measure is the VDL. However, this remains a conjecture for the moment.

4.8.2 Non-Polynomial Dispersion Coefficient

We can avoid the notion of the r-limit measure by considering a dispersion coefficient which is not a power of the mesh size Δx but which tends to zero slower than any power of Δx:

$$\varepsilon = \alpha(\Delta x), \quad \forall r > 0 : \Delta x^r = o(\alpha(\Delta x)). \tag{61}$$

By the above results, the Young measure corresponding to the resulting scheme will satisfy the whole DiPerna characterization:

Theorem 4.2 (Non-polynomial dispersion coefficient)**.** *Let $\nu^k = (\nu_0^k, \dots \nu_{k-1}^k)$ be the k-dimensional Young measure associated with the implicit FDS where the dispersion coefficient $\varepsilon = \alpha(\Delta x)$ is chosen such that*

$$\forall r > 0 : \Delta x^r = o(\alpha(\Delta x)).$$

Assuming $J_k^{\Delta x}$ to be uniformly bounded in $L^\infty(\mathbb{R}/\mathbb{Z} \times (0,T))$, ν^k will be a k-jet MV solution for any $k \in \mathbb{N}$.

This again indicates that the one-dimensional Young measure associated with the implicit FDS is the VDL provided we choose ε to behave as in (61). However, this again remains a conjecture for the moment.

5 Crank-Nicolson Finite Difference Scheme

Even though we payed a lot of attention to the diffusion contained in the dispersive operator $D_+^2 D_-$ (see sections 4.1.4, 4.5 and 4.6), it is also mainly the implicity of the scheme (36) resp. (60) which is responsible for diffusion. This is also indispensable for deriving the weak BV estimates that are needed for proving the DiPerna characterization. As an example, we look at the L^2-norm of the numerical solution: The inequality (41) shows that it is not only non-increasing but indeed decreasing. It is this undesirable property which we try to avoid in this section.

Attempting to improve the numerical results, we thus present a Crank-Nicolson finite difference scheme and use it to perform numerical experiments. The construction of the FDS is such that the L^2-norm is not decreasing but completely conserved. This however makes it impossible to prove the above theoretical result concerning the DiPerna characterization. For fixed ε, we nevertheless believe that we can prove it to converge to the classical KdV solution doing a similar proof as in [11]. As a KdV scheme, the Crank-Nicolson FDS works much better than the implicit scheme which is the reason for the numerical improvement when computing the VDL.

5.1 The Scheme

It is a fact that being *implicit* adds a considerable amount of diffusion to a FDS. We eliminate this source of diffusion by evaluating the numerical terms corresponding to $6uu_x$ and εu_{xxx} at the $n-\frac{1}{2}$-th time step. Also, we use the *symmetric third order operator* $D_+D_-D_0$ which was already discussed in section 4.6. The result is the following Crank-Nicolson scheme:

$$\frac{u_{j,n}-u_{j,n-1}}{\Delta t} - 6Eu_{j,n-1/2}D_0u_{j,n-1/2} + \varepsilon^2 D_+D_-D_0u_{j,n-1/2} = 0 \qquad (62)$$

where

$$u_{j,n-1/2} := \frac{u_{j,n-1}+u_{j,n}}{2}.$$

Multiplying equation (62) with $u_{j,n-1/2}$ and summing over j, we see that

$$||u_{j,n}||_{\Delta x} = ||u_{j,n-1}||_{\Delta x},$$

i.e. the L^2-norm of the numerical solution is completely conserved. It is this property which is mainly responsible for the numerical improvement compared to the implicit scheme.

5.2 Numerical Experiments

In this section, we perform numerical experiments with the perturbation approach using the Crank-Nicolson FDS. Since it approximates the KdV solution much better than the implicit scheme, it allows us to choose the dispersion coefficient much smaller which yields a more faithful statistical analysis.

In addition to the one-bump initial function, we shall present the numerical result for the initial function $u_0(x) = cos(x)$, and perform a stability experiment. Finally, we shall demonstrate how well this scheme approximates the KdV oscillations for small values of ε.

5.2.1 One-Bump and $cos(x)$ Initial data

We apply the MC-LR-approach resp. MC-UD-approach to the same one-bump initial function as in subsection 4.7.2. We set

$$\begin{aligned} M &= 200, \\ N &= 1000, \\ \varepsilon &= 0.01 \\ t &= 0.15, \\ \varepsilon' &= 0.1 \text{ and} \\ \lambda &= 0.1 \end{aligned}$$

and show the resulting plots in figure 17. We can observe quite some improvement compared to the implicit FDS (figure 12). In figure 18, we furthermore show the results of the UNI-LR-approach with parameters

$$\begin{aligned} N &= 4000, \\ \varepsilon &= 0.003 \\ t &= 0.15, \\ \varepsilon' &= 0.1 \text{ and} \\ \lambda &= 0.1. \end{aligned}$$

We can see a further improvement compared to the Monte-Carlo method from figure 17.

In figure 19, we show the histograms corresponding to the points $(x, t) = (0.7, 0.15)$ resp. $(x, t) = (0.9, 0.15)$ generated with the UNI-LR-approach and parameters

$$\begin{aligned} N &= 4000, \\ \varepsilon &= 0.006 \\ t &= 0.15, \\ \varepsilon' &= 0.1 \text{ and} \\ \lambda &= 0.1. \end{aligned}$$

We can observe two broad peaks which presumably correspond to the maxima and minima of the KdV oscillations. The fact that the right peak is higher is explained by the fact that the KdV maxima are broader than the minima.

As a second example, we apply the UNI-LR-approach to the initial function $u_0(x) = cos(x)$. We show the result with parameters

$$\begin{aligned} N &= 4000, \\ \varepsilon &= 0.008 \\ t &= 0.23, \\ \varepsilon' &= 0.1 \text{ and} \\ \lambda &= 0.1 \end{aligned}$$

in figure 20. Not surprisingly, the picture looks similar to the one-bump case: The non-atomicity is propagating out of the shock to the left.

5.2.2 Stability of the VDL Revisited

As in subsection 3.2.3, we would like to present numerical indication that the VDL is stable with respect to small perturbation around atomic initial data. However this

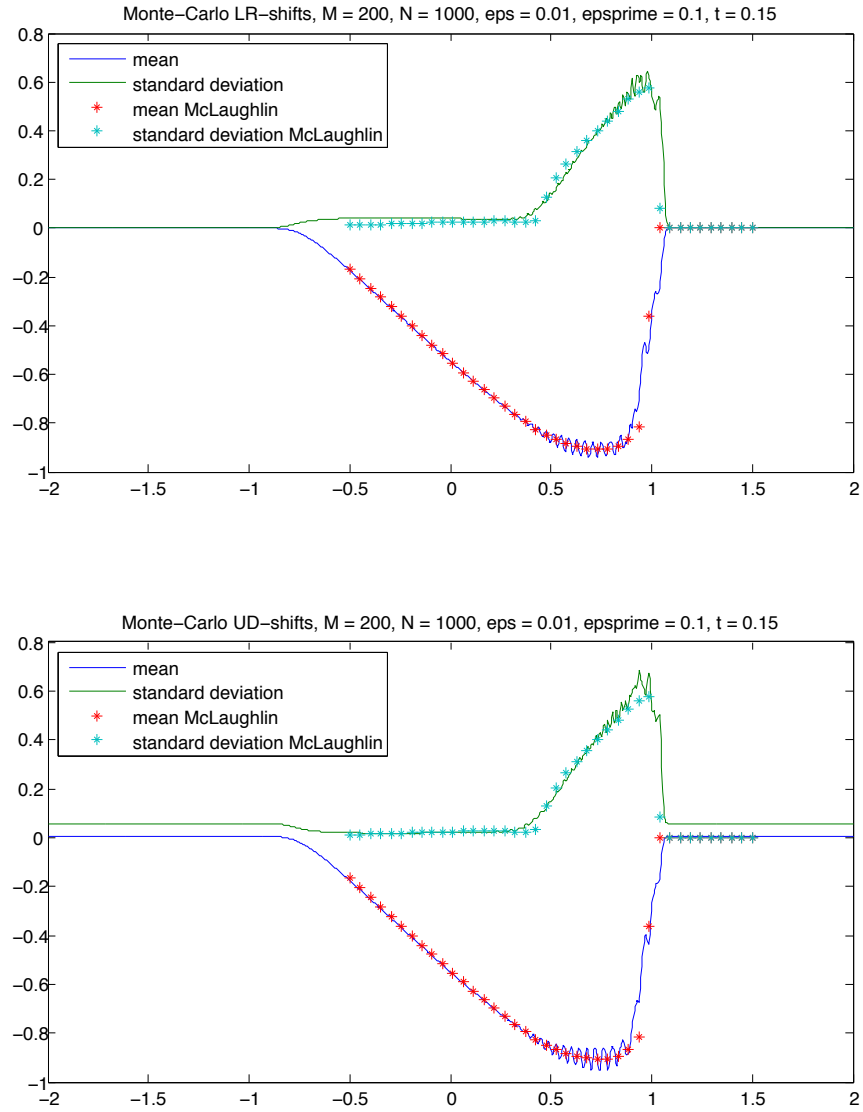

Figure 17: Approximative Young measure (mean and standard deviation) with Crank-Nicolson FDS and MC-LR-approach resp. MC-UD-approach, compared to simplified method of McLaughlin and Strain.

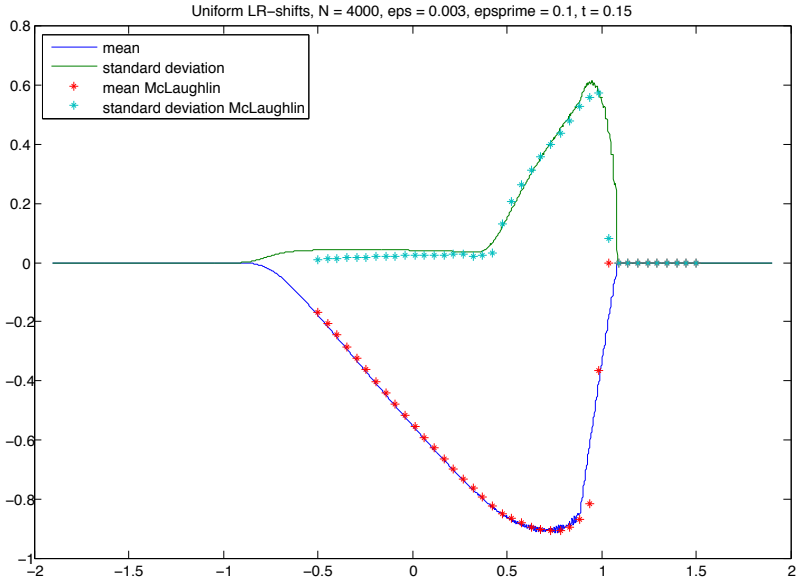

Figure 18: Approximative Young measure (mean and standard deviation) with Crank-Nicolson FDS and UNI-LR-approach, compared to simplified method of McLaughlin and Strain.

time, we use the Crank-Nicolson FDS. We apply the UNI-LR-approach to the initial function $u_0(x) = cos(x)$ but perturb it by an up-shift: $u_0^\delta(x) = cos(x) + \delta$. For each δ, we obtain an approximative Young measure $\nu^{\Delta x,\delta}$. We then study the behavior of the mean and standard deviation of $\nu^{\Delta x,\delta}$ as $\delta \to 0$ by measuring the L^1-error with respect to the numerical solution corresponding to $\delta = 0$:

$$\text{error of mean}^{\Delta x}(\delta) = \left|\left|\mathbb{E}(\nu_{x,t}^{\Delta x,\delta}) - \mathbb{E}(\nu_{x,t}^{\Delta x,0})\right|\right|_{L^1(0,2\pi)}$$
$$\text{error of standard deviation}^{\Delta x}(\delta) = \left|\left|\sqrt{\text{Var}(\nu_{x,t}^{\Delta x,\delta})} - \sqrt{\text{Var}(\nu_{x,t}^{\Delta x,0})}\right|\right|_{L^1(0,2\pi)}.$$

The resulting error plot with

$$\begin{aligned} N &= 4000, \\ t &= 0.23, \\ \varepsilon &= 0.008, \\ \varepsilon' &= 0.1 \text{ and} \\ \lambda &= 0.1 \end{aligned}$$

is shown in figure 21. We can clearly see that the errors are converging to zero as $\delta \to 0$ which indicates that the VDL is stable with respect to small perturbation around atomic initial data.

5.2.3 Resolving the KdV Solution

In subsection 4.7.5, we have seen that the implicit FDS failed to produce a good approximation of the KdV solution for small dispersion coefficients ε. We now compute

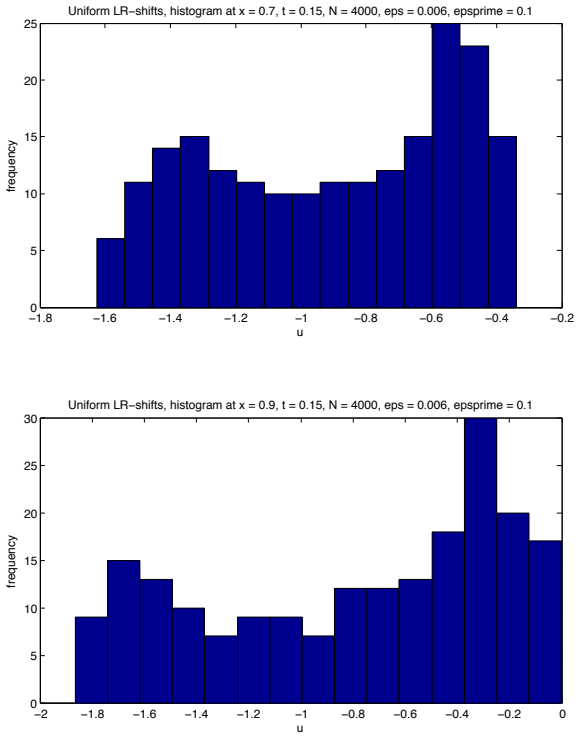

Figure 19: Histograms at the points $(x,t) = (0.7, 0.15)$ resp. $(x,t) = (0.9, 0.15)$, generated with the Crank-Nicolson FDS and UNI-LR-approach.

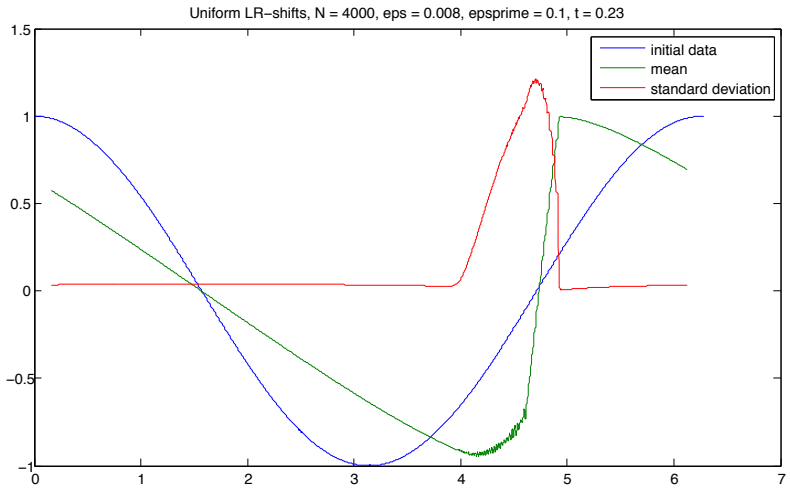

Figure 20: Approximative Young measure (mean and standard deviation) with Crank-Nicolson FDS and UNI-LR-approach for $cos(x)$-initial data.

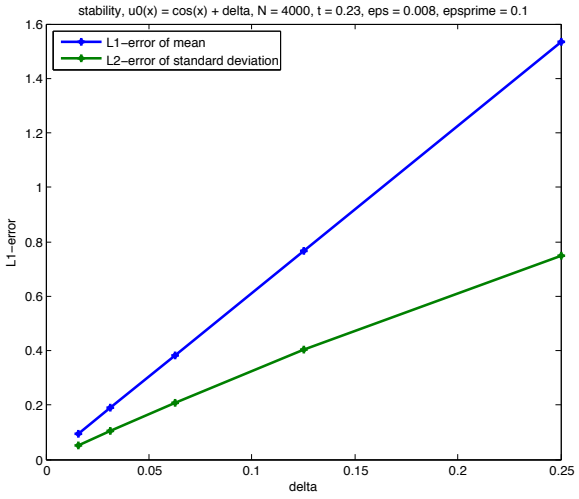

Figure 21: Stability check with Crank-Nicolson FDS: Error plot for the mean and standard deviation.

the KdV oscillations with the Crank-Nicolson FDS with parameters

$$\begin{aligned} \varepsilon &= 0.003, \\ N &= 4000, \\ t &= 0.15 \text{ and} \\ \lambda &= 0.1 \end{aligned}$$

and compare it with the LaL KdV reference solution. The result is shown in figure 22. Even though there is a slight x-shift, we see that the Crank-Nicolson scheme reproduces both shape and amplitude of the KdV oscillations much more accurately than the implicit scheme, and this for a value of ε which is more than 10 times smaller than the first ε in figure 15!

6 Conclusion, Summary

In this thesis, we have presented an implicit finite difference scheme (FDS) with perturbation of the initial data to compute the vanishing dispersion limit (VDL) of Burgers' equation $u_t - (3u^2)_x = 0$. This was motivated by the numerical work on systems of conservation laws done by Fjordholm and co-workers [5] and by the theoretical work of Lax and Levermore (LaL) on the VDL of Burgers' equation [12],[13],[14]. The main concept behind all considerations is the concept of measure valued (MV) solutions introduced by DiPerna [4]. As opposed to the vanishing viscosity solution which is atomic, the vanishing *dispersion* limit is indeed a non-atomic measure.

To *theoretically* sustain the validity of our computations, we attempted to show that our numerical MV solution satisfies DiPerna's characterization of the VDL, see ([4], section 7). This characterization includes infinitely many levels, called k-jets. We could prove that for a fixed rate $\varepsilon = \Delta x^r$ of the dispersion coefficient ε, the numerical MV solution satisfies the first k levels of DiPerna's characterization provided that r is small enough. Indeed, we have seen that $r \to 0$ as $k \to \infty$. Our discretization of the

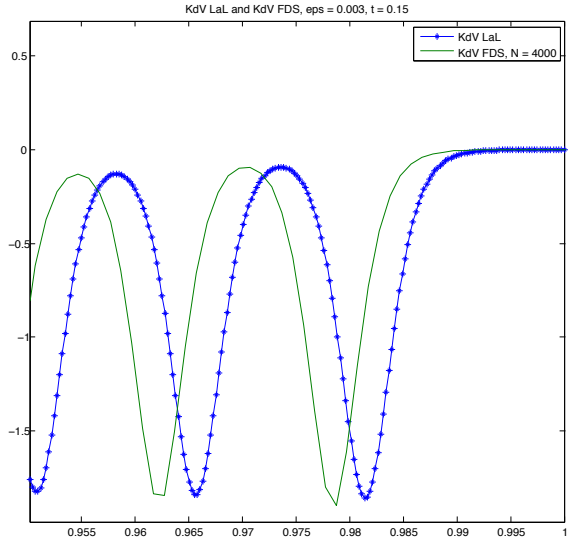

Figure 22: KdV oscillations for $\varepsilon = 0.003$ computed with Crank-Nicolson FDS and compared to LaL reference.

dispersive term consists of both numerical dispersion *and diffusion*:

$$D_+^2 D_- u(x) \approx \varepsilon^2 u_{xxx} + \frac{\varepsilon^2 \Delta x}{2} u_{xxxx}.$$

As $r \to 0$, the diffusive term tends to zero faster than the dispersive term which lead to the conjecture that the numerical MV solution converges to the VDL as $r \to 0$. *Since a smaller rate r means a better resolution of the KdV equation,* these theoretical considerations are also consistent with mere common sense.

To *numerically* sustain the validity of our computations, we mainly used the perturbation approach presented in [5] and compared the results with a simplified method of McLaughlin and Strain which is based on the theoretical work of LaL [12]. This indicated that at least the mean and variance of our numerical MV solution converge to the correct limit. Also, in accordance with our theoretical results and conjecture, the results get better for *increasing* dispersion coefficients ε if we keep Δx fixed since this imitates the behavior of a slower rate r.

Even though the theoretical and numerical results look promising at first sight, the fact that we rely on resolving the KdV oscillations as accurately as possible raised some concerns about the accuracy of the *whole* Young measure. Since the implicit FDS is very diffusive, it is difficult to obtain a good approximation of the KdV solution for small values of ε. This is why we furthermore applied a Crank-Nicolson FDS for which we can't prove the theoretical result concerning the DiPerna characterization but which resolves the KdV oscillations much better.

Comparing the finite difference approach with the algorithm of McLaughlin and Strain, we have to stress the following points: The McLaughlin method avoids exactly the one challenge we faced throughout this whole thesis, namely resolving the KdV solution. This big advantage however is overshadowed by the following three drawbacks which are resolved by the finite difference approach: First, McLaughlin is a *local* method which means that for each point (x, t), a different minimization problem has to be solved. This also makes an efficiency comparison rather difficult. Second, it only

computes the mean and variance of the VDL. Third, it is only applicable to a very small class of initial functions satisfying the requirements of the LaL theory.

We would like to stress that the theoretical results of this thesis are mainly based on the special structure of the implicit FDS. We therefore doubt whether they can be generalized to *higher-dimensional* problems. However, stability results might similarly be obtained for *higher-order* dispersive regularization. Nevertheless, a characterization in the spirit of DiPerna's is only available for the *third-order* dispersion since it relies on the special properties of the KdV equation.

Acknowledgments. I would like to thank my adviser Prof. Dr. Siddhartha Mishra for supervising this thesis and for many interesting discussions.

References

[1] A. Bressan, G. Crasta and B. Piccoli. Well-posedness of the Cauchy problem for $n \times n$ systems of conservation laws. Memoirs of the AMS, 146 (694), 2000.

[2] M. G. Crandall and A. Majda. Monotone difference approximations for scalar conservation laws. Math. Comp. 34, 1980, 1-21.

[3] C. Dafermos. Hyperbolic conservation laws in continuum physics. Springer, Berlin, 2000.

[4] R. J. DiPerna. Measure valued solutions to conservation laws. Arch. Rational Mech. Anal., 88(3), 1985, 223-270.

[5] U. S. Fjordholm, R. Käppeli, S. Mishra, E. Tadmor, Construction of approximate entropy measure valued solutions for hyperbolic systems of conservation laws.

[6] C. S. Gardner, J. M. Greene, M. D. Kruskal, and R. M. Miura, Method for solving the Korteweg-de Vries equation, Phys. Rev. Lett. 19, 1967, pp. 1095-1097.

[7] J. Glimm. Solutions in the large for nonlinear hyperbolic systems of equations. Comm. Pure Appl. Math. 18 (4), 1965, 697-715.

[8] Y. Kametaka. 123. Korteweg-de Vries Equation. II. Finite Difference Approximation. Proc. Japan Acad., 45 (1969)

[9] S. N. Kruzkhov. First order quasilinear equations in several independant variables. USSR Math. Sbornik., 10 (2), 1970, 217-243.

[10] S. Laumer, KdV Equation: Convergence of a Finite Difference Scheme suggested by Y. Kametaka (Bachelor's Thesis).

[11] S. Laumer, KdV-type Equations: Convergence of a Finite Difference Scheme (Semester Thesis).

[12] P. D. Lax & C. D. Levermore, The small dispersion limit for the KdV equation I, Comm. Pure Appl. Math. 36 (1983), 253-290.

[13] P. D. Lax & C. D. Levermore, The small dispersion limit for the KdV equation II, Comm. Pure Appl. Math. 36 (1983), 571-594.

[14] P. D. Lax & C. D. Levermore, The small dispersion limit for the KdV equation III, Comm. Pure Appl. Math. 36 (1983), 809-829.

[15] D. W. McLaughlin and J. A. Strain. Computing the Weak Limit of KdV. Comm. Pure Appl. Math. 47, 1319-1364 (1994).

[16] R. M. Miura, C. S. Gardner & M. D. Kruskal, Korteweg-de Vries equation and generalizations, II. Existence of conservation laws and constants of motion, J. Math. Phys. 9 (1968), 1204-1209.

[17] A. Sjöberg. On the Korteweg-de Vries Equation: Existence and Uniqueness. Journal of Mathematical Analysis and Applications 29, 569 - 579 (1970), p. 573